

GLYCOGEN METABOLISM IN LAFORA DISEASE

Christopher J. Contreras

Submitted to the faculty of the University Graduate School
in partial fulfillment of the requirements
for the degree
Doctor of Philosophy
in the Department of Biochemistry and Molecular Biology
Indiana University

February 2018

Accepted by the Graduate Faculty of Indiana University, in partial fulfillment of the requirements for the degree of Doctor of Philosophy.

Doctoral Committee

Peter J. Roach, Ph.D., Chair

Anna A. DePaoli-Roach, Ph.D.

September 12, 2017

Thomas D. Hurley, Ph.D.

B. Paul Herring, Ph.D.

© 2017

Christopher J. Contreras

DEDICATION

This work is dedicated to the memory of my friend and my grandmother, Keith "Buster" Norwood Jr. and Siprianita Ortega. Both have had a significant impact on my life and are dearly missed.

I would also like to dedicate this work to my parents Diana and Juan Contreras, who have always supported me throughout my life.

Last but not least, I would like to dedicate this work to all of my friends and those who have supported me throughout my education and inspired me to keep pressing on.

ACKNOWLEDGEMENTS

I would like to first thank Dr. Peter J. Roach for allowing me to be a part of his lab and for his guidance throughout my research. Dr. Roach is a great person to have a discussion about research with. Our discussions always encouraged thought and ideas for testing hypotheses. I would next like to thank Dr. Anna A. DePaoli-Roach for her guidance and extensive knowledge of glycogen metabolism and she has taught me to be critical of data. Working with Dr. Roach and Dr. DePaoli-Roach has been a great experience and has made me a better scientist. One of the things I enjoyed most about interacting with Dr. Roach and Dr. DePaoli-Roach was hearing about how they conducted research and how they purified glycogen and enzymes from primary sources.

I would also like to thank the other members of the Roach lab, Dyann Segvich and Sasha Skurat. There have been a few past members of the Roach lab and it has been a joy working with those great people. One in particular is Dr. Vincent Tagliabracci, who taught me how to measure phosphate and sparked my interest in Lafora disease research. All of the people in the Roach lab, present and past, have always offered great advise, been encouraging and have a great deal of knowledge that is always appreciated.

I would like to thank my committee members, Dr. Thomas D. Hurley and Dr. Paul B. Herring, who have given valuable advise that helped move projects forward.

I would like to thank everyone in the Department of Biochemistry and Molecular Biology for all they do, Jack Arthur, Sandy McClain, Melissa Tarrh, Sheila Reynolds and Patty Dillworth.

Last but not least I would like to thank my family and my close friends.

Christopher J. Contreras

GLYCOGEN METABOLISM IN LAFORA DISEASE

Glycogen, a branched polymer of glucose, serves as an osmotically neutral means of storing glucose. Covalent phosphate is a trace component of mammalian glycogen and has been a point of interest with respect to Lafora disease, a fatal form of juvenile myoclonus epilepsy. Mutations in either the *EPM2A* or *EPM2B* genes, which encode laforin and malin respectively, account for ~90% of disease cases. A characteristic of Lafora disease is the formation of Lafora bodies, which are mainly composed of an excess amount of abnormal glycogen that is poorly branched and insoluble. Laforin^{-/-} and malin^{-/-} knockout mice share several characteristics of the human disease, formation of Lafora bodies in various tissues, increased glycogen phosphorylation and development of neurological symptoms. The source of phosphate in glycogen has been an area of interest and here we provide evidence that glycogen synthase is capable of incorporating phosphate into glycogen. Mice lacking the glycogen targeting subunit PTG of the PP1 protein phosphatase have decreased glycogen stores in a number of tissues. When crossed with mice lacking either laforin or malin, the double knockout mice no longer over-accumulate glycogen, Lafora body formation is almost absent and the neurological disorders are normalized. Another question has been whether the abnormal glycogen in the Lafora disease mouse models can be metabolized. Using exercise to provoke glycogen degradation, we show that in laforin^{-/-} and malin^{-/-} mice the insoluble, abnormal

glycogen appears to be metabolically inactive. These studies suggest that a therapeutic approach to Lafora disease may be to reduce the overall glycogen levels in cells so that insoluble, metabolically inert pools of the polysaccharide do not accumulate.

Peter J. Roach, Ph.D., Chair

TABLE OF CONTENTS

LIST OF TABLES	xiv
LIST OF FIGURES	xv
LIST OF ABBREVIATIONS	xvii
I. INTRODUCTION	1
1. Glycogen Structure	1
2. Glycogen Metabolism	4
2.1 Overview	4
2.2 Glycogen Metabolism, Enzymes and Regulation	
Glycogen synthase	7
2.2.1 Glycogenin	7
2.2.2 Branching Enzyme	8
2.2.3 Glycogen Synthase and Regulation	8
2.2.4 Glycogen Phosphorylase	11
2.2.5 Debranching Enzyme	13
3. Insulin Signaling and Glycogen Metabolism	13
4. Regulation of Glycogen Metabolism by Epinephrine and Glucagon	15
5. Regulation of Glycogen Metabolism by Exercise	16
6. Glycogen Storage Diseases	19
6.1 Glycogen Storage Disease Type 0	20
6.2 Glycogen Storage Disease Type I: Von Gierke Disease	20
6.3 Glycogen Storage Disease Type II: Popme Disease	22
6.4 Glycogen Storage Disease Type III: Cori Disease	22

6.5 Glycogen Storage Disease Type IV: Andersen Disease	22
6.6 Glycogen Storage Disease Type V: McArdle Disease	23
6.7 Glycogen Storage Disease Type VI: Hers Disease	23
6.8 Glycogen Storage Disease Type VII: Tarui Disease	23
7. Lafora Disease	24
7.1 Laforin	26
7.2 Laforin, Malin and Autophagy	28
7.3 Laforin as a Glycogen Phosphatase	28
7.4 Malin	30
7.5 Lafora Disease and Glycogen	32
8. Glycogen Phosphate	33
8.1 Preface	33
8.2 Phosphate Abundance and Chemistry	33
8.3 Introduction of Glycogen Phosphate	34
8.4 Phosphate and Glycogen Metabolism	38
II. METHODS	41
1. Purification of Rabbit Skeletal Muscle Glycogen for Phosphate Determination	41
1.1 TCA Method	41
1.2 KOH Method	43
2. Preparation of Potato Amylopectin for Phosphate Analysis	44
3. Mouse Models of Lafora Disease	45
4. Mouse Skeletal Muscle Glycogen Purification for Phosphate Determination	45
5. Purified Glycogen and Inorganic Phosphate Determination	47
5.1 Glycogen Determination	47

5.2 Total Phosphate Determination	48
6. Measurement of Phosphate at the C6 Position in Glycogen	48
7. Purification of Glycogen for Total Glycogen Content in Mouse Tissue	49
8. Fractionation of Glycogen by Low Speed Centrifugation and Western Blotting Analysis	50
8.1 Branching Analysis of Purified Glycogen and Glycogen in the Low Speed Supernatant and Pellet	52
9. Synthesis of [β-32P]UDP-glucose	53
9.1 One Step Reaction	54
9.2 Two Step Reaction	54
9.3 Purification of [β - 32 P]UDP-glucose	55
10. Radiolabeling and Visualization of Glycogen	56
11. Treatments of 32P- and 14C- Labeled Glycogen	57
11.1 Glucosidase and Laforin Treatment of Labeled Glycogen	57
11.2 Treatment of Glycogen with PiBind™ Resin	58
11.3 Spin Column and Gel Filtration	58
11.4 Hydrolysis of UDP with Recombinant Human Soluble Calcium Activated Nucleotidase (hSCAN-1)	59
11.5 Competition with Unlabeled UDP	59
11.6 Binding of 32 P-UDP to Glycogen	50
12. Thin Layer Chromatography	60
13. Recombinant Laforin Purification and Reactions	61
13.1 Purification of Recombinant His-Tagged Laforin	61
13.2 Laforin Phosphatase Activity using <i>pNPP</i> as a substrate	62
13.3 Dephosphorylation of Phospho-oligosaccharides with Laforin and HPAEC Analysis	63
13.4 Laforin Nucleotide Reactions and HPAEC Analysis	63

14. Phosphooligosaccharide Purification and Analysis	64
14.1 HPAEC Analysis of Phospho-oligosaccharides	65
14.2 Analysis of Phospho-oligosaccharide by Mass Spectroscopy	65
14.3 Analysis of Phospho-oligosaccharide by NMR Analysis	66
15. Recombinant Glycogen Branching Enzyme Purification	67
16. Branching Enzyme Activity	68
16.1 Indirect Branching Enzyme Activity	68
16.2 Branching Enzyme Activity using Amylose and HPAEC	71
17. Measuring Reducing Ends of Carbohydrates	72
18. Synthesis of Glucose-1,2-Cyclic Phosphate and Glucose-3,6 and 4,6-Cyclic Phosphate	72
19. Synthesis of Glucose-2-Phosphate	73
20. Mouse Exercise Protocol	74
21. Tissue Staining	75
III. RESEARCH OBJECTIVES	76
IV. RESULTS	78
1. Glycogen Phosphate	78
1.1 Phosphate Chemistry and Abundance	78
1.2 Phosphorylation of Glycogen at C6 in Mouse and Rabbit Glycogen	86
1.3 C6 Phosphorylation of Glycogen from Mouse Models of Lafora Disease	87
2. Incorporation of Phosphate into Glycogen by Glycogen Synthase	90
2.1 Assay for Monitoring Incorporation of the β -Phosphate	

of UDP-Glucose into Glycogen	90
2.2 Evidence that Phosphate Incorporation by Glycogen Synthase is Associated with Glycogen	92
2.2.1 Gel Filtration	92
2.2.2 Laforin Removal of ³² P from Glycogen and UDP Hydrolysis	93
2.2.3 Further Investigations of Potential [β- ³² P] UDP Binding to Glycogen	98
3. Glycogen Phosphate, Branching and Solubility	104
3.1 Analysis of Glycogen and Glycogen Phosphate from PTG/Laforin and PTG/Malin Double Knockout Mice	104
3.1.1 Skeletal Muscle Glycogen Levels in WT, Single and Double Knockout Mice	104
3.1.2 Skeletal Muscle Glycogen Phosphate in WT, Single and Double Knockout Mice	106
3.2 Glycogen Solubility and Branching in the Double Knockout Mice	109
3.2.1 Skeletal Muscle Glycogen Solubility	110
3.2.2 Skeletal Muscle Glycogen Branching	111
4. Glycogen Metabolism in Mouse Models of Lafora Disease Subjected to Exercise	114
4.1 Exercise Performance and Blood Glucose	114
4.2 Effect of Exercise on Enzyme Phosphorylation and Distribution	116
4.3 Effect of Exercise on Glycogen and Glycogen Phosphate Metabolism	124
V. Discussion	132
1. Location of the Phosphate in Glycogen	132
2. Origin of the Phosphate in Glycogen	133
3. Glycogen Structure and Metabolism in Mouse Models of	

Lafora Disease	134
4. Glycogen Metabolism During Exercise in Mouse Models of Lafora Disease	139
5. Overall Discussion	140
REFERENCES	142
CURRICULUM VITAE	

LIST OF TABLES

Table 1. Proton, carbon, and phosphorus chemical shifts (in ppm) of phosphorylated amylopectin and glycogen oligosaccharides	85
Table 2. Phosphomonester distribution in phospho-oligosaccharides from glycogen and amylopectin based on NMR analyses	86
Table 3. Determination of total phosphate and glucose-6-P in glycogen and amylopectin	88
Table 4. Exercise performance	115
Table 5. Blood glucose pre- and post-Exercise	116

LIST OF FIGURES

Figure 1. Glycosidic linkages	2
Figure 2. Glycogen structure	2
Figure 3. Glycogen metabolism	6
Figure 4. Regulation of glycogen metabolism	14
Figure 5. Regulation of glycogen metabolism by exercise	17
Figure 6. Glycogen Storage Diseases	21
Figure 7. Lafora body	24
Figure 8. Proposed location of phosphoesters in glycogen	33
Figure 9. Glucose-1-phosphate transferase	34
Figure 10. Proposed mechanism for phosphate incorporation by glycogen synthase	35
Figure 11. HPAEC branching analysis	53
Figure 12. Phosphate elution profile for phospho-oligosaccharide purification	65
Figure 13. Branching enzyme activity	70
Figure 14. Rabbit skeletal muscle glycogen content	79
Figure 15. HPAEC analysis of phospho-oligosaccharides from glycogen and amylopectin	81
Figure 16. Analysis of phospho-oligosaccharides purified from glycogen by MALDI-TOF mass spectrometry	82
Figure 17. Analysis of phospho-oligosaccharides purified from glycogen and amylopectin by NMR	84
Figure 18. Total phosphate and C6 phosphate content of rabbit and mouse glycogen and amylopectin	89
Figure 19. Time-dependent incorporation of ^{32}P into synthesized glycogen by glycogen synthase	91
Figure 20. Effect of gel filtration on ^{32}P -labeled glycogen	94
Figure 21. Effect of treating ^{32}P -labeled glycogen with laforin or glucosidases	95

Figure 22. Release of $^{32}\text{P}_i$ from ^{32}P -glycogen by laforin	97
Figure 23. Effect of unlabeled UDP on ^{32}P -labeling of glycogen	99
Figure 24. Analysis of the progress of glycogen synthesis by glycogen synthase	100
Figure 25. Effect of hSCAN-1 treatment on ^{32}P -labeling of glycogen	101
Figure 26. Test for ^{32}P -UDP binding to glycogen	103
Figure 27. Skeletal muscle glycogen content	105
Figure 28. Skeletal muscle glycogen phosphate content	107
Figure 29. Total skeletal muscle glycogen phosphate	109
Figure 30. Low speed supernatant and pellet glycogen content	111
Figure 31. HPAEC analysis of skeletal muscle glycogen	113
Figure 32. Effect of exercise on AMPK phosphorylation	118
Figure 33. Effect of exercise on glycogen synthase and glycogen synthase phosphorylation	119
Figure 34. Effect of exercise on glycogen synthase and glycogen synthase phosphorylation in the LSS and LSP	120
Figure 35. Laforin protein levels in the malin knockout mice	122
Figure 36. Laforin protein levels in the LSS and LS of malin knockout mice	123
Figure 37. Effect of exercise on glycogen	125
Figure 38. Lafora bodies and response to exercise	126
Figure 39. Skeletal muscle glycogen distribution in response to exercise	127
Figure 40. Glycogen phosphate levels in response to exercise	128
Figure 41. Total glycogen phosphate in response to exercise	129
Figure 42. Skeletal muscle glycogen distribution and branching	131

LIST OF ABBREVIATIONS

AGL	Amylo-1,6-glucosidase, 4- α -glucanotransferase
AMP	Adenosine monophosphate
AMPK	AMP activated protein kinase
ATP	Adenosine triphosphate
Ba(OH) ₂	Barium hydroxide
BE	Branching enzyme
CaCl ₂	Calcium chloride
cAMP	3'-5'-cyclic adenosine monophosphate
cAZY	Carbohydrate active-enzymes
CBM20	Carbohydrate binding domain subtype 20
Ci	Curries
CK-1	Casein kinase-1
CK-2	Casein kinase-2
cpm	Counts per minute
Cys/C	Cysteine
DCC	Dicyclohexylcarbodiimide
DEAE	Diethylaminoethyl
DSP	Dual specificity phosphatase
DTT	Dithiothreitol
EDTA	Ethylenediaminetetraacetic acid
EGTA	Ethyleneglycol-O, O'-bis(2-aminoethyl)-N, N, N', N'-tetraacetic acid
Epm2a	Epilepsy progressive myoclonus type 2a
Epm2aIP	Epm2a interacting protein
Epm2b	Epilepsy progressive myoclonus type 2b
F6P	Fructose-6-phosphate
F-1,6-BP	Fructose-1,6-bisphosphate
G1	Glucose
G2	Maltose

G3	Maltotriose
G4	Maltotetraose
G5	Maltopentaose
G6	Maltohexaose
G7	Maltoheptaose
G8	Maltooctaose
GAA	Lysosomal acid- α -glucosidase
GAPDH	Glyceraldehyde-3-phosphate dehydrogenase
gHMQC	Gradient heteronuclear multiple quantum coherence
Glc	Glucose
G6P	Glucose-6-phosphate
GLUT	Sodium independent glucose transporter
Gly/G	Glycine
GN	Glycogenin
GP	Glycogen phosphorylase
G6PT	Glucose-6-phosphate translocase
G6Pase	Glucose-6-phosphatase
GS	Glycogen synthase
GSK3	Glycogen synthase kinase-3
GSD	Glycogen storage disorder
HCl	Hydrochloric acid
HClO ₄	Perchloric acid
HK	Hexokinase
HMQC	Heteronuclear multiple quantum coherence
HPAEC	High performance anion exchange chromatography
HPTLC	High performance thin layer chromatography
H ₂ SO ₄	Sulfuric acid
Hz	Hertz
I ₂	Iodide
IR	Insulin receptor
IRS	Insulin receptor substrate

kDa	Kilodalton
KH ₂ PO ₄	Potassium dihydrogen phosphate
KI	Potassium iodine
KOH	Potassium hydroxide
KOMP	Knockout mouse project repository
LDH	Lactate dehydrogenase
LB	Lafora body
LD	Lafora disease
LiCl	Lithium chloride
LSS	Low speed supernatant
LSP	Low speed pellet
MALDI	Matrix assisted laser desorption/ionization
MCT-1	Monocarboxylate transporter-1
MCT-2	Monocarboxylate transporter-2
MGSKO	Muscle glycogen synthase knockout
MS	Mass spectrometry
NaCl	Sodium chloride
NaCl	Sodium chloride
NaOH	Sodium hydroxide
NADP ⁺	Nicotinamide adenine dinucleotide phosphate
NaOAc	Sodium acetate
NH ₄ HCO ₃	Ammonium bicarbonate
NHL	NCL-1, HT2A and LIN-41
NHLRC1	NHL repeat-containing protein 1
NH ₄ OH	Ammonium hydroxide
NMR	Nuclear magnetic resonance
NP:	Number of points in the directly detected dimension
NT	Number of transients
OH	Hydroxyl
PAS	Periodic acid/Schiff
PASD	Periodic acid/Schiff diastase (α -amylase) treated

PDK-1	Phosphoinositide-dependent kinase-1
PFK	Phosphofructokinase
PGI	Phosphoglucose isomerase
PGM	Phosphoglucomutase
Ph	Phosphorylase
PIP2	Phosphatidylinositol (4,5) bisphosphate
PIP3	Phosphatidylinositol (3,4,5) triphosphate
PKA	cAMP dependent protein kinase / protein kinase A
PI3K	Phosphatidylinositol-3-kinase
PKB/Akt	Protein kinase B
PM	Plasma membrane
PMSF	Phenylmethylsulfonylfluoride
<i>p</i> NPP	<i>para</i> -Nitrophenylphosphate
PP1c	Protein phosphatase-1, catalytic subunit
PP1G	Glycogen associated phosphatase
PTG	Protein targeted to glycogen
RT	Room temperature
SDS	Sodium dodecyl sulfate
SDS-PAGE	Sodium dodecyl sulfate polyacrylamide gel electrophoresis
Ser/S	Serine
SEX4	Starch excess-4
SFRQ	Spectrometer frequency for proton nucleus
SM	Skeletal muscle
SW	Spectral width in the directly detected dimension (¹ H)
SW1	Spectral width in the indirectly detected dimension (¹³ C or ³¹ P)
TBS	Tris-buffered saline
TBST	Tris-buffered saline containing tween-20
TCA	Trichloroacetic acid
TCA cycle	Tricarboxylic acid cycle
TFA	Trifluoroacetic acid

Tris	Tris(hydroxymethyl)aminomethane
TLC	Thin layer chromatography
Trp/FIGURE	Tryptophan
Tyr	Tyrosine
THAP	2',4',6'-Trihydroxyacetophenone monohydrate
Thr/T	Threonine
TOCSY	Total correlation spectroscopy
TOF	Time of flight
Tyr	Tyrosine
Ub	Ubiquitin
UDP	Uridine diphosphate
UDP-glucose	Uridine diphosphate glucose
UGP	UDP-glucose pyrophosphorylase
UGPPase	UDP-glucose pyrophosphatase
UMP	Uridine monophosphate
UTP	Uridine triphosphate
WT	Wild type

INTRODUCTION

1. Glycogen Structure

Many organisms store excess glucose in the form of branched polymers, such as glycogen or amylopectin. Glycogen is mainly stored in the liver and skeletal muscles of mammals, which can be catabolized to individual glucose units to meet energy demands (4). Plants store glucose in the form of starch, which is composed of amylose, a long mainly unbranched glucose polymer, and amylopectin, a branched polymer of glucose. Amylopectin and glycogen are similar in that they are branched polymers of glucose. However, the branching patterns, topology and average chain length of each is different, which contributes to their distinct physical properties.

Glycogen is a highly branched polymer of glucose that is readily soluble in water and serves as an osmotically neutral means of storing glucose. Glucose residues are linked together via α -1,4 glycosidic linkages, which make up the polymer chains, and branch points are introduced by α -1,6 glycosidic linkages (Figure 1). Because of the heterogeneous structure and size of glycogen it is impossible to obtain a three dimensional structure by conventional structural techniques. However, chemical analysis of glycogen chain length and branching has led to a widely accepted model of its structure (5-7) (Figure 2). In this model, the average glucose chain length would be \sim 13 glucose residues long and would consist of inner B chains, which would be branched twice, and the outer unbranched A chains (Figure 2). On average, branch points occur about 1 in every 8-12 glucose residues, which is inconsistent with the average chain length of \sim 13 glucose residues long. However, if the outer unbranched A chains make up 50% of the total glucose then the average chain length and branching frequency are consistent with the model. Additionally, it has been calculated that a 13th tier added to glycogen would result in an impossible density of glucose. Therefore, the largest possible glycogen molecule would consist of

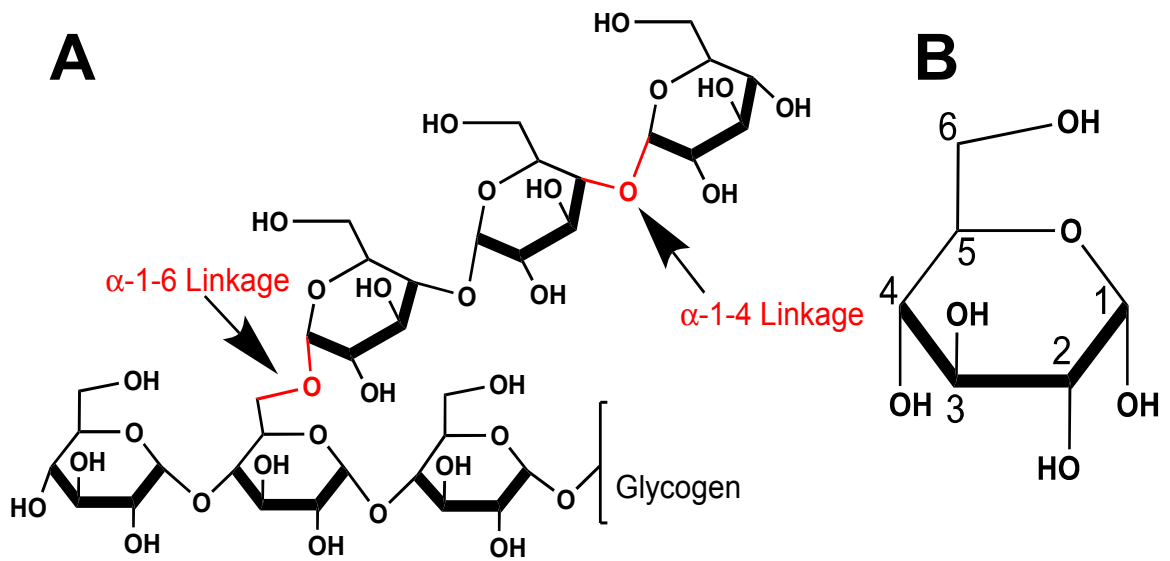


Figure 1. Glycosidic linkages. **A)** Glucose residues are linked together via α -1-,4- and α -1-6-glycosidic linkages, which make up the bulk of the polymerization of glycogen. **B)** Structure of glucose, numbers indicate the numerical nomenclature of the carbons, C1, C2, C3, C4, C5 and C6.

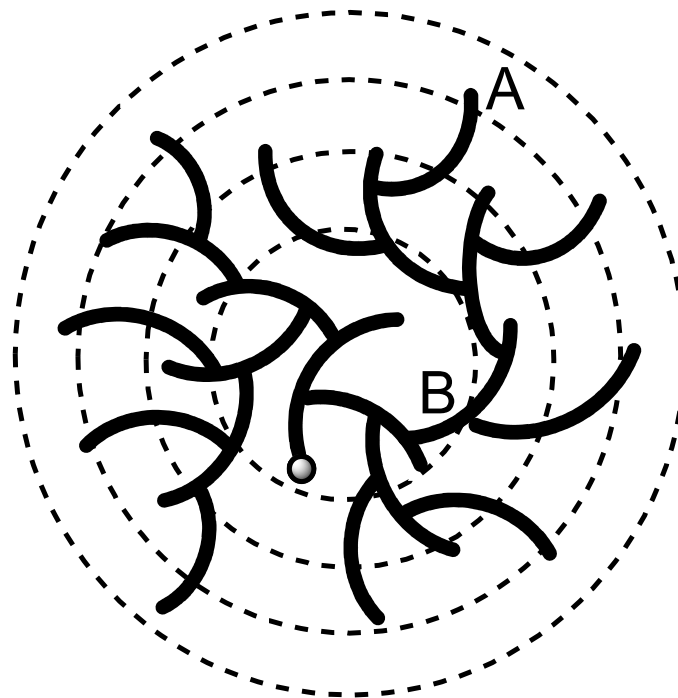


Figure 2. Glycogen structure. A portion of a glycogen molecule is shown, indicating branching pattern and tiered structure.

12 tiers, have a molecular mass of $\sim 10^7$ kDa, a diameter of ~ 44 nm and contain about 55,000 glucose residues (5,8). Interestingly, electron microscopy analysis of skeletal muscle glycogen shows that glycogen granule size is normally distributed, the average size being ~ 25 nm and the maximum size being ~ 44 nm, consistent with the proposed model of glycogen (7,9).

Although glycogen is mainly composed of glucose it also contains trace amounts of phosphate and glucosamine (10,11). There has been more research on phosphate in glycogen due to its association with a juvenile form of myoclonus epilepsy known as Lafora disease. Recent studies have shown phosphate to be present in a range from 1 phosphate per 500 – 2000 glucose residues depending on the source of glycogen (12-14). Covalently bound phosphate was originally proposed to exist as a monoester at the C6-OH and as a phosphodiester which would link the C1 to the C6 of another glucose residue, effectively forming a novel type of branch point. (2,3). Nuclear magnetic resonance (NMR) analysis of phospho-oligosaccharides purified from glycogen has shown that phosphate is located at the C2, C3 and C6 positions of glucose residues but no evidence for a phosphodiester bond has been observed (14,15). Amylopectin, also a branched polymer of glucose, contains covalently bound phosphate monoesters at the C3 and C6 positions (14,16,17). Phosphate in starch is well known and plays a role in disrupting its semicrystalline structure to allow for proper breakdown and utilization (17). However, the role of phosphate in glycogen is not well understood but excess accumulation of phosphate in glycogen has been associated with Lafora disease (12-14,18,19).

The metabolism of glycogen is dynamic and involves multiple bouts of degradation and synthesis, which could result in the accumulation of modifications, such as phosphate, throughout its lifespan. The accumulation of modifications could potentially lead to an altered structure and negatively impact its metabolism. It has been proposed that the chemical modifications in glycogen might indicate the age of the molecule and serve as signal for its disposal (3). Interestingly, in normal aging tissue poorly branched insoluble glycogen-like material, polyglucosan, accumulates and forms deposits in the brain, known as

corpora amylacea (20) and in heart as cardiac colloid (21). These observations support the idea that chemical modifications may reflect the age of the molecule and the need to dispose abnormal glycogen in order to avoid adverse outcomes.

2. Glycogen Metabolism

2.1 Overview

In mammals, the liver and skeletal muscle contain the major deposits of glycogen but other tissues such as heart, fat, kidney and brain are capable of storing glycogen. Although many of the processes involved in glycogen metabolism are similar in skeletal muscle and liver, there are significant differences that reflect metabolic flexibility along with tissue-specific enzyme isoform expression. Glucose, derived from ingested carbohydrates or from gluconeogenesis, is the major precursor for glycogen synthesis, utilized in a direct pathway, but gluconeogenic precursors, such as lactate or alanine can serve as precursors in an indirect pathway (22,23). The direct pathway begins with glucose entering cells through one or more of the glucose transporters (GLUTs) (24). Skeletal muscle takes up glucose from the bloodstream via the GLUT4 transporter, which is translocated to the plasma membrane in response to insulin signaling. In the liver and beta cells of the pancreas, GLUT2 is the major glucose transporter that allows glucose to be transported down a positive gradient between the blood stream and the tissue. Intracellular glucose is then converted to glucose-6-phosphate by hexokinase, in the muscle, and by glucokinase, in the liver. In times when nutrients intake is low, glucose that enters tissues is typically oxidized through glycolysis. However, when nutrients are plentiful excess glucose is converted to UDP-glucose through a series of enzymatic reactions (Figure 3). Following conversion to glucose-6-phosphate, glucose-1-phosphate is generated by phosphoglucomutase and converted to UDP-glucose by UDP-glucose pyrophosphorylase. UDP-glucose serves as a substrate for glycogen synthase, which transfers the glucose moiety to existing glycogen molecules or as substrate for glycogenin during *de novo* glycogen

synthesis. Bulk glycogen synthesis requires three key enzymes, glycogenin, glycogen synthase and the glycogen branching enzyme (Figure 3).

Glycogenin serves as a primer for glycogen synthesis and self-glucosylates to form an oligosaccharide primer chain (25-27). Branch points, α -1,6-glycosidic linkages are introduced by the branching enzyme. Multiple rounds of elongation by glycogen synthase and branching result in the formation of glycogen molecules and provide an efficient and osmotically neutral means of storing glucose. The regulation of glycogenin and the branching enzyme are not well understood, but glycogen synthase, the rate-limiting enzyme in glycogen synthesis, is highly regulated and many of the regulatory mechanisms are well known.

Glycogen degradation occurs by two distinct pathways. The first, known as phosphorolysis, occurs in the cytosol of cells and is mediated by the actions of glycogen phosphorylase, the rate-limiting enzyme, and the debranching enzyme (AGL). Phosphorolysis produces glucose-1-phosphate and free glucose is produced by AGL, which hydrolyzes α -1,6-glycosidic linkages and liberates a free glucose residue (28). In the liver, glycogen breakdown is stimulated by nutrient deprivation and by hormonal signaling, mainly glucagon, which results in the breakdown of glycogen to glucose for export into the blood stream. The breakdown of glycogen is initiated by conditions that elevate cAMP and Ca^{2+} levels, such as exercise (4). The second pathway for degradation occurs in the lysosome. Glycogen is transported to the lysosome, by mechanisms that are not well understood at this point, where it is directly hydrolyzed to glucose by the lysosomal α -glucosidase, also known as acid α -glucosidase (GAA) (29) (Figure 3).

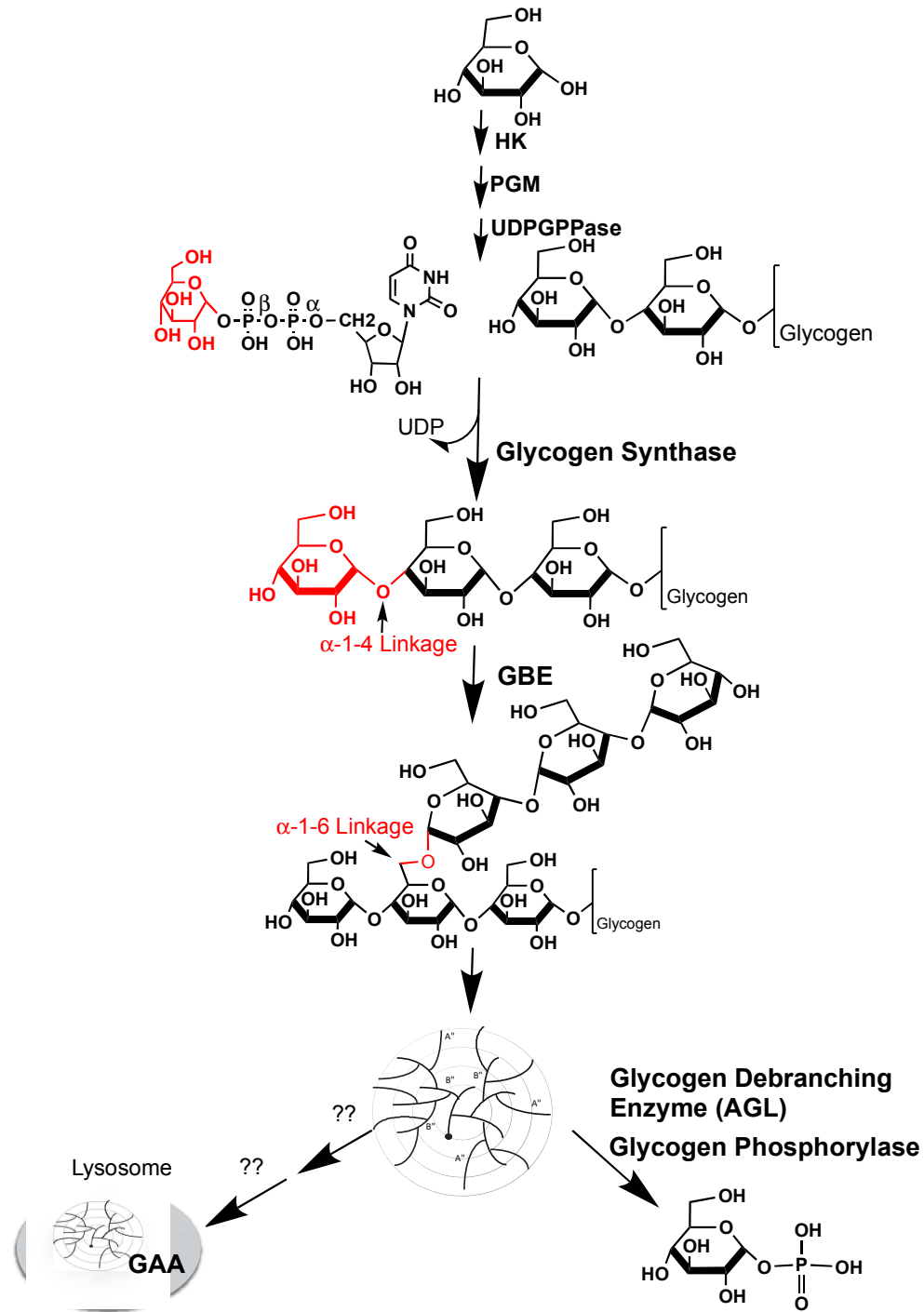


Figure 3. Glycogen metabolism. HK, hexokinase/glucokinase; PGM, phosphoglucomutase; UDPGPPase, UDP-glucose pyrophosphorylase; BE, branching enzyme; AGL, debranching enzyme; GAA, lysosomal α -glucosidase

2.2 Glycogen Metabolism, Enzymes and Regulation

2.2.1 Glycogenin

In the early 1930's the Cori's observed that *in vitro* glycogen synthesis by phosphorylase occurred only in the presence of trace amounts of glycogen, suggesting that a 'primer' was necessary for polysaccharide synthesis (30). Krisman and Barengo later proposed that the initial primer for glycogen synthesis was a protein (26). This led to the discovery of a specialized self-glycosylating enzyme, glycogenin, that was found to be necessary for the initiation of glycogen synthesis (31,32). Glycogenin can be co-purified with glycogen synthase from rabbit muscle (27) and is found covalently bound to glycogen from muscle (33) and liver glycogen (34).

Glycogenin is a member of the family 8 retaining glycosyltransferases (35,36), which serves as a primer for glycogen synthesis. Humans have two genes that encode glycogenin, *GYG1* and *GYG2* (37) whereas rodents only have a single gene (38,39). *GYG1* is widely expressed while *GYG2* is mainly expressed in the liver, heart and to a lesser extent pancreas of humans (37). Glycogenin from rabbit muscle is the most studied form of the enzyme, but the corresponding human enzyme is 90% identical in amino acid sequence (40). A crystal structure of glycogenin from rabbit muscle has been solved and shows that the enzyme functions as a dimer (41).

Glycogenin catalyzes two distinct reactions: the first involves glucosylation of Try194 through the formation of the α -C1-O-tyrosyl linkage, using UDP-glucose as the glucose donor, and the second is the subsequent addition of glucose residues, forming α -1,4-glycosidic linkages, which can be extended to a length of 10—20 glucose residues (33,42-44). For the initiation of bulk glycogen synthesis, glycogenin interacts directly with glycogen synthase through a conserved amino acid sequence in its C-terminus. Glycogen synthase is then able to associate with the glucosyl-primer and elongate the nascent polyglucose chain

There are no known modes of regulating glycogenin at this time. However, Roach and colleagues proposed that glycogenin could be regulated by glucose

(45). When overexpressing glycogenin in COS cells and in the presence of high glucose, they observed an increased molecular weight of glycogenin, suggesting that glucose might initiate glycogen synthesis by controlling the glucosylation state of glycogenin (46) (32).

2.2.2 Branching Enzyme

Branch points are formed by the branching enzyme which excises an oligosaccharide from glycogen by hydrolyzing an α -1,4-glycosidic linkage and forming a new α -1,6-glycosidic linkage between the excised oligosaccharide and an existing chain within glycogen (47,48). The frequency of branching determines the topology and solubility properties of glycogen molecules and is what distinguishes glycogen from amylopectin. For example, glycogen has branch points every \sim 12 glucose residues and amylopectin has branch points every \sim 30 glucose residues. In mammals, the glycogen branching enzyme is encoded by the *GBE1* gene, which operates as a monomer and has a predicted Mr of 81.5 KD (47). The glycogen branching enzyme contains a domain similar by sequence (residues 222-568) to α -amylase and a smaller region (residues 73-168) similar to polysaccharide-modifying enzymes that act on branched structures (49). The mechanism for the branching enzyme is a two step reaction that involves the catalytic amino acids Asp 357 and Glu 412 (50). The branching of glycogen is critical in maintaining its solubility and function. Defects in the branching enzyme lead to formation of poorly branched and insoluble glycogen-like material known as polyglucosan and is associated with glycogen storage disease type IV. However, not much is known about its regulation.

2.2.3 Glycogen Synthase and Regulation

Glycogen synthase is the rate-limiting enzyme in glycogen synthesis and is highly regulated. Glycogen synthase is responsible for the formation of glucose polymer chains by forming the α -1,4-glycosidic linkages by transferring glucose residues from UDP-glucose to the non-reducing end of existing glycogen molecules or to the oligosaccharide attached to glycogenin. The enzyme is negatively regulated by phosphorylation and allosterically activated by glucose-6-phosphate, which can completely restore the activity of the enzyme in the

phosphorylated state (28). In fact, glycogen synthase was the third enzyme discovered that is regulated by reversible phosphorylation (51). *In vitro* assays take advantage of the allosteric activation of glycogen synthase by glucose-6-phosphate by assaying for its activity in the presence and absence of glucose-6-phosphate, which gives an activity ratio that can be used as indication of its phosphorylation status (52).

Glycogen synthase belongs to the family 3 retaining glycosyltransferases (GT3) and mammals have two isoforms of the enzyme encoded by *GYS1* and *GYS2*, with *GYS1* expressed in skeletal muscle and many other cells while *GYS2* expression is restricted to the liver (28). *GYS2* is 70% identical in sequence to the muscle isoform (53,54). The yeast, *Saccharomyces cerevisiae*, also contains two genes that encode for glycogen synthase, *Gsy1* and *Gsy2*, with *Gsy2p* being the predominant protein isoform. It has ~50% sequence identity to the human enzyme (55). Based on sequence identity, the skeletal muscle isoform seems to be conserved between mammals, for example human and rabbit skeletal muscle glycogen synthases are 97% identical (56).

Rabbit skeletal muscle glycogen synthase, which was initially the most studied enzyme, contains 9 serine phosphorylation sites, clustered at the N- and C- termini, that can be phosphorylated *in vivo* (57). The sites, 1a, 1b, 2, 2a, 3a, 3b, 3c, 4 and 5 correspond respectively to amino acids 697, 710, 7, 10, 640, 644, 648, 652, and 656. Yeast glycogen synthase also contains phosphorylation sites but lacks the phosphorylation sites at its N-terminus (58). Studies on glycogen synthase phosphorylation have led to the concept of hierarchical phosphorylation (59,60), where the phosphorylation of one site promotes the phosphorylation of a secondary site. Several protein kinases are capable of phosphorylating glycogen synthase *in vitro*: glycogen synthase kinase-3 (GSK3) (61,62), phosphorylase kinase (PhK) (63), cAMP dependent protein kinase (PKA) (64), protein kinase-CK1 (previously known as casein kinase 1) (CK1) (65,66), protein kinase-CK2 (CK2) (67), AMP activated protein kinase (AMPK) (68), PAS kinase (69), DYRK1A (70) and p38 MAPK (71). An example of hierarchical phosphorylation comes from *in vitro* studies where site 2 can be phosphorylated by cyclic AMP-

dependent kinase (64) and phosphorylase kinase (63), which then allows for the phosphorylation of site 2a by casein kinase 1 but only when site 2 is phosphorylated (65). Additionally, mutation of site 2 prevents phosphorylation of site 2a in COS cells, which is consistent with the idea of hierarchical phosphorylation (72). The skeletal muscle isoform of glycogen synthase, *GYS1*, contains 7 phosphorylation sites at its C-terminus while the liver isoform, *GYS2*, has 5 phosphorylation sites and is lacking the 1a and 1b sites found in *GYS1*. Phosphorylation of the 3a and 3b sites have been found to have the largest effect on enzyme activity (57). These regulatory sites can be phosphorylated by glycogen synthase kinase-3 (GSK3), *in vitro*, by the hierarchical and sequential phosphorylation of sites 4, 3c, 3b, and 3a (60,61,67). Phosphorylation of site 5 by casein kinase II results in a recognition motif –S-X-X-X-S(P) (where X can be any amino acid) for GSK3, which primes glycogen synthase for sequential phosphorylation of sites 4, 3c, 3b and 3a (62,67). However, cell based experiments, where the GSK3 recognition sites were mutated from serine to alanine, have demonstrated that glycogen synthase can still be phosphorylated at sites 3a or 3b, suggesting that other kinases are able to phosphorylate glycogen synthase at those sites (73). A member of the dual-specificity tyrosine phosphorylated and regulated protein kinase, DYRK1A, was purified from rabbit skeletal muscle and shown to be a site 3a kinase (70). Additionally, a site 3a kinase, PAS kinase (69), was identified based on an ortholog in *S. cerevisiae* and found to be required for normal maintenance of glycogen stores (74).

Dephosphorylation and activation of glycogen synthase is mediated by members of a family of glycogen-associated protein phosphatases (PP1Gs) that are composed of a catalytic subunit (PP1C) bound to a glycogen-targeting (G) subunit (75,76). Regulatory G subunits contain carbohydrate-binding domains, which localize them to glycogen and recruit the catalytic PP1C subunits, thus allowing the complex to dephosphorylate substrates, such as glycogen synthase (77). Biochemical and bioinformatics analysis have identified seven glycogen-targeting subunits (75,76). Of the seven identified, three have been extensively studied. The R_{GL} or GM subunit is mainly expressed in the skeletal muscle and

heart (78). Expression of the G_L subunit is found mainly in the liver and its expression is induced by insulin (79,80). A more ubiquitously expressed subunit, the protein targeting to glycogen (PTG) or (R5) is expressed in several insulin-sensitive tissues, such as skeletal muscle, liver and fat (80). Less is known about the other family members but they seem to have roles in glycogen metabolism and some are highly expressed in brain (81).

There are crystal structures for two eukaryotic glycogen synthase enzymes, *S cerevisiae* (82) and *Caenorhabditis elegans* (83). The *C. elegans* glycogen synthase structure was solved in complex with 34 amino acids of the C-terminus of human glycogenin, and is superimposable with the basal state of the yeast enzyme. Interestingly, structures of the yeast enzyme have been solved for the intermediate state and the glucose-6-phosphate activated state (82). The binding of glucose-6-phosphate to an arginine rich region of the C-terminus induces structural changes that allow for more efficient binding of substrates and catalysis. Recently, a crystal structure of a mutant yeast enzyme, which based on kinetic data mimics a phosphorylated state of the enzyme, has been solved and shows structural changes that occur when the enzyme is in an inhibited state (84).

The dynamic process for activation and inactivation of glycogen synthase is necessary to maintain proper stores of glycogen and to release stored glucose in an appropriate manner. Excessive activation of glycogen synthase results in the aberrant structure and over accumulation of glycogen in mice that overexpress skeletal muscle glycogen synthase (85). Defects in glycogen synthase or lack of glycogen synthase leads to glycogen storage disease type 0 (86-89). Additionally, Irimia et al demonstrated the importance of liver glycogen stores in maintaining whole body glucose homeostasis and that mice lacking liver glycogen synthase physiologically mimic glycogen storage disease type 0 (90).

2.2.4 Glycogen Phosphorylase

Phosphorylase catalyzes the phosphorolysis of α -1,4-glycosidic linkages to generate glucose-1-phosphate and stalls four glucose residues from an α -1,6-glycosidic linkage. In mammals, it is widely expressed and tissue specific

isoforms, liver, skeletal muscle, and brain, have been identified (91,92). The skeletal muscle and liver isoforms are thought to dominate in their specific tissues, but there is some evidence for expression of multiple isoforms in the same tissue (93). The liver isoform is ~83% identical to the skeletal muscle isoform (93). Like glycogen synthase, rabbit skeletal muscle glycogen phosphorylase has been extensively studied and shares a 97% amino acid identity with the human muscle ortholog (91,92,94). A three-dimensional structure of glycogen phosphorylase is known and much effort has been made to relate mechanistic catalysis and regulation to the structure of the enzyme (92,95-97). Like glycogen synthase, glycogen phosphorylase is regulated by reversible phosphorylation and by allosteric ligands. The enzyme undergoes structural changes between the less active T state and a more active R state, which is dependent on its phosphorylation status and the binding of allosteric ligands (94,98).

Phosphorylation of glycogen phosphorylase, unlike glycogen synthase, occurs at a single site and activates the enzyme. In fact, phosphorylase was the first enzyme shown to be controlled by both covalent and allosteric modifications (99-101). Phosphorylase kinase is responsible for the phosphorylation of glycogen phosphorylase at Ser14 (102,103). Phosphorylase kinase is thought to be activated by two primary mechanisms, phosphorylation by cAMP-dependent protein kinase and by increased cellular Ca^{2+} levels (104,105). During exercise or epinephrine signaling intracellular Ca^{2+} and cAMP levels increase, which causes activation of cyclic AMP-dependent protein kinase and results in the phosphorylation of phosphorylase kinase thus allowing for activation of glycogen phosphorylase (104,106,107). The phosphorylated form of phosphorylase can be fully activated by binding of AMP. The binding affinity for AMP is increased when the enzyme is phosphorylated and occurs at a major allosteric binding site. The liver isoform shares similar properties with regards to regulation, but is not as readily activated by AMP (92). The ratio of the phosphorylase activity, in the presence or absence of AMP, is used as a kinetic index for its activity status (108). Dephosphorylation of skeletal muscle glycogen phosphorylase and

phosphorylase kinase is mediated by glycogen associated protein phosphatases containing a glycogen targeting subunit, such as R_{GL} or PTG.

2.2.5 Debranching Enzyme

Glycogen breakdown is accomplished by the coordinated actions of glycogen phosphorylase and the debranching enzyme (AGL), which is responsible for the hydrolysis of α -1,6-glycosidic linkages. The enzyme has two catalytic activities in two domains. The N-terminal domain has α -amylase-like activity, which hydrolyzes an α -1,4-glycosidic linkage and transfers a maltotriose unit from the four glucose residues left by phosphorylase, to the main chain of glucose residues via an α -1,4-glycosidic linkage. The remaining glucose at the branch point is hydrolyzed by the C-terminus of AGL, which contains a domain with amylo-1,6-glucosidase activity that hydrolyzes the α -1,6-glycosidic linkage to liberates a free glucose residue. Little is known about the regulation of AGL but defects in the enzyme lead to Type III glycogen storage disease or Cori's disease, which is characterized by the formation of abnormal glycogen with short outer chains.

3. Insulin Signaling and Glycogen Metabolism

Insulin is the primary hormone responsible for driving glycogen synthesis in skeletal muscle (Figure 4). Impairments in insulin signaling or insulin secretion are associated with impaired glycogen metabolism, which occurs in the diabetic state (109). Besides glycogen synthesis, insulin promotes the uptake of glucose in insulin sensitive tissues, inhibits hepatic gluconeogenesis, promotes fat synthesis and protein synthesis. Insulin secretion, by the β -cells, occurs when blood glucose levels increase post-prandially, and once in the blood stream it binds to the insulin receptor found on the plasma membrane of insulin sensitive cells. The insulin receptor consists of two subunits, α and β , with the α subunit on the extracellular side of the plasma membrane. Binding of insulin to the α subunit causes a conformational change that activates a tyrosine kinase domain on the β -subunit, which autophosphorylates a series of its own tyrosine residues promoting the phosphorylation of insulin receptor substrates. There are four

members of the insulin receptor substrate (IRS) family that are phosphorylated on tyrosine residues by the activated insulin receptor (110). In addition to IRS family members, Shc adapter proteins and SIRP family members are also phosphorylated. The phosphorylation of tyrosine residues on IRS-1 forms docking sites for proteins that contain SH2 (Src-homology-2) domains (111), such as the p85 regulatory subunit of phosphatidylinositol-3 kinase (PI3K). Phosphorylation of IRS-1 promotes the activation of PI3K and the production of phosphatidylinositol-3,4,5-triphosphate (PIP3) by phosphorylating phosphatidylinositol-4,5-bisphosphate.

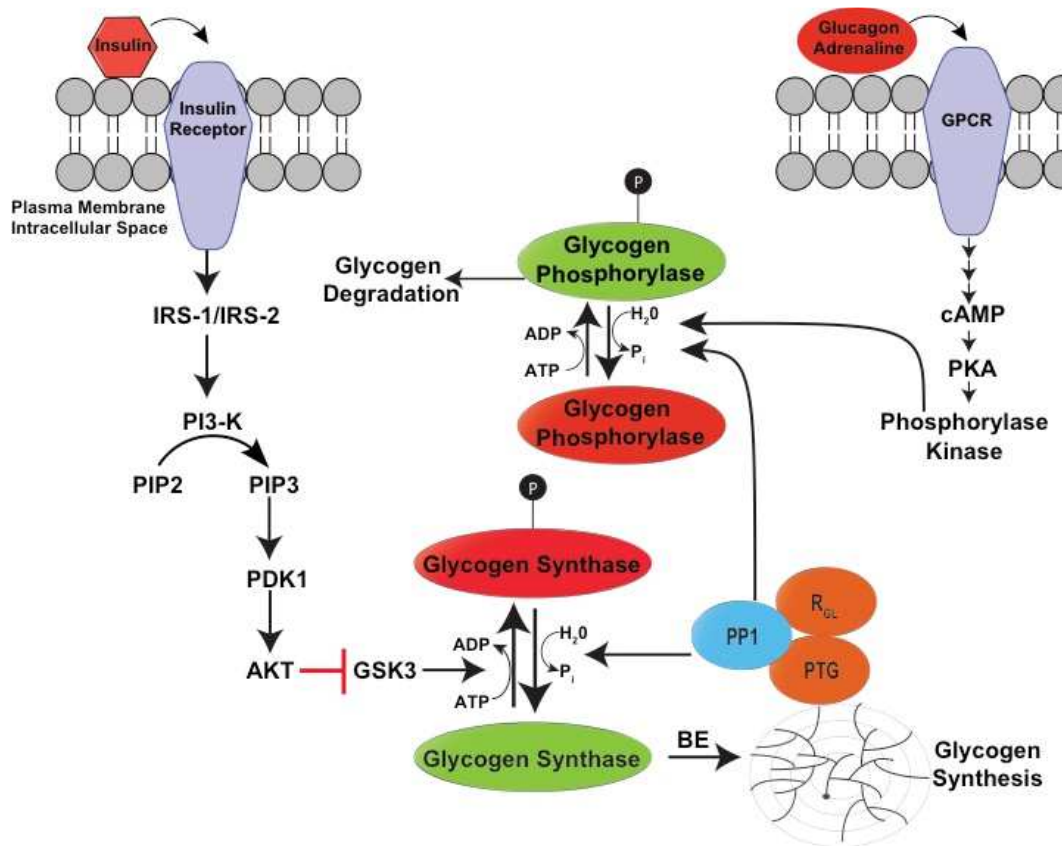


Figure 4. Regulation of glycogen metabolism. Schematic represents major signaling pathways that regulate glycogen metabolism. GSK3, glycogen synthase kinase 3; PIP2, phosphatidylinositol-4-5-bisphosphate; PIP3, phosphatidylinositol-3-4-5-bisphosphate; PI3-K phosphatidylinositol kinase; PP1, protein phosphatase 1.

PIP3 binds to and activates the protein kinase PDK1, which in turn phosphorylates and activates the protein kinase Akt (112). Akt, a major signaling kinase, once activated, can phosphorylate glycogen synthase kinase-3 (GSK3), which is a negative regulator of glycogen synthase. Therefore, the phosphorylation of GSK-3 through insulin signaling prevents the phosphorylation of glycogen synthase and allows for increased activity of glycogen synthase.

Glycogen associated phosphatases also play a role in the hormonal control of glycogen synthase. In skeletal muscle, it had been proposed that insulin signaling involves a protein phosphatase 1 containing the glycogen binding subunit R_{GL} (113) but these results were later shown to be incorrect (114). Studies in mice lacking the R_{GL} subunit showed that glycogen synthase was still activated by insulin (115), suggesting that other mechanisms or phosphatases are involved in regulating glycogen synthase during insulin signaling. The protein targeting to glycogen, PTG has also been implicated in insulin control of glycogen synthase (116,117).

4. Regulation of Glycogen Metabolism by Epinephrine and Glucagon

Epinephrine and glucagon promote glycogen degradation, with epinephrine mainly acting on the muscle and glucagon on the liver (Figure 4). Epinephrine binds to β -adrenergic receptors and induces a signaling cascade that activates adenylyl cyclase, which converts ATP to cAMP. The production and increased concentration of cAMP activates protein kinase A (PKA) by binding to the regulatory subunit and releasing the catalytic subunit. PKA, once activated, can phosphorylate a large number of target proteins, one of which is phosphorylase kinase. In response to epinephrine signaling phosphorylase kinase is phosphorylated by PKA on its α and β subunits, which activates the enzyme and allows it to phosphorylate phosphorylase on Ser¹⁴ to activate it as described above. Glucagon and epinephrine signaling also inhibits glycogen synthesis through PKA dependent phosphorylation of glycogen synthase (118-121). Epinephrine signaling has been associated with the PKA dependent phosphorylation of PP1 inhibitory protein, inhibitor 1 (122). In the liver glucagon

signaling increases cAMP and causes the activation of PKA, which in turn promotes the phosphorylation and activation of glycogen phosphorylase, inhibits glycogen synthesis by binding to G_L and inhibits phosphatases that target glycogen synthase, effectively promoting glycogenolysis and inhibiting glycogen synthesis (123,124).

5. Regulation of Glycogen Metabolism by Exercise

Glycogen serves as a major source of energy during muscle activity and is critical for prolonged exercise endurance (125,126). It is well established that the ability for muscle to perform is seriously compromised when glycogen stores are depleted even when other fuel sources are available (126). The most recognized theory for the association between impaired muscle contraction and reduced glycogen stores is that glycogen is an essential substrate, and its depletion results in a decreased rate of ATP regeneration (125). There has been a great deal of research into the exact mechanisms that regulate glycogen metabolism during exercise and much progress has been made, but the exact mechanism still remain elusive.

Glycogen is catabolized during exercise and is utilized locally to meet energy demands in the skeletal muscle while breakdown in the liver results in the export of glucose to maintain blood glucose levels (Figure 5). Following a bout of exercise glycogen stores must be replenished, which involves the activation of glycogen synthase. Experimentally, and depending on the experimental conditions, it has been observed that glycogen synthase can either be activated or inactivated during exercise (127,128).

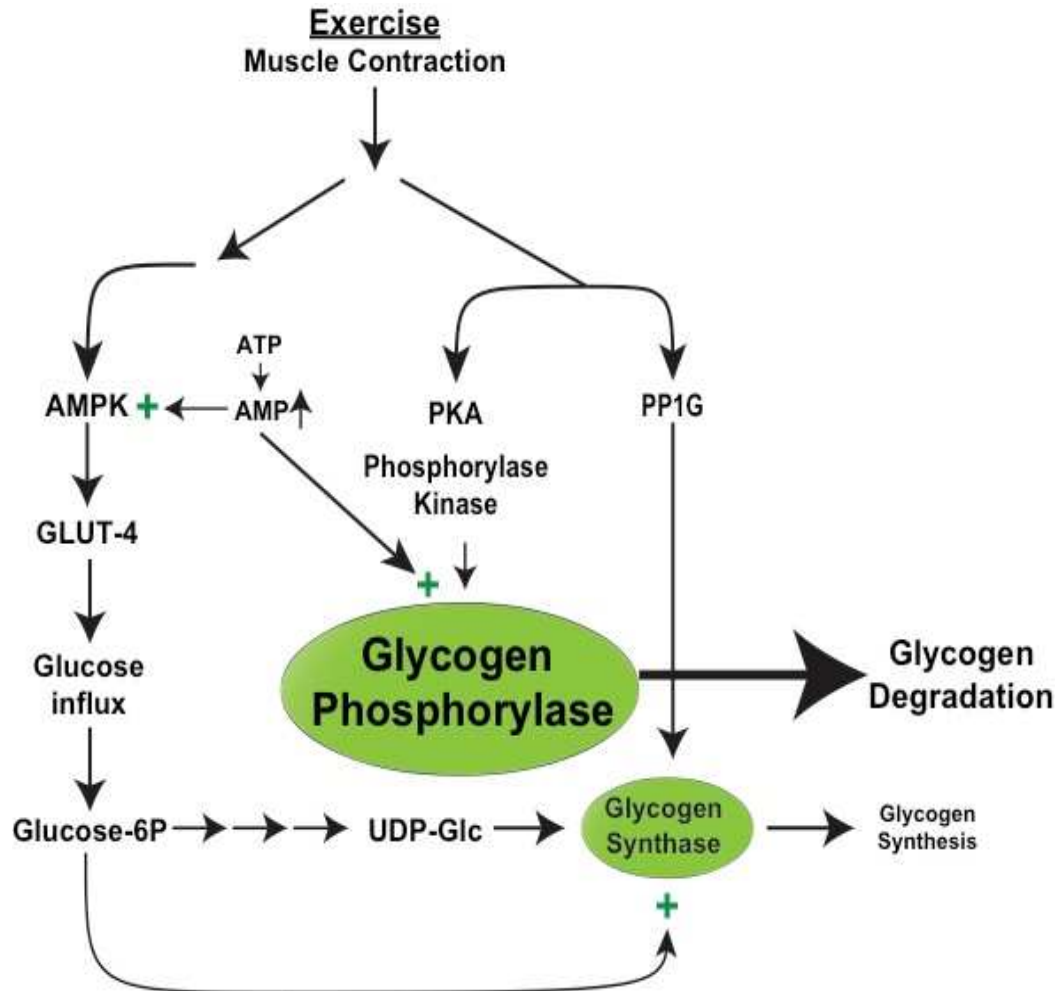


Figure 5. Regulation of Glycogen Metabolism by Exercise. Schematic represents pathways responsible for glycogen metabolism in response to exercise. AMPK, AMP activated kinase; GLUT-4, glucose transporter-4, PKA, protein kinase-A; Glucose-6P, glucose-6-phosphate; UDP-Glc, uridine diphosphate glucose; PP1G, protein phosphatase type 1 associated with glycogen; +, indicate allosteric activators.

It has also been observed that glycogen synthase can be activated post exercise (127). Activation of glycogen synthase during exercise can be viewed as paradoxical since there is an overall net loss of glycogen during exercise. There are three possible explanations for the activation of glycogen synthase during exercise. One is that activation of glycogen synthase 'primes' the enzyme for rapid glycogen synthesis once muscle contraction has decreased. The second explanation would involve other factors besides phosphorylation to inhibit the enzyme to prevent 'futile cycling' of glycogen. The third reason for the activation of glycogen synthase during exercise would be to actually synthesize and utilize glycogen during exercise (129).

The exact mechanism for glycogen synthase regulation during exercise is not clear. However, there is a consensus that it differs from insulin-mediated regulation (127). Mice with muscle specific insulin-receptor knockout show that glycogen synthase can be activated by exercise (130). Mice with inactive mutation on GSK3 were generated to investigate the role GSK-3 plays in insulin and Wnt signaling by generating knockin mice where the Akt phosphorylation sites were mutated, GSK3 α (Ser21) and GSK-3 β (Ser9) were changed to alanine (131). The authors determined, in muscle, that GSK-3 β is the major enzyme that regulates glycogen synthase in response to insulin signaling. However, muscle contraction induced activation of glycogen synthase remained normal suggesting that exercise activates glycogen synthase by a different mechanism, possibly through the G_M/R_{GL}-PP1 complex since activation of glycogen synthase by exercise or by *in situ* electrical stimulation is blocked in mice lacking the PP1 glycogen targeting subunit R_{GL}(132). However, how R_{GL} is regulated is not known. Additionally, it has been observed that glycogen synthase can be phosphorylated by exercise at sites 2 and 2a (128). However, upon more prolonged exercise, sites 3a and 3b can be dephosphorylated, which would result in activation of the enzyme (133). Site 2, *in vitro*, serves as a substrate for a variety of kinases, some of which could be activated by muscle contraction (128) One such kinase could be AMPK. A possible role for AMPK as a site 2 kinase has been investigated. AMPK is activated under exercise conditions (134) and when ATP

levels decrease (135). Additionally, AMPK is viewed as a cellular energy sensor. It has been proposed that AMPK bound to the outer chains in glycogen, via its CBM20 domain on the β -subunit, could be active and able to phosphorylate glycogen synthase (136,137). There seems to be a correlation between AMPK activation and decreases in glycogen content, particularly in muscle under exercise conditions (134). However, studies of Hampshire pigs (138) or humans with mutations in the *PRKAG2* gene, that encodes the $\gamma 2$ non-catalytic subunit of AMPK (139), where AMPK is more active, indicated an accumulation of glycogen in the skeletal muscle of the pigs and in the heart of the humans, suggesting the opposite, that AMPK is not a negative regulator of glycogen synthase.

Although the regulation of glycogen synthase remains complex and not fully understood, the regulation of glycogen phosphorylase is well established. Breakdown of glycogen during exercise is mediated by glycogen phosphorylase, resulting in the phosphorolysis of α -1,4 glycosidic linkages and the release of glucose-1-phosphate. During exercise, ATP is consumed and AMP levels increase. Glycogen phosphorylase is allosterically activated by AMP, which would result in the degradation of glycogen. Additionally, during muscle contraction Ca^{2+} levels increase, which binds to the δ subunit (calmodulin) of phosphorylase kinase and participates in allosteric control by relieving autoinhibition of the γ subunit. Additionally, cAMP levels increase during exercise resulting in the phosphorylation and activation of phosphorylase kinase by PKA, which activates phosphorylase kinase. During exercise there is a paradoxical activation of glycogen synthase and the activation of glycogen phosphorylase that results in the decrease of glycogen levels, which is utilized to meet energy demand. Figure 5 shows an overview of glycogen metabolism and exercise

6. Glycogen Storage Diseases

Glycogen storage diseases (GSDs) or glycogenoses are rare inherited disorders of glycogen metabolism that result in alterations of amounts and/or structure of glycogen (Figure 6). Mutations that affect either glycogen synthesis, degradation or enzymes whose products are involved with glycogen metabolism

result in GSDs and mainly affect the liver, skeletal muscle and heart although other tissues may also be affected.

6.1. Glycogen storage disease type 0

Glycogen storage disease type 0 is caused by mutations in the *GYS2* gene, the liver isoform of glycogen synthase. The mutations are autosomal recessive and result in fasting hypoglycemia that is present in infancy. Patients have postprandial hyperglycemia hyperlactatemia, hyperlipidimia along with high blood ketones, low alanine and lactate concentrations (88). Mice lacking the *Gys2* gene have a similar phenotype to human patients, although not as severe, but they have a 95% reduction in liver glycogen content, develop mild hypoglycemia, have impaired insulin suppression of endogenous glucose production and have an elevated rate of gluconeogenesis (90). More recently mutations in the muscle isoform *GYS1*, have been reported in humans (86,87,89) (90). In humans, mutations in *GSY1* result in cardiomyopathy and exercise intolerance (87), which is in contrast to the phenotype of mice lacking *Gsy1* which have no impaired ability to exercise (140)

6.2. Glycogen Storage Disease Type I: von Gierke Disease

The most common of the GSDs is glycogen storage disease type I or von Gierke Disease, resulting from mutations in the *G6PC* and *G6PT* genes, which encode glucose-6-phosphatase and glucose-6-phosphate translocase (G6PT) respectively, and characterized by the accumulation of glycogen and fat in the liver and kidneys. The disease results in hypoglycemic seizures, hepatomegaly, growth retardation and severe lactic acidosis (141). In the absence of glucose-6-phosphatase, which hydrolyzes glucose-6-phosphate to glucose, glucose is not transported out of the liver to maintain blood glucose levels in the fasted state.

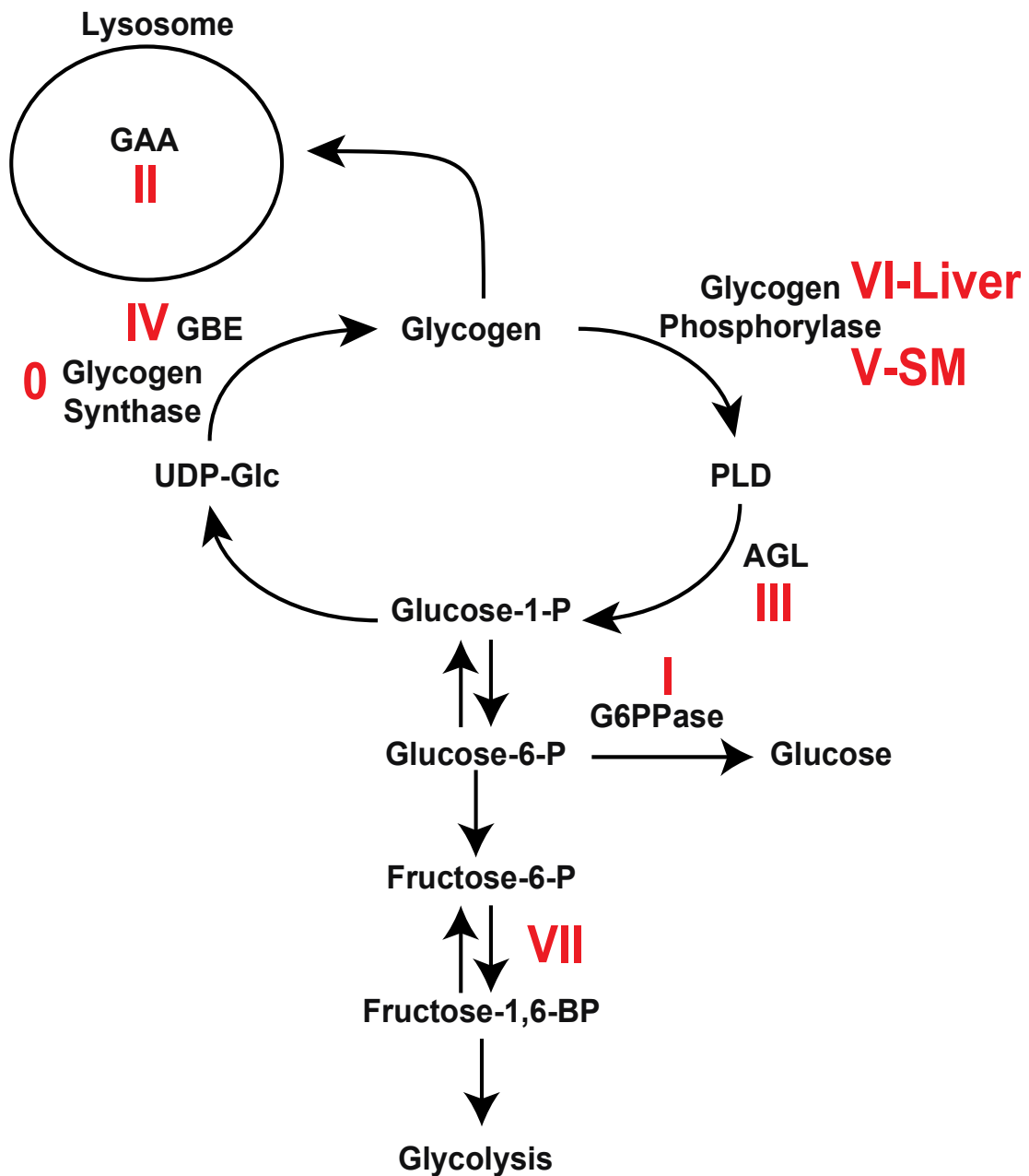


Figure 6. Glycogen Storage Diseases. Schematic of glycogen metabolism and some of the glycogen storage diseases (GSD), represented by Roman numerals. GAA, lysosomal enzyme, acid α -glucosidase; GBE, glycogen branching enzyme; UDP-glc, uridine diphosphate glucose; PLD, phosphorylase limit dextrin; AGL, glycogen debranching enzyme; G6PPase, glucose-6-phosphatase.

G6PT is involved in the terminal steps of gluconeogenesis and glycogenolysis where cytoplasmic glucose-6-phosphate is transported to the lumen of the endoplasmic reticulum by G6PT to be dephosphorylated by glucose-6-phosphatase (142). Loss of G6PT results in the same phenotype as loss of glucose-6-phosphate (142).

6.3. Glycogen storage disease type II: Pompe Disease

Mutations in the lysosomal enzyme, acid α -glucosidase (GAA), result in the accumulation of glycogen in the lysosomes of heart and skeletal muscle and leads to GSDII. Patients with Pompe Disease mutations in the *GAA* gene develop cardiomegaly, cardiomyopathy, hypotonia, muscle weakness, failure to thrive, which is dependent on the severity of the mutations, and death can occur within the first year of life (143) (144). The acid- α -glucosidase enzyme is localized in the lysosome and is responsible for the lysosomal catabolism of glycogen. The enzyme does not participate in the cytosolic degradation of glycogen. Mice lacking the *GAA* gene have a similar phenotype to the human disease. However, the symptoms develop later in life and they do not die (145). Interestingly, mice lacking both *GAA* and *GYS1* have a marked reduction in the heart and skeletal muscle glycogen levels, reduced lysosomal swelling and a complete reversal of the cardiomegaly (146).

6.4. Glycogen Storage Disease Type III: Cori Disease

Cori's disease is caused by infantile autosomal mutations in the *AGL/DBE* gene that leads to defects in the glycogen debranching enzyme, AGL (147). Symptoms usually present themselves during infancy with hypoglycemia and failure to thrive. The disease is characterized by accumulation of glycogen with shorter branches in the liver, muscles and heart (147).

6.5. Glycogen Storage disease Type IV: Andersen Disease

Mutations in the *GBE1* gene, which encodes the glycogen branching enzyme, results in one of the most severe of the GSDs, GSD IV or Andersen's

disease (148). Patients have symptoms of hepatosplenomegaly, failure to thrive and cirrhosis of the liver (149). There are several subtypes of GSD IV that have been recognized, but the phenotype is a continuum that ranges from mild to severe (150). Since the glycogen branching enzyme is responsible for introducing branch points into glycogen, patients with Andersen disease develop poorly branched insoluble glycogen, also known as polyglucosan that accumulates in the muscle and liver.

6.6. Glycogen Storage Disease Type V: McArdle Disease

McArdle disease was identified as a glycogenolytic defect in the muscle due to the absence of muscle phosphorylase (151,152) resulting from mutations in the *PYGM* gene, which encodes the muscle glycogen phosphorylase isoform. The disease is characterized by exercise intolerance and muscle cramps in childhood or adolescence. Patients may experience transient myoglobinuria after bouts of exercise, which is due to rhabdomyolysis. In some cases severe myoglobinuria may lead to acute renal failure (153). However, the disease is relatively benign and patients may report muscle weakness, myalgia, and lack of endurance during childhood or adolescence (154).

6.7. Glycogen Storage Disease Type VI: Hers Disease

Glycogen storage disease type VI is caused by mutations in the *PYGL* gene, which encodes the liver isoform of glycogen phosphorylase. The disease is characterized by hypoglycemia, hyperlipidemia, hyperketosis, hepatomegaly and growth retardation (155).

6.8. Glycogen Storage Disease Type VII: Tarui Disease

Tarui disease is caused by mutation in the *PFKM* gene, which encodes the muscle form of phosphofructokinase. Phosphofructokinase is a rate limiting enzyme in glycolysis that catalyzes the phosphorylation of fructose-6-phosphate and generates fructose-1,6-bisphosphate. Loss of function leads to the accumulation of glycolytic intermediates, such as glucose-6-phosphate. The build

up of glucose-6-phosphate can allosterically activate glycogen synthase and lead to an over-accumulation of glycogen (156).

7. Lafora Disease

Lafora Disease is a fatal juvenile form of progressive myoclonus epilepsy, with onset usually occurring in the teenage years followed by death within ten years after diagnosis (157,158). Gonzalo Lafora first described Lafora disease over a century ago, from an autopsy of a patient with teenage-onset myoclonus epilepsy with associated dementia (159). A hallmark and diagnosis marker of Lafora Disease is the presence of Lafora bodies, which were described by Lafora as a material that stained positive for starch in the ganglion cells, also known as amyloid bodies (Figure 7). Lafora bodies are mainly composed of polyglucosan, poorly branched insoluble glycogen-like carbohydrate found in the brain, skeletal muscle and heart. Their presence in the brain is considered to be causative of the disease (20,160-162). Patients present stimuli-sensitive grand mal, absences, visual and myoclonic seizures, which progress to dementia, cerebellar ataxia, psychosis, amaurosis and muscle wasting (163-167). Autosomal recessive mutations in either the *EPM2A* or *EPM2B* genes, which encode laforin and malin respectively, account for ~90% of Lafora Disease cases (168).

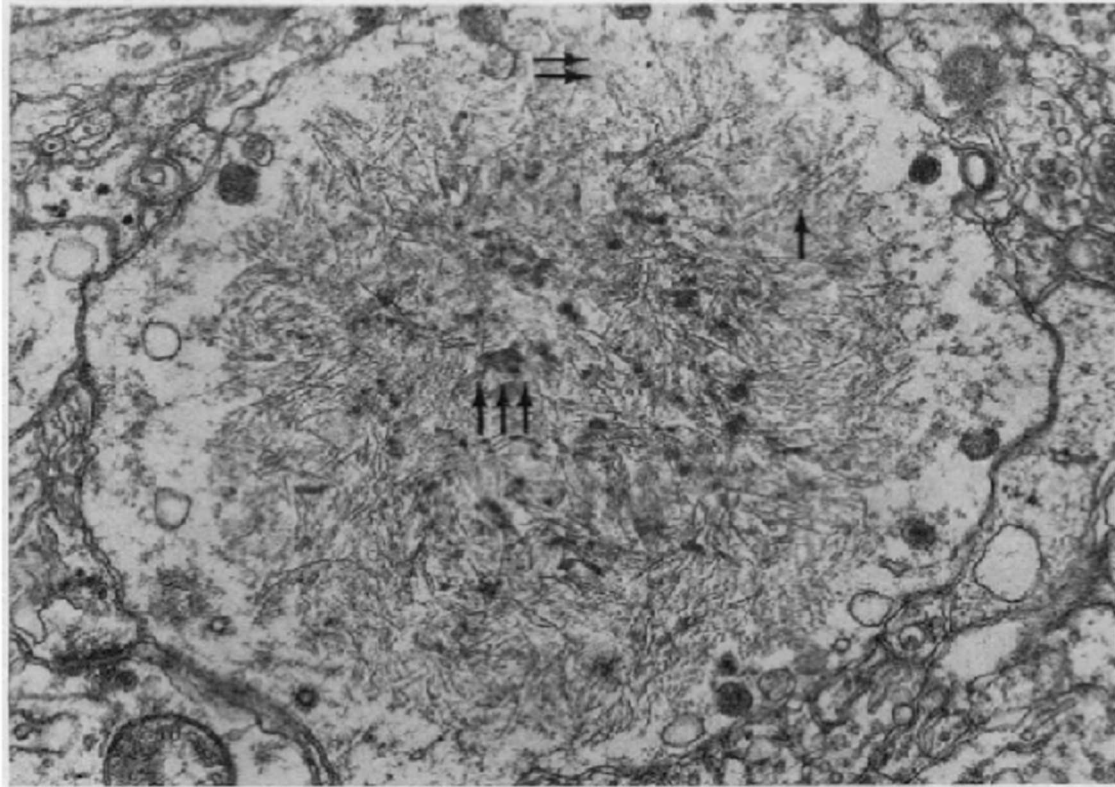


Figure 7. Lafora Body. Electron micrograph of a Lafora body in the center of an unidentified process. Single arrows represent filamentous material, double arrows represent amorphous material and triple arrows represent high electron density material (1).

7.1. Laforin

Lafora Disease patients have either homozygous or compound heterozygous loss of function mutations in laforin (169). Laforin is conserved among vertebrates and in a small group of protists that are able to produce floridean starch, a carbohydrate that resembles amylopectin (170,171). Expression of laforin in mammals is ubiquitous with the highest levels of expression in the skeletal muscle, liver, kidney, heart and brain, which are also the tissues that develop Lafora bodies (172,173). Based on primary structure, laforin belongs to the dual specificity protein phosphatase (DSP) family and also contains a carbohydrate binding module (CBM20) within the same peptide (169), making laforin unique in that no other known protein phosphatases share these same features. To date there are 79 different mutations described in the EPM2A gene (The Lafora Progressive Myoclonus Epilepsy Mutation and Polymorphism database, <http://project.tcag.cal/lafora/>). The mutations are evenly distributed across the four exons of the gene and affect the ability of the enzyme to bind to polysaccharides or the dual specificity phosphatase activity.

Laforin is able to bind to branched polymers of glucose such as glycogen, amylopectin and polyglucosan, via its CBM20 (174-176). One of the disease mutants, W32G (177), is located in the CBM20 domain and affects carbohydrate binding. Although it retains a significant amount of phosphatase activity towards PNPP as a substrate it loses activity toward glycogen (12,174,178), suggesting that impaired glycogen binding by laforin may be sufficient to cause the disease. Additionally, levels of laforin have been correlated with the levels of glycogen in a series of mouse models where glycogen content has been altered by genetic manipulation (179).

A common hypothesis in Lafora research has been that polyglucosan formation results from an imbalance between the glycogen synthase and branching enzyme activities, the 'imbalance hypothesis'. One example of an imbalance between glycogen branching and polymer synthesis is Andersen disease, which results from loss of function mutations in the glycogen branching enzyme (180). The impaired glycogen branching enzyme activity results in the

development and accumulation of polyglucosan (181). Tarui disease results in a build up of glucose-6-phosphate, due to defects in phosphofructokinase, which allosterically activates glycogen synthase and leads to the accumulation of abnormal glycogen (156). Additionally, overexpression of glycogen synthase in the skeletal muscle of mice leads to the accumulation of glycogen that was poorly branched and developed structures similar to Lafora bodies (85,145). As a result of the “imbalance hypothesis” many researchers have looked for a link between laforin and glycogen metabolizing enzymes. In fact, many have suggested that, besides glycogen, laforin can bind to several proteins involved in glycogen metabolism including glycogen synthase, GSK3, PTG, malin, the α 2 and β 2 subunit of AMPK and the Alzheimer’s disease protein Tau (182-187). One mutation of laforin has been found that does not affect carbohydrate binding or phosphatase activity, instead it is said to affect its interaction with PTG (185). It has also been proposed that laforin could be responsible for regulating GSK3, which would affect glycogen synthase activity (186,188). In this proposal, laforin would dephosphorylate and activate GSK3, which would negatively regulate glycogen synthase. In Lafora disease, where laforin is defective, GSK3 would be less active and result in a more active glycogen synthase and allow for excess glycogen production. However, in mouse models of Lafora disease it was shown that the phosphorylation status of GSK3 remains unchanged (12,189), suggesting that GSK3 regulation of glycogen synthase is not affected by laforin or malin. Wang *et al.* also showed that there was no observable change in glycogen synthase or branching enzyme activity in mice over expressing a dominant-negative form of laforin (190). Additionally, skeletal muscle and brain tissue of mice lacking laforin or malin did not show altered glycogen synthase or the branching enzyme activity (12,189), arguing against the imbalance theory for Lafora body formation.

7.2. Laforin, Malin and Autophagy

Autophagy is an intracellular process that delivers cell components to the lysosome. Autophagy plays a role in glycogen metabolism and defects in the GAA enzyme result in an inability for glycogen to be broken down in the lysosome where it accumulates, such as in Pompe disease. The mechanism for delivery of glycogen to the lysosome is not well understood but is believed to involve an autophagy-like process. Defects in autophagy also lead to neurodegeneration, behavioral changes and early death in mice (191), suggesting that it is an essential process for the function of the central nervous system. Autophagy is also thought to play a role in removing disease-associated cytoplasmic aggregate-prone proteins, which can be detected by anti-ubiquitin antibodies associated with Lafora bodies (192,193). Aguado et al. reported that laforin activates autophagy by acting upstream of the TSC (tuberous sclerosis complex) 2 (194). Loss of TSC2 leads to activation of mTOR (mammalian target of rapamycin), which causes activation of protein synthesis, cell growth and inhibits autophagy (195,196). Therefore, when laforin is disabled, autophagy would be inhibited via mTOR activation and lead to the disease phenotype. These results however are controversial. Indeed, patients with TSC2 mutations do not develop Lafora bodies. Additionally, there are no reports of TSC-like tumors in Lafora disease patient or in Lafora disease mouse models, suggesting that laforin may not be acting upstream of TSC2. Other studies have suggested that malin and not laforin affects autophagy (197). However unpublished work from our laboratory and work from the Guinovart laboratory (198) have shown that normalization of glycogen in malin knockout mice normalizes markers of autophagy arguing that defective autophagy is not pathogenic in Lafora Disease and may only be a consequence of the abnormal glycogen accumulation.

7.3. Laforin as a Glycogen Phosphatase

Glycogen contains trace amounts of covalently linked phosphate (see below). Amylopectin, a component of plant starch, also contains covalently linked phosphate, in fact much more phosphate than glycogen. The abnormal glycogen,

polyglucosan, which makes up Lafora bodies, is often described as having a structure more like amylopectin. In plants starch phosphate plays a critical role in the metabolism of starch. The plant enzyme starch excess 4 (SEX4) is responsible for hydrolyzing phosphate from starch and loss of SEX4 causes starch accumulations in Arabidopsis (170,199,200). Plants lacking SEX4 are unable to degrade starch during the night cycle and develop a starch excess phenotype, suggesting that phosphate removal is necessary for proper starch breakdown. Dixon and colleagues (184) demonstrated that laforin was able to dephosphorylate amylopectin. Tagliabracci et al. (13) later showed that, *in vitro*, laforin can also remove phosphate from rabbit skeletal muscle glycogen. When laforin is incubated with rabbit skeletal muscle glycogen, *in vitro*, ~25% of the phosphate can be removed by laforin. However, when glucosidase enzymes are added to the reaction, ~90% of the total phosphate can be released by laforin (13). This demonstrated that a majority of covalently bound phosphate is located in the inner tiers which can be accessed by laforin only after the outer tiers are degraded. Additionally, structural analysis of laforin demonstrates that the binding of carbohydrate is necessary for phosphatase activity (201).

The hypothesis that laforin functions as a physiological glycogen phosphatase has gained strength from analysis of highly purified glycogen from mice lacking the *Epm2a* gene. Mice lacking the *Epm2a* gene (will be designated as laforin^{-/-}) accumulate glycogen, glycogen phosphate and develop Lafora bodies in an age dependent manner (13). Skeletal muscle glycogen phosphate levels in the laforin^{-/-} mice were 4 – 6 times higher compared to wild-type littermates. Additionally, the skeletal muscle glycogen became less branched and decreased in solubility, consistent with the ability to form Lafora body. Glycogen from 12 – month old mice, when viewed by electron microscopy, had a larger diameter than wild type glycogen and appeared to be aggregated (12). Interestingly, when the glycogen purified from 12-month-old laforin^{-/-} mice was treated with recombinant laforin it alleviated the aggregation of the glycogen and resulted in more of a rosette like appearance, much like the wild-type glycogen (12). How phosphate disrupts glycogen structure is still not known, but a

possibility is that it may disrupt hydrogen bonding that is associated with helical polyglucose (8,202).

7.4. Malin

Malin is a putative E3-ubiquitin ligase encoded by the *EPM2B* gene. It is a 395-amino acid protein with an N-terminal RING finger domain followed by 6 NHL domains (203). To date there are some 75 disease-causing mutation, polymorphisms and deletions in the *EPM2B* gene (The Lafora Progressive Myoclonus Epilepsy Mutation and Polymorphism Database; <http://projects.tcag.ca/lafora/>). The RING finger domain is a characteristic of E3 ubiquitin ligases (204). It has been reported, in cell culture experiments, that malin interacts with laforin and catalyzes its polyubiquitylation, which results in its proteasomal degradation (187). Based on these observations, a defect in malin would cause an upregulation of laforin. This upregulation of laforin would be difficult to reconcile with the phenotype of the malin knockout mice as well with the development of Lafora disease in patients bearing malin mutations.

It has also been proposed that malin is responsible for regulating enzymes involved in glycogen metabolism. Mainly based on cell culture experiments, it has been reported that proteins such as glycogen synthase, PTG and AGL are malin substrates (205-208). Co-expression of malin and laforin, in cell culture, resulted in the ubiquitylation and proteasomal degradation of PTG (207,208). The authors of these studies proposed that laforin, bound to glycogen, would recruit malin resulting in PTG ubiquitinatylation. In this model, if malin were defective this would result in a build up of PTG, which would result in a more active form of glycogen synthase and excess glycogen synthesis, polyglucosan and Lafora body formation. Cheng et al (205) reported that the debranching enzyme AGL is a substrate for malin and that the ubiquitylation of AGL was independent of laforin. The authors proposed that a loss of function mutation in malin would prevent the proteasomal degradation of AGL and result in excessive AGL activity, removal of α -1,6-glycosidic linkages, which would lead to polyglucosan formation. However, glycogen degradation involves the coordinated actions of both AGL

and phosphorylase. Excessive AGL activity would only reduce branching frequency if phosphorylase were limiting. Furthermore, analysis of skeletal muscle from 3-month-old *Epm2b* knockout mice (which will be designated as malin^{-/-}) show no changes in the protein levels of glycogen synthase, AGL or PTG (189), suggesting that malin is not a major regulator of their protein levels. It has also been proposed that AMPK phosphorylates laforin, which would promote association with malin and degradation of laforin (183). However, analysis of skeletal muscle from WT exercised mice revealed that although AMPK was phosphorylated no changes in the levels of laforin were observed (189).

There seems to be an increase in laforin levels in the malin^{-/-} mice, particularly in the brain, and it is associated with enrichment in the insoluble fraction of extracts with depletion from the cytosol (189). This would be consistent with the idea that laforin is a malin substrate. However, increased levels of laforin have been observed in several mouse models that accumulate glycogen and viceversa, decreased in animal model where glycogen is decreased, indicating that laforin, like glycogen synthase, tracks with glycogen (178). Laforin has been shown to preferentially bind to starch over glycogen (175), suggesting that it might also prefer to bind to the polyglucosan. In the malin^{-/-} mice glycogen phosphate content is increased suggesting that a majority of the laforin may be inactive or that the insoluble glycogen and its associated phosphate and proteins may not be subject to normal metabolism. Therefore, we proposed that the abnormal glycogen accumulation in the malin knockout mice binds and sequesters laforin away from the metabolically active soluble glycogen pools (189). Furthermore work in our laboratory and by Duran et al (198) has shown that genetically decreasing glycogen by deficiency in PTG or glycogen synthase in either malin or laforin knockout mice, rescues the glycogen phenotype and normalizes the levels of glycogen synthase and/or laforin, arguing that these proteins are not malin substrates.

7.5. Lafora Disease and Glycogen

There has been serious debate as to whether Lafora body formation is a cause or consequence of the disease, for example (209). However, there is growing evidence that accumulation of glycogen, and most likely abnormal glycogen, leads to Lafora body formation and the disease pathology. Besides elevated phosphate, abnormal glycogen found in mouse models of Lafora disease also has reduced branching, which contributes to its insolubility. The relationship between phosphorylation, branching and structure remains unknown.

Our laboratory and others have also shown that suppressing or eliminating glycogen synthesis in mouse models of Lafora disease reduced Lafora body formation and restored neurological function (198,210-212). Furthermore, when PTG knocked mice were crossed with malin or laforin knockouts there was no longer an over-accumulation of glycogen, Lafora body formation is suppressed and neurological dysfunction is alleviated (210,211). Additionally, knockout of the *GYS1* gene and either laforin or malin completely or partially eliminates brain glycogen, abolishes Lafora body formation along with restoring neurological function (198,212). Duran et al (213) have reported that over expression of an active form of glycogen synthase in neurons of mice resulted in neuronal loss, locomotion defects. Interestingly, in two different mouse models where glycogen accumulates in the brain, defects in autophagy, similar to those found in mouse models of Lafora disease, have been observed and is independent of malin function (198).

Therefore, evidence is suggesting that Lafora disease may be dependent on the accumulation of glycogen and could be considered a glycogen storage disease. Mice lacking brain glycogen do not display any severe neurological defects. These observations offer a therapeutic approach for Lafora disease along with other glycogen storage diseases by targeting glycogen synthesis.

8. Glycogen Phosphate

8.1. Preface

Our understanding of the role of phosphate in glycogen and glycogen metabolism has advanced in recent years but its function, if any, remains something of a mystery. It has become clear that defects in glycogen phosphate metabolism are associated with Lafora disease (12-14,18,19,214). In the 1970's it was established that starch, specifically amylopectin, contained covalent phosphate (215). However, because phosphate would often be a contaminant of purified biological components, due to its ubiquitous abundance, low phosphate content in early glycogen preparations was viewed as an indicator of its purity (216-218). Then in 1980, Fontana had the first convincing report that phosphate was stably bound to glycogen (11).

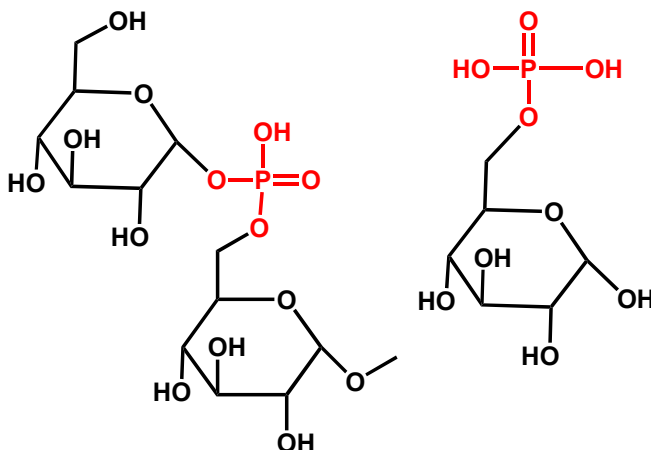


Figure 8. Proposed location of phosphoesters in glycogen. Structure on the left represents the phosphodiester and the structure on the right represents a phosphohomoester at the C6 location proposed by Lomako and colleagues (3)

8.2. Phosphate Abundance and Chemistry

Phosphate is present in glycogen in low amounts ranging from 1 phosphate per ~650 glucose residues to 1 in 2000 glucose residues, with the abundance of phosphate being dependent on the source (12-14). In mouse

models of Lafora disease, either laforin^{-/-} or malin^{-/-}, there is increased glycogen phosphate that is further increase with age (13,14,189). The location of the phosphate has been an area of interest for some time. Whelan and colleagues originally proposed that the phosphate existed as a phosphomonoester that would be located at the C6 of glucose residues or as a glucose-1,6-phosphodiester (3) (Figure 8). The first report of phosphate location was in 2011 when Tagliabracci et al. reported that phospho-oligosaccharides, purified from enzymatically hydrolyzed rabbit skeletal muscle glycogen, had phosphate monoesters located at the C2 and C3 carbons of glucose residues (16). In 2013 Nitschke et al reported that NMR analysis of phospho-oligosaccharides showed phosphate at the C2, C3 and C6 carbon atoms of glucose residues and that the C6 phosphomonoester was the predominant site of phosphorylation that could affect glycogen structure.

8.3. Introduction of Glycogen Phosphate

The incorporation of phosphate into glycogen is still not fully understood. There is evidence that glycogen synthase is capable of incorporating phosphate during glycogen synthesis (16,219). Lomako et al had earlier proposed that an uncharacterized enzyme, distinct from glycogen synthase, could be responsible for phosphate incorporation into glycogen (2) (Figure 9). They proposed that the enzyme, a glucose-1-P-transferase, would form the proposed C1-C6 phosphodiester bond, forming a novel branch point, by transferring the β -phosphate from UDP-glucose (2). This hypothesis was tested in our laboratory using skeletal muscle extracts of mice lacking the skeletal muscle isoform of glycogen synthase, which was incubated with radiolabeled [β -³²P]UDP-glucose and no phosphate incorporation was observed, while wild type skeletal muscle extract did show the incorporation of phosphate (16).

These data suggested that glycogen synthase might be responsible for incorporating phosphate into glycogen. A second possible mechanism for phosphate incorporation would involve phosphorylation by a glycogen water dikinase, similar to enzymes found in plants. In plants, amylopectin is

phosphorylated at the C3 and C6 carbon atoms of glucose. The glucan water dikinase enzyme is responsible for transferring the β -phosphate from ATP to the glucan at the C6 position (220,221). Phosphorylation of the C6 position promotes the phosphorylation of the C3 site by a second enzyme, phosphoglucan water dikinase (PWD), which prefers substrates that have been previously phosphorylated at the C6 position (222,223). One might predict that a similar type of enzyme could exist in mammals. However, at this time neither bioinformatics nor biochemical analysis has found evidence for such enzymes.

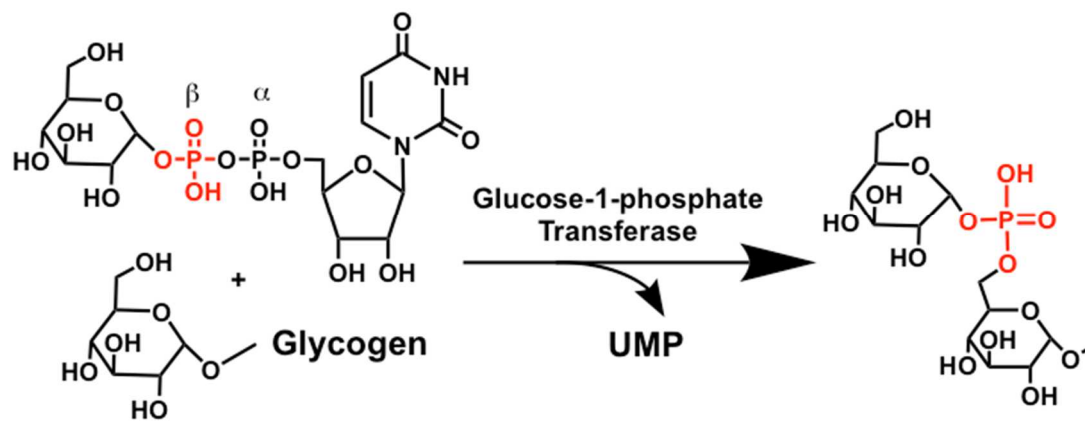


Figure 9. Glucose-1-phosphate transferase. Proposed mechanism for phosphate introduction by Lomako and colleagues. (2).

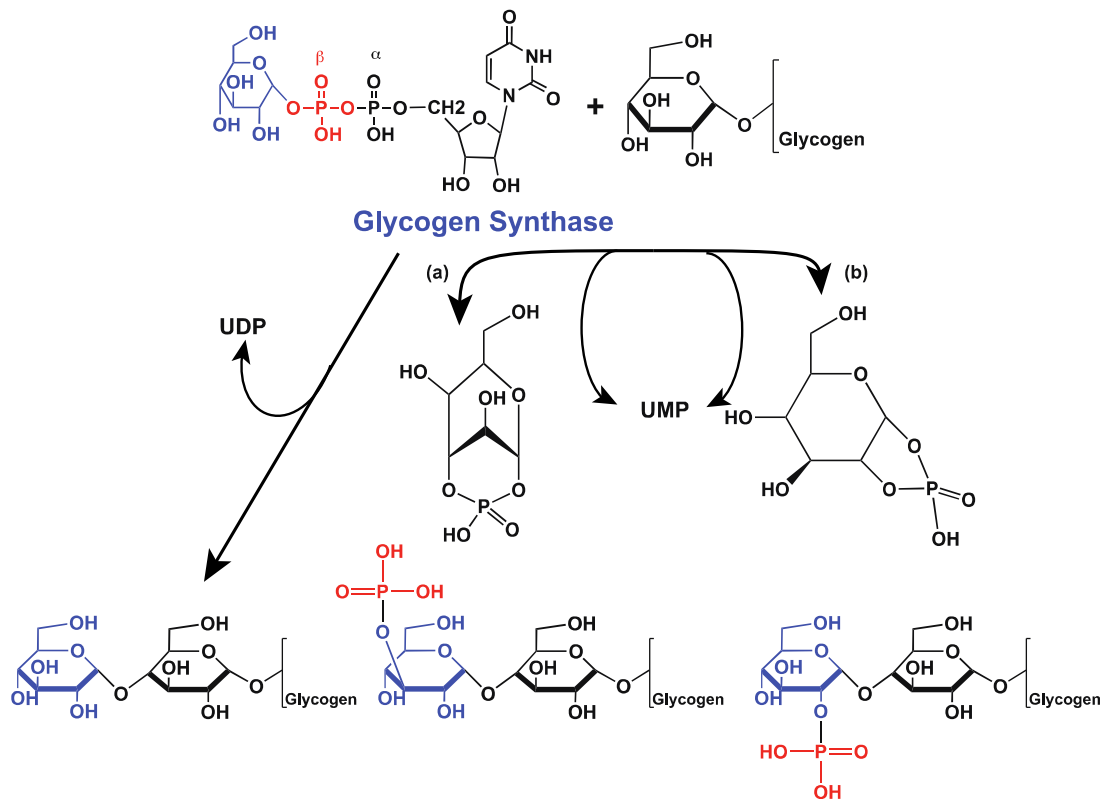


Figure 10. Proposed mechanism for phosphate incorporation by glycogen synthase. The normal glycogen synthase reaction is shown on the left where glucose from UDP-glucose is added to the non-reducing end. The proposed mechanism for phosphate introduction would involve the formation of either glucose-1,3-cyclic phosphate (a) or a glucose-1,2-cyclic phosphate (b) in the active site of glycogen synthase, which would result in the incorporation of either a glucose-3-phosphate or a glucose-2-phosphate into glycogen.

Tagliabracci et al. proposed a mechanism for the incorporation of phosphate by glycogen synthase that would involve the a glucose 1,2- or 1,3-cyclic phosphate that would form in the active site of glycogen synthase, which would result in UMP leaving and the incorporation of a glucose-2 or glucose-3 phosphate into the growing glucose polymer (16) (Figure 10). Using purified glycogen synthase from rabbit skeletal muscle (224), yeast (82) and human (225) recombinant glycogen synthase the rate of phosphate incorporation was measured to be ~1 phosphate per 10,000 glucose residues (16). However, the results and conclusions from Tagliabracci *et al* 2011 were challenged by Nitschke *et al* 2013. Nitschke et al. labeled glycogen with [β - ^{32}P]UDP-glucose in a similar manner to that described in Tagliabracci et al. 2011 and reported that the signal could be removed by gel filtration, and concluded that the ^{32}P signal observed was due to [β - ^{32}P]-UDP produced during the glycogen synthase reaction, which was binding non-specifically to the glycogen (15).

The mechanism for phosphate incorporation by glycogen synthase has not been confirmed, but there is some evidence that supports the mechanism proposed by Tagliabracci et al. (16). The formation of a glucose cyclic phosphate from UDP-glucose has been known since the mid 1900's and was described by Paladini and Leloir (226). The glucose cyclic compound described was known as “fast ester,” due to its mobility on TLC, where it migrated ahead of UDP-glucose. The fast ester is formed from UDP-glucose in the presence of divalent metals under slightly alkaline condition, to yield the glucose-1,2-cyclic phosphate. The formation of glucose-1,2-cyclic phosphate and glucose-1,3-cyclic phosphate are known (227) and may account for the introduction of phosphate at the C2 or C3 positions. Structural and enzymatic studies of glycogen synthase provide further support of the hypothesis proposed by Tagliabracci et al. (16,228). A crystal structure of glycogen synthase shows glucose-1,2-cyclic phosphate and UMP bound to the active site of the enzyme. Also, glycogen synthase, when incubated with UDP-glucose, produces the cyclic phosphate (228). These data suggest that glycogen synthase can incorporate phosphate at the C2 and possibly the C3 locations but proving the proposed mechanism (Figure 10) (16) is challenging.

There are still many unknowns regarding the source of phosphate in glycogen and what its role may be. For instance, how phosphate is incorporated at the C6 location remains unknown. Cyclic phosphates of glucose-6,3- or glucose 6,4-phosphates are known and can be chemically synthesized (227). Formation of glucose-1,6-cyclic phosphate from UDP-glucose would be sterically impossible. There is evidence that phosphate groups can migrate between hydroxyl groups on glucose residues, under alkaline or acidic conditions (229-231). However, at this point there is no evidence for phosphate migration within glycogen.

8.4 Phosphate and Glycogen Metabolism

Elevated levels of phosphate have been associated with the formation of Lafora bodies, which are mainly composed of insoluble glycogen like material known as polyglucosan (145,161,232). Mice lacking either the Epm2a or Epm2b genes have an age dependent accumulation of glycogen, glycogen phosphate and formation of Lafora bodies (12,13,19,189,214). The mechanism linking excess phosphate and its relationship between glycogen becoming poorly branched and insoluble is not well understood at this time. In plants, the phosphorylation of starch is critical for its degradation (17,233-235). Although starch and glycogen share some similarities the overall metabolism and functions between the two carbohydrates are distinctly different. Starch forms a semi-crystalline structure with highly organized branching patterns and is mostly insoluble and inaccessible to enzymes (233,236,237). The incorporation of phosphate into starch is thought to disrupt the semi-crystalline structures, which makes it more soluble and accessible for enzymes. However, a similar role for glycogen degradation is unlikely because glycogen is typically soluble and the accumulation of phosphate in glycogen is associated with glycogen insolubility (12).

The metabolism of glycogen may be associated with its structure and solubility properties. Laforin^{-/-} mice, at 3 months of age, have elevated levels of phosphate but do not have an excessive accumulation of glycogen and the

glycogen is only slightly less branched compared to wild type (12). As the laforin *-/-* mice age, up to 12 months of age, glycogen levels increase, glycogen phosphate levels further increase, branching decreases, solubility decreases and Lafora bodies are formed in many tissues (12,13). Using exhaustive exercise to metabolize glycogen, 3 month-old laforin *-/-* mice were able to utilize skeletal muscle glycogen to the same extent as the wild type animals (238). Immediately following exercise in both the wild type and laforin *-/-* mice there is a significant increase in phosphate levels (238). Glycogen phosphate content, as determined on a mmole of phosphate per mole of glucose, increases following a bout of exhaustive exercise. This is due the release of glucose from glycogen, which effectively increases the ratio of phosphate to glucose.

Additionally, pervious reports demonstrated that laforin was capable of liberating ~25% of the total phosphate from glycogen and that only after treating with amyloglucosidase, in order to degrade the outer tiers of glycogen and exposing the inner core, laforin was able to release the remaining phosphate (13). These data show that a majority of the phosphate is located within the inner tiers of glycogen and is inaccessible for removal by laforin. Therefore, the observation that glycogen phosphate increases after exercise in both wild type and the laforin *-/-* mice is in agreement (238) with previous observations (12). Furthermore, glycogen phosphate, as mole of phosphate per gram of tissue (total phosphate), can be used to determine if there is a loss of glycogen phosphate during a given experimental procedure, within the mouse tissue. Indeed, Irimia et al observed that total phosphate decreases in the wild type animals. However, when laforin is lacking there was no change in the total glycogen phosphate levels, and the authors concluded that laforin can remove phosphate from glycogen *in vivo* during exercise and possibly acts during glycogen degradation (238)

Analysis of branching following exercise showed that the laforin *-/-* mice had a slower rate of branching remodeling, suggesting that the high levels of phosphate may affect branching (238). Irimia et al. concluded that the laforin *-/-* mice had a delay in the remodeling of their glycogen compared to wild type mice. This would suggest that perhaps the high amount of phosphate in the laforin *-/-*

mice, and most likely in Lafora disease patients, might inhibit the ability for branching to properly occur and with multiple rounds of degradation and synthesis would eventually lead to Lafora body formation.

METHODS

1. Purification of Rabbit Skeletal Muscle Glycogen for Phosphate Determination

Rabbit muscle glycogen was purified by either of two procedures, one involving treatment of muscle extracts with 10% TCA (Figure/v) at 4°C to remove protein prior to precipitation with ethanol (TCA Method) and the other involving direct KOH digestion of muscle (KOH Method). Two male New Zealand white rabbits, ~ 2 kg each, were sacrificed by lethal injection with pentobarbital (150mg/kg body weight) followed by exsanguination. Back and hind limb muscles were removed, ~ 75% of the harvested muscle was placed immediately under ice and used for glycogen purification by the TCA method. The remaining tissue was flash frozen in liquid N₂ and stored at -80°C for glycogen purification by the KOH method.

1.2. TCA Method.

Immediately following exsanguination, skeletal muscle was harvested from rabbits, ~1.45 kg, cut into small pieces and then homogenized with three volumes of 4 mM EDTA in a large Waring blender, 60 seconds at low speed and 30 sec at high speed. All steps, such as homogenizations, centrifugations and other steps were conducted at 4°C. The homogenate was centrifuged for 45 min at 7,000 x g. The supernatant was then passed through two layers of Miracloth to remove floating fat. The recovered supernatant (2.8 L) was transferred to a 4 L glass beaker placed in an ice bath and 100% (Figure/v) TCA was slowly added under constant stirring to a final concentration of 10% TCA. The suspension was then centrifuged for 30 min at 7,000 x g, the supernatant (2.7 L) transferred to a 4 L glass beaker placed in a ice-salt bath and glycogen was precipitated by slowly adding 1 volume of -80°C 100% ethanol. After stirring in the ice-salt bath for an additional 20 min, the sample was centrifuged at 7,000 x g for 60 min, the supernatant was decanted and the precipitate dissolved in water using a motor driven pestle of a Dounce homogenizer. The solution (80 ml) was transferred to a

glass Corex tube and lipids were extracted with an equal volume of a 3:1 chloroform:octanol solution followed by vigorous mixing and centrifuged at 6,000 x g for 10 min to separate the aqueous and organic phases. The aqueous layer was collected and re-extracted with an equal volume of 3:1 chloroform:octanol. Ten ml of water was added to the organic phase of the first extraction, mixed and centrifuged. The process was repeated once more and all aqueous phases were combined, 90 ml total. Glycogen was then precipitated from the aqueous phase by slow addition under stirring of an equal volume of -20°C 100% ethanol and the suspension was kept overnight at -20°C. The precipitated glycogen was collected by centrifugation, 7,000 x g for 30 min, the pellet was re-dissolved with 45 ml of 1% SDS and then subjected to ultracentrifugation in a Ti45 rotor at 196,000 x g for 3 hr at 4°C. After ultracentrifugation, the supernatant was decanted and 30 ml of water was added to the translucent glycogen pellet which was re-dissolved by rocking on a Nutator overnight at 4°C. The solution was then placed on ice for 1 hr to precipitate any remaining SDS, which was removed by centrifugation at 12,000 x g for 20 min. The glycogen in the supernatant (45 ml) was precipitated with two volumes of -20°C 100% ethanol and kept at -20°C for 2.5 hr followed by centrifugation at 15,300 x g for 30 min. The precipitated glycogen was washed with -20°C 100% ethanol, centrifuged at 15,300 x g and then dissolved in 30 ml of water. The glycogen solution was dialyzed using Spectra/Por (Spectrum) 16 mm diameter with 12-14,000 MW cutoff dialysis tubing at 4°C against 4L of water, which was changed after 4.5 hr and allowed to dialyze overnight. The dialyzed glycogen solution was centrifuged at 23,000 x g for 20 min to remove insoluble material. Glycogen in the supernatant (53 ml) was then precipitated with two volumes of -20°C 100% ethanol with stirring and then kept at -20°C for 2 hr. After centrifugation at 23,000 x g for 20 min, the precipitated glycogen was washed with -20°C 100% ethanol and re-centrifuged. The pellet was kept at room temperature to evaporate all residual ethanol. After the glycogen was completely dried, it was pulverized using a ceramic mortar and pestle. From the 1.45 kg of muscle 4.0 g of glycogen was recovered and kept at -20°C until use.

1.2. KOH Method

Liquid N₂ flash frozen rabbit skeletal muscle (~105 g) stored at -80°C was rapidly broken into small pieces and added to 10-volumes of boiling 30% KOH and maintained in a 100°C water bath for 1 hr with mixing about every 10-15 min. The digested tissue was then placed on ice to cool and centrifuged at 10,000 x g for 10 min. All centrifugations were done at 4°C. The supernatant, 1 L, was filtered through 2 layers of Miracloth to remove floating fat, transferred to a 4 L glass beaker placed in a ice-salt bath and glycogen was precipitated by slowly adding two volumes of -80°C 100% ethanol with constant stirring in the presence of 10 mM LiCl and 0.02% Na₂SO₄ to aid precipitation. After an additional 5-10 min stirring, the suspension was placed overnight at -20 °C. All subsequent ethanol precipitations included 6 mM LiCl. The precipitated glycogen was collected by centrifugation, 7,000 x g for 45 min, the pellet was re-dissolved in 30 ml water and centrifuged at 10,000 x g for 25 min to remove insoluble material. The supernatant (36 ml) was precipitated by adding two volumes of -20°C 100% ethanol with the addition of LiCl and kept at -20°C for 2 hr. The sample was then heated in a boiling water bath for 3 min, which causes glycogen flocculation, then cooled on ice followed by centrifugation at 10,000 x g for 30 min. The pellet was re-dissolved in 20 ml of water and 13 ml of the solution was added to each of two glass Corex tubes. Ten volumes of 4:1 methanol:chloroform was added to each tube, vigorously mixed and incubated at 80°C for 5 min. The tubes were then cooled on ice and centrifuged at 5,500 x g for 30 min to pellet the glycogen. The pellets were dried in a Speed Vac for 10 min to remove residual solvents, re-dissolved with ~25 ml of water, heated to aid solubilization and centrifuged at 10,000 x g for 25 min to remove insoluble material. The supernatant was precipitated again with two volumes 100% ethanol and kept at -20°C overnight. After heating for 2 min in a boiling water bath and cooling on ice, the sample was centrifuged at 15,000 x g for 30 min. The glycogen pellet was dried in a Speed Vac for 5 min. The pellet was then re-dissolved with 20 ml of water and TCA was added under stirring to a final concentration of 10% (Figure/v) followed by centrifugation at 15,000 x g for 30 min. The glycogen in the supernatant, 27 ml,

was precipitated with ethanol and centrifuged at 15,000 x g for 30 min. The pellet was re-dissolved in 20 ml of water and filtered by passing through one layer of Miracloth that had been extensively washed with water. The filtered solution was then transferred to dialysis tubing, Spectra/Por, 16 mm diameter, 12-14,000 MW cutoff, and dialyzed against 4 L of water, which was changed after 2.5 hr and dialysis continued overnight at 4°C. After dialysis, the glycogen solution (19 ml) was precipitated with ethanol and the pellet was dried in a Speed Vac. The dried pellet was minced and weighed, yielding 0.48 g of glycogen.

2. Preparation of Potato Amylopectin for Phosphate Analysis

Potato amylopectin (Sigma-Aldrich #A8515), to be analyzed for phosphate content and as a positive control for the presence of glucose-6-P, was also subjected to the KOH purification procedure. Four aliquots of ~ 3 mg amylopectin were treated with 10 volumes of boiling 30% KOH as described for glycogen. After boiling, the samples were cooled on ice, precipitated with two volumes of -20°C 100% ethanol and LiCl and Na₂SO₄ to final concentrations of 10 mM and 0.02%, respectively and kept overnight at -20°C. The samples were then heated in a boiling water bath for 2 min, cooled on ice for 10 minutes and centrifuged at 15,000 x g for 20 min at 4°C. The pellets were re-dissolved in 300 µl of water. The precipitation was repeated two more times with LiCl at a final concentration of 6 mM. After the last precipitation, the amylopectin pellets were dried in a Speed Vac, re-dissolved in 500 µl H₂O and dialyzed in Spectra/Por tubing of 10 mm diameter and 12-14,000 MW cutoff. The samples were dialyzed against 4 L of water overnight at 4°C. The dialysates were ethanol precipitated again. The pellets were dried in a Speed Vac to completely remove any residual liquid, weighed, dissolved in water at a final concentration of ~ 5 mg/ml and stored at -20°C until use. Glucose equivalents were determined as in the Glycogen and Inorganic Phosphate Determination section.

3. Mouse Models of Lafora Disease

Epm2a^{-/-} (laforin^{-/-}) mice were generated as previously described (239) and were backcrossed five times with C57BL/6 mice. From this generation, heterozygotes were crossed to generate the *Epm2a*^{+/+} (wild type, WT) and the laforin^{-/-} mice (240). The *Epm2b*^{-/-} (malin^{-/-}) mice were generated as previously described (189). The PPP1R3C gene, which encodes the protein phosphatase 1 (PP1) glycogen targeting subunit PTG, was deleted as previously described (241) to generate the PTG knockout (PTG^{-/-}) mice. Crossing PTG^{-/-} mice with either laforin^{-/-} or malin^{-/-} mice generated double knockout mice, PTG/laforin^{-/-} (211) or PTG/malin^{-/-}. All mice were kept in temperature and humidity controlled housing with a 12:12 light-dark cycle at the Indiana University School of Medicine Laboratory Animal Resource Center. Mice were fed standard chow (Harlan Tekland global diet 2018SX), and allowed food and water ad libitum. All studies were conducted in accordance with federal guidelines and were approved by the Institutional Animal Care and Use Committee of Indiana University School of Medicine.

4. Mouse Skeletal Muscle Glycogen Purification for Phosphate Determination

Animals were sacrificed by cervical dislocation, were decapitated and the heads dropped directly in liquid nitrogen. Other tissues (skeletal muscle, liver and heart) were rapidly harvested and immersed in liquid nitrogen. Tissues were kept at -80°C until use.

Flash frozen mouse skeletal muscle was pulverized under liquid nitrogen and a minimum of 500-600 mg of tissue was weighted in a 15 ml screw cap centrifuge tube (ENEMate, C-3313-15). Ten volumes of boiling hot 30% KOH were added to the tubes and heated in a 100°C water bath for 1 hour, with mixing about every 15 minutes, to hydrolyze the tissue. The digested tissue was then placed on ice for 10 minutes and centrifuged at 10,000 x g for 10 min. All centrifugations were done at 4°C. The supernatant was filtered through 2 layers of Miracloth to remove floating fat and transferred to a new 15 ml screw cap tube.

Glycogen was precipitated by adding two volumes of -20°C 100% ethanol, LiCl and Na_2SO_4 , with a final concentration of 66% ethanol, 10 mM LiCl and 0.02% Na_2SO_4 . The mixture was mixed by inverting and placed overnight at -20°C . The tubes were incubated in a boiling water bath for 2 minutes and then cooled on ice for 10 minutes. The precipitated glycogen was collected by centrifugation, $10,000 \times g$ for 30 min, the pellet was re-dissolved in 500 μl water (occasionally heating to fully dissolve the pellet) and transferred to a 1.5 ml screw cap centrifuge tube. The sample was then centrifuged at $17,500 \times g$ at 4°C for 20 minutes in a microcentrifuge to remove insoluble material. The supernatant was then transferred to a new 1.5 ml screw cap tube and 2 volumes of -20°C 100% ethanol and LiCl were added to precipitate the glycogen. All subsequent ethanol precipitations included 6 mM LiCl. The tubes were mixed by inverting and incubated at -20°C overnight. Samples were incubated in a boiling water bath for 2 min, cooled on ice for 10 minutes and glycogen was collected by centrifugation, $17,500 \times g$ for 20 minutes at 4°C . The supernatant was removed and the glycogen pellet was dried in a Speed Vac for 10 minutes. The glycogen pellet was re-dissolved in 100 μl of water, and heated in a boiling water bath to aid in solubilization. Lipids were removed by adding ten volumes of 4:1 methanol:chloroform solution to each tube, vigorously mixed and incubated at 80°C for 5 min. The tubes were then cooled on ice and centrifuged at $17,500 \times g$ for 20 min to pellet the glycogen. The pellets were dried in a Speed Vac for 10 min to remove residual solvents, redissolved with 500 μl of water, heated to aid solubilization and centrifuged at $17,500 \times g$ for 25 min to remove insoluble material. The supernatant, after transfer to a new tube, was precipitated again with two volumes 100% ethanol and kept at -20°C for a minimum of 1 hour. After heating for 2 min in a boiling water bath and cooling on ice, the sample was centrifuged at $17,500 \times g$ for 20 min. The glycogen pellet was dried in a Speed Vac for 10 min. The glycogen pellets were then re-dissolved with 400 μl of water and 100 μl of 50% TCA was added to a final concentration of 10%, mixed well by vortexing and centrifuged at $17,500 \times g$ for 20 min. The glycogen in the supernatant was precipitated with ethanol and centrifuged at $17,500 \times g$ for 20

min. The pellet was redissolved in 500 μ l of water, transferred to dialysis tubing, Spectra/Por, 10 mm diameter, 12-14,000 MW cutoff, and dialyzed against 4 L of water, overnight at 4°C. After dialysis, the glycogen solution was transferred to a new weighed 1.5 ml tube, precipitated with ethanol, the supernatant removed and the pellet was dried in a Speed Vac. The dried pellet and tube were weighed and the glycogen weight was determined. The glycogen was dissolved in MilliQ water for a final 5 mg/ml. The final glycogen concentration was determined using the method described in (115) (see Glycogen and Inorganic Phosphate Determination for details).

5. Purified Glycogen and Inorganic Phosphate Determination

5.1 Glycogen Determination

Glucose equivalents from purified mouse and rabbit skeletal muscle glycogen, and amylopectin were determined using the assay previously described in Suzuki *et al.* (115) by the method of Bergmeyer (242). Approximately 50-150 μ g of polysaccharide, based on a 5 mg/ml solution, described above, was enzymatically digested with 300 μ g/ml amyloglucosidase in 200 mM sodium acetate (NaOAc) pH 4.8 in a final volume of 50 μ l at 40°C overnight. Glucose equivalents from the digest were determined using a coupled enzymatic reaction involving the formation of glucose-6-phosphate by hexokinase (Roche) followed by the reduction of NADP⁺ to NADPH by glucose-6-phosphate dehydrogenase (G6PDH) (Roche). Briefly, the glycogen and amylopectin digest were typically diluted 1:2 and 10 μ l of the digest was added to 300 μ l of the glucose assay buffer consisting of 0.3 M triethanolamine pH7.6, 4 mM MgCl₂, 0.9 mM NADP⁺, 2 mM ATP and 2 μ g/ml G6PDH. Background readings of the reaction were determined at 340 nm. Hexokinase was then added, 5 μ l of 100 μ g/ml in 3.2 M (NH₄)₂SO₄, and incubated at room temperature in the dark for 30 minutes. After the hexokinase incubation, the absorbance at 340 nm was again measured and using the extinction coefficient for NADPH (6.22 mM⁻¹), glucose equivalents were determined. The glucose equivalents were

used to normalize phosphate measurements from the same samples to give the mol phosphate/mol glucose ratio.

5.2 Total Phosphate Determination

Polysaccharide phosphate content from mouse and rabbit skeletal muscle glycogen, and amylopectin was determined using the sensitive Malachite green assay as previously described (13,243). Briefly, ~200 µg of polysaccharide was taken in triplicate, one non-hydrolyzed and two hydrolyzed samples, from a solution of glycogen or amylopectin, placed in borosilicate glass tubes and dried in a Seed Vac. The polysaccharide was hydrolyzed by adding 40 µl of a 3:1 solution of 60% HClO₄:10N H₂SO₄ and incubated at 190°C for 2 hours. After hydrolysis, 100 µl of water was added to the samples and mixed. The Malachite green solution (400 µl) was added to the samples and mixed. The solution was then transferred to a cuvette and the absorbance at 620 nm was measured using a spectrophotometer. Phosphate amounts were determined using a standard curve of KH₂PO₄, which was linear from 0-70 nmols.

The Malachite green solution was prepared by dissolving 13.5 mg of Malachite green oxalate salt (Sigma) in 30 ml of H₂O. After the Malachite green was completely dissolved, 10 ml of 4.2% ammonium molybdate in 4 N HCL was added, mixed and placed on a Nutator at 4°C for 1 hour. The solution was then filtered through a 0.22 µm syringe filter and Tween-20 was added for a final concentration of 0.01%.

6. Measurement of Phosphate at the C6 Position in Glycogen

Dr. DePaoli-Roach developed a method for measuring glucose-6-phosphate in hydrolysates of glycogen or amylopectin (14). The procedure was based on that described in Zhu et al. (244). Highly purified glycogen from mouse and rabbit skeletal muscle, and amylopectin, 0.5 mg of each, were hydrolyzed in 75 µl of 1 N HCL for 3 hours in a boiling water bath. The reaction was neutralized by adding 37.5 µl of 2 N NaOH. For glycogen samples 10 µl of sample, in triplicate, were added to wells of a 96-well plate (Costar 3603, Corning) with a

clear bottom and black walls. Amylopectin samples were diluted 1:10 and 10 μ l of sample was added to the 96-well plate in triplicate. The reaction mixture (90 μ l) of 50 mM triethanolamine, pH 7.6, 1 mM $MgCl_2$, 100 μ M NADP⁺, 10 μ M high purity resazurin (Acros Organics #18990), and 0.2 units/ml *Clostridium kluyveri* diaphorase (Sigma #D2322), was added to each well. Samples were centrifuged at 2000 rpm for 45 seconds in a Fisher Marathon 8K centrifuge and then mixed at 700 rpm for 45 seconds in an Eppendorf Mixmate. Background fluorescence was measured using a FlexStation II plate reader (Molecular Devices) with excitation at 530 nm and emission at 590nm. The reaction was started by adding 0.1 units/ml *Leuconostoc mesenteroids* glucose-6-phosphate dehydrogenase (Roche Applied Science #10165875001), centrifuged, mixed and incubated at room temperature for 30 minutes in the dark. Fluorescence was again measured and the background readings subtracted. Each assay included a set of standards which contained 0 – 150 pmols of glucose-6-phosphate. Due to the low amounts of glucose-6-phosphate relative to glucose in the hydrolysates, it was determined that a 4000-fold molar excess of glucose to glucose-6-phosphate did not interfere with the measurements of glucose-6-phosphate (data not shown).

7. Purification of Glycogen For Total Glycogen Content in Mouse Tissue

Total glycogen in skeletal muscle, liver and brain was determined by a protocol similar to that described in Suzuki *et al.* (115) using the method of Bergmeyer (242). Under liquid nitrogen, brain tissue was harvested by breaking open the skulls and transferred to a new tube. Flash frozen tissues were pulverized under liquid nitrogen and 30 – 50 mg of muscle, heart, brain or liver, were weighed in a 1.5 ml screw cap tube. The tissue was hydrolyzed by adding 300 μ l of boiling 30% KOH and incubating in a boiling water bath for 30 minutes, with mixing every 5-10 minutes. Samples were then cooled on ice for 10 minutes. Glycogen was precipitated by adding 100 μ l of 2% Na_2SO_4 and 800 μ l of -20°C 100% ethanol, for a final 0.25% Na_2SO_4 and 66% (v/v) ethanol. The samples were then mixed, by inverting, and incubated at -20°C for a minimum of 1 hour. Samples were then incubated in a boiling water bath for 2 minutes and cooled on

ice for 10 minutes. Glycogen was collected by centrifugation, 17,500 x g for 20 minutes at 4°C. The supernatant was decanted and tubes were quickly centrifuged to collect any remaining supernatant, which was removed. Glycogen pellets were dried in a Speed Vac to remove residual ethanol and re-suspended by adding 200 µl of MilliQ water and vortexing. Precipitation of glycogen was repeated two more times by adding two volumes of -20°C 100% ethanol to the re-suspended glycogen and incubating at -20°C for a minimum of 1 hour. After each precipitation, the samples were incubated in a boiling water bath, cooled on ice, centrifuged and dried in a Speed Vac as described above. Once the last precipitation was completed the dried glycogen pellet was re-suspended in 100 – 200 µl of 0.2 M NaOAc (NaOAc) buffer, pH 4.8, that contains 300 µg/ml amyloglucosidase and incubated for a minimum of 4 hours at 40°C to digest the glycogen. Glucose equivalents were determined as described above (Glycogen Determination).

8. Fractionation of Glycogen by Low Speed Centrifugation and Western Blotting Analyses

Skeletal muscle was powdered under liquid nitrogen and homogenized using a tissue Tearor, ~75 mg for glycogen content and Western blot and between 800 -1000 mg for glycogen branching and phosphate determination, in 10 volumes of buffer consisting of 50 mM Tris-HCl, pH 7.8, 10 mM EDTA, 2 mM EGTA, 100 mM NaF, 2 mM benzamidine, 0.1 mM N-Tosyl-L-lysine chloromethyl ketone hydrochloride (TLCK), 50 mM β-mercaptoethanol, 0.5 mM phenylmethane sulfonyl fluoride (PMSF), 10 µg/ml leupeptin, 1 mM sodium orthovanadate and 0.2% Triton-20. Homogenization was done at maximum speed for ~30 seconds. After homogenization, 80 µl of the total extract was taken and 20 µl of 5X SDS loading buffer (60 mM Tris-PO₄ pH 6.8, 40% glycerol, 5% SDS (Figure/v), 0.08% Bromophenol Blue, and 5%(v/v) β-mercaptoethanol) was added, incubated in a boiling water bath for 5 minutes and frozen for later use. The remaining homogenate was subjected to centrifugation at 5,000 X g for 10 minutes, as previously described (12,14). Following centrifugation, the

supernatant was removed and measured. Typically, the removed supernatant was ~70% of the original volume of homogenization buffer. The low speed pellet (LSP) was re-suspended by adding 70% of the original volume of homogenization buffer. Equal amounts (100 μ l) of the LSS and LSP were taken for western blot analysis, 1/5 the volume of 5X SDS loading buffer was added, samples were incubated in a boiling water bath for 5 minutes, cooled on ice and stored at -20°C for later use. From the LSS 10 μ l of sample was taken and diluted 1:30 with water and used to determine protein concentration using the Bradford assay (245).

For Glycogen determination, equal amounts (350 μ l) of the LSS and LSP, and boiling 50% KOH was added to the samples for a final 30% KOH (v/v), which was heated in a boiling water bath for 30 minutes. The samples were then cooled on ice and quickly centrifuged to collect condensation. Glycogen was then precipitated by adding 2 volumes of -20°C 100% ethanol and 100 μ l of 2% Na₂SO₄, mixed and incubated at -20°C for a minimum of one hour. The glycogen was precipitated two more times, similarly to what is described in the measuring total glycogen content section. Glucose equivalents were then determined.

For Western blot analysis an equivalent volume, based on the protein concentration of the LSS, of the LSP or total extract was used to separate proteins by SDS – PAGE followed by Western blotting (12,189). Typically, 10 – 40 μ g of LSS protein and equivalent samples of LSP or total extracts were loaded on to 10% SDS-PAGE gels. Proteins were separated by electrophoresis, 180 volts for 45 minutes, and transferred to a 0.45 μ m nitrocellulose membrane at 15 volts overnight at 4°C. Nitrocellulose membranes were then stained with Ponceau S (0.5% Ponceau S in 1% glacial acetic acid) to monitor loading and proper transfer of proteins to the membrane. Membranes were destained with H₂O and blocked with 5% non-fat milk powder in 1X Tris-buffered saline, consisting of 50 mM Tris-HCl, 150 mM sodium chloride, pH 7.6 with 0.1% Tween-20 (TBST). Various antibodies were used to probe the membranes for proteins by incubating the membranes in a solution containing the antibody of interest diluted into 2% non-fat milk powder solution in 1X TBST and incubated

for 3 hours at room temperature or overnight at 4°C. Following incubation with antibodies, the membranes were washed three times for 10 minutes with 1X TBST. Secondary antibodies, conjugated to horseradish peroxidase, diluted in 2% non-fat powdered milk solution in 1X TBST, were incubated at room temperature for one hour followed by 3 washes in 1X TBST. Detection of antibodies was achieved by chemiluminescence using the Pierce ECL Western blot substrate. The levels of proteins were quantitated by densitometric analysis of the autoradiograph using Quantity One Software (BioRad).

Antibodies used were the following: glycogen synthase (Cell Signaling Technology #3886), laforin (Abnova, H00007957-M02), phospho-glycogen synthase (3a), AMP activated protein kinase α subunit (AMPK) and pAMPK (Thr172) (Cell Signaling Technology #3891, #2532 and #2535 respectively).

8.1 Branching Analysis of Purified Glycogen and Glycogen in the Low Speed Supernatant and Low Speed Pellet

Total purified glycogen or glycogen from the low speed supernatant and pellets were prepared as described above, except that 700 – 800 mg of skeletal muscle from 9-10 month old male wild type and laforin^{-/-} or malin^{-/-} mice were used. Once the LSS and LSP were prepared, the glycogen was purified and measured as described above. Glycogen solutions were prepared, 100 μ l of a 1 mg/ml glycogen, and treated with 25 μ g/ml isoamylase (Sigma, 15284-5MU) in 100 mM NaOAc pH 4.0 or 4.8 and incubated for 16 hours at 42° C. The reaction was terminated by heating in a boiling water bath for 5 minutes, cooled on ice and centrifuged at 14,000 x g to remove any denatured proteins. After centrifugation, the supernatant was transferred into a new tube. A sample of the reaction was diluted 10 x with water and filtered through a centrifuge spin filter (Costar SpinX) and loaded onto a Dionex ICS3000 high performance anionic exchange chromatography (HPAEC) for branching analysis. The glucose polymer chains were then separated by the HPAEC as previously described (238). Briefly, 2.5 μ g of the debranched glycogen was loaded on to a PA200 column with a mobile phase of 100mM NaOH, eluent A, and eluted with a eluent

B, 100mM NaOH and 1M NaOAc with a continuous gradient of 0 – 50% eluent B over 60 minutes with a flow rate of 0.3 ml/min. Data is analyzed as relative peak area, the product of the individual area over the sum of all peak areas. Figure 11 shows HPAEC branching analysis of purified glycogen from WT LSS and laforin-/- LSP.

9. Synthesis of [β - 32 P]UDP-Glucose

The synthesis of [β - 32 P]UDP-glucose was conducted in two different ways, each of which followed a similar protocol to that described previously (16,246). The procedure was conducted either in a one step reaction where all the enzymes and substrates were added together or a two-step reaction, where the hexokinase reaction was carried out first, terminated and transferred to a new tube for the second set of enzymatic reactions.

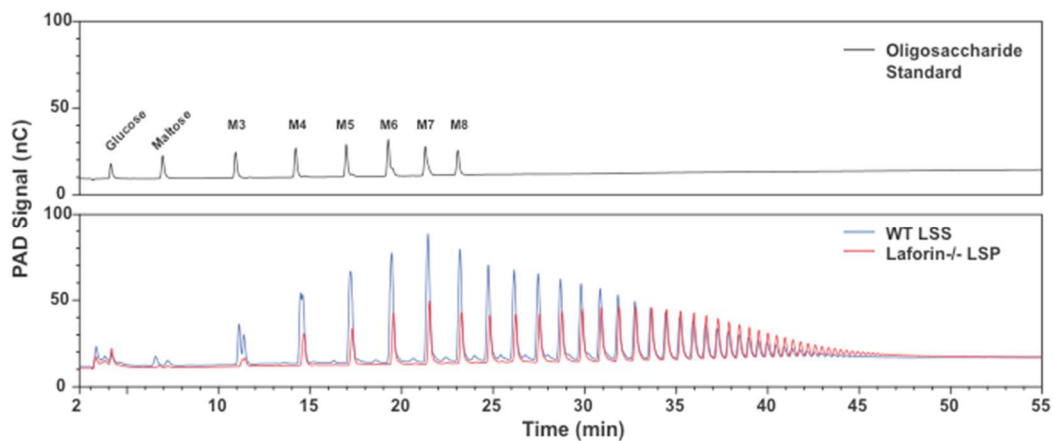


Figure 11. HPAEC branching analysis. High performance anionic exchange chromatography (HPAEC) chromatograph of isoamylase treated glycogen. The top panel is a chromatograph of glucose – maltooctoase (M8) and the bottom panel is a chromatograph of glucose polymer chains from isoamylase treated glycogen from either WT LSS glycogen (blue line) or laforin-/- LSP (red line).

9.1 One Step Reaction

The one step enzymatic synthesis of [γ - ^{32}P]UDP-glucose was carried out in a single tube that contained ~ 1.5 mCi of [γ - ^{32}P]ATP (Perkin Elmer), which was dried under nitrogen. The dried [γ - ^{32}P]ATP was dissolved in 160 μl of a 1.25X reaction mixture, which consisted of 62.5 mM Tris-HCl pH 7.6, 6.25 mM glucose, 7.5 mM MgCl_2 , 1 mM UTP, 1.125 mM DTT, 0.016 U/ μl pyrophosphatase (Roche), 0.038 U/ μl phosphoglucomutase (PGM) (Megazyme) and 17 $\mu\text{g/ml}$ of *Leishmania* UDP-glucose-pyrophosphorylase (LMUGP). The LMUGP recombinant enzyme was produced and purified by Dr. Vimbai M. Chikwana as previously described (247). The reaction was started by adding 40 μl of hexokinase (Roche) for a final concentration of 0.03 U/ μl , which brought all other reaction components to a final 1X concentration and was incubated at 30°C for 2 hours. The reaction was terminated by placing the reaction in a boiling water bath for 5 minutes, cooled on ice and centrifuged for 10 minutes at 15,000 x g at 4°C to pellet denatured proteins. [β - ^{32}P]UDP-glucose was purified from the reaction mixture as described below.

9.2 Two Step Reaction

The two step reaction was used for the majority of the [β - ^{32}P]UDP - glucose production because the yields were better than that of the one step reaction ($\sim 50\%$ vs $\sim 70\%$ respectively). One main difference between the two step and the one step reaction is that in the two step reaction cold ATP was added to the reaction mixture to yield more UDP-glucose total mass, which may have contributed to the higher yields with this method. The first step in the synthesis of [β - ^{32}P]UDP-glucose was to dry ~ 1.5 mCi of [γ - ^{32}P]ATP under nitrogen. The dried [γ - ^{32}P]ATP was then dissolved in 80 μl of 1.25X hexokinase reaction mixture, which consisted of 62.5 mM Tris-HCl pH 7.6, 6.25 mM glucose, 7.5 mM MgCl_2 and 31.25 μM ATP. To start the reaction, 20 μl of hexokinase was added for a final concentration of 0.03 U/ μl and all other reaction components were brought to a final 1X concentrations (100 μl of 50 mM Tris-HCl

pH 7.6, 5 mM glucose, 6 mM MgCl₂ and 25 μM ATP). The reaction was incubated at 30°C for one hour and terminated by heating in a boiling water bath for 5 minutes. The reaction was then cooled on ice and centrifuged for 10 minutes at 15,000 x g at 4°C. The reaction mixture was then transferred to a new tube and the remaining synthesis components were added for a final 200 μl reaction containing 50 mM Tris-HCl pH 7.6, 6 mM MgCl₂, 0.9 mM DTT, 0.8 mM UTP, 0.013 U/ μl pyrophosphatase, 0.03 U/ μl PGM and 0.136 mg/ml LMUGP. The second step of the reaction involved incubation at 30°C for one hour and termination by heating in a boiling water bath for 5 minutes. The reaction was then cooled on ice and centrifuged for 10 minutes at 15,000 x g at 4°C to pellet denatured proteins. [β -³²P]UDP-glucose was purified from the reaction mixture as described below.

9.3 Purification of [β -³²P]UDP-glucose

Once the enzymatic reactions were terminated, centrifuged and the supernatant removed, [β -³²P]UDP-glucose was purified by binding to ~7 mg of activated charcoal, vortexing for 1 minute and incubating on ice for 10 minutes. The charcoal was collected by centrifugation at 15,000 x g for 2 minutes at 4°C. The supernatant was removed and the activated charcoal was washed 3 times with 1ml each of ice cold MiliQ water. The mixture was vortexed for 30 seconds, centrifuged at 15,000 x g for 2 minutes at 4°C and the supernatant was removed. After three washes, the [β -³²P]UDP-glucose was eluted by adding 200 μl of elution buffer, 0.16 M NH₄OH in 50% (v/v) ethanol, vortexing for 30 seconds and centrifugation at 15,000 x g for 2 minutes at 4°C for a total of 4 elutions. After each elution, the supernatant was removed and transferred to a new tube; all eluates were combined. To remove any residual charcoal, the eluates were once again centrifuged and the supernatant was passed through a Costar Spin-X Centrifuge Tube Filter that had been equilibrated with the elution buffer. The filtered eluates were then completely dried in a Speed Vac and the dried material was dissolved in 100 μl of 10 mM Tris-HCl pH 7.5, aliquoted and stored at -80°C.

10. Radiolabeling and Visualization of Glycogen

Purified rabbit skeletal muscle (RSM) glycogen was labeled with recombinant yeast or human glycogen synthase essentially as described previously (16). A 1.25 x glycogen synthase reaction mixture was prepared which was composed of 62.5 mM Tris-HCl pH 7.8, EDTA 6.25 mM, glucose-6-phosphate (G6P) 9 mM, RSM glycogen at 8.3 mg/ml, UDP-glucose added to a concentration of 2 - 5 μ M with a specific activity of 330-400 cpm/pmol for UDP-[U¹⁴C]-glucose and 75,000-260,000 cpm/pmol for [β -³²P]-UDP-glucose. For control samples, an aliquot of the 1.25 x reaction mix was taken and GS dilution buffer (50 mM Tris-HCl pH 7.8, 0.1% RSM glycogen and 1 mM DTT) was added for a final 1 x reaction mixture (50 mM Tris HCL pH7.8, 5 mM EDTA, 7.2 mM G6P, 6.7 mg/ml RSM glycogen, and 2-5 μ M of UDP-[U¹⁴C]-glucose or [β -³²P]-UDP-glucose). Glycogen synthase reactions were incubated at 30°C with 2 – 5 μ g/ml yeast glycogen synthase or 20 μ g/ml human glycogen synthase. At given time points, a sample of the glycogen synthase reaction was taken and terminated by heating in a boiling water bath for 5 minutes, then cooled on ice and centrifuged to collect condensation. From each time point, samples were taken for thin layer chromatography (TLC) analysis, typically ~5 μ l. From the remaining reaction sample, glycogen was precipitated by adding two-volumes of cold (-20°C) 100% ethanol, as well as Na₂SO₄ and LiCl to a final concentration of 2.8 mM and 20 mM respectively to aid in precipitation. The samples were then mixed and incubated at -20°C for a minimum of 4 hours to allow for precipitation, heated in a boiling water bath for 2 minutes, cooled on ice for 10 minutes, centrifuged at 15,000 x g for 30 minutes, and the supernatant was removed. The glycogen pellet was dried with a Speed Vac and dissolved in water or buffer as needed, typically to the original sample volume. If further precipitations were required, two volumes of cold 100% ethanol were added and LiCl was added to a final concentration of 2 mM. For SDS-PAGE, the glycogen pellets were dissolved in 25 μ l of water or buffer and 1/5 of the volume of 5 x SDS loading buffer (60 mM Tris-PO₄ pH 6.8, 40% glycerol, 5% SDS (Figure/v), 0.08% Bromophenol Blue, and 5%(v/v) β -mercaptoethanol) was added. The samples were then

heated in a boiling water bath for 5 minutes and loaded into wells of a 10% polyacrylamide gel with a 4% stacking gel. Loading corresponded to 250 – 375 μg of the initial glycogen present in the reactions. Gels were developed at 180 V for ~45 minutes. Following electrophoresis gels were incubated in a solution containing 20% methanol (v/v) and 5% glycerol (v/v) for a minimum of 10 minutes. The gels were then dried and imaged with a FujiFilm FLA-5100 Phosphorimager.

11. Treatments of ^{32}P - and ^{14}C -labeled glycogen

^{32}P - and ^{14}C -labeled glycogen produced by glycogen synthase reactions was purified through ethanol precipitation(s) and subjected to various additional treatments prior to analysis by SDS-PAGE.

11.1. Glucosidase and Laforin Treatment of Labeled Glycogen

Rabbit skeletal muscle glycogen labeled with UDP-[U- ^{14}C]glucose or [β - ^{32}P]UDP-glucose was purified by ethanol precipitation and digested with a mixture of α -amylase and amyloglucosidase or treated with either mouse recombinant WT or the catalytically inactive C266S laforin, similar to what has been previously described (16). Following ethanol precipitation, glycogen was dissolved in water and adjusted to 20 mM NaOAc, pH 4.8 for glucosidase or laforin treatment. The glycogen was incubated with 25 – 50 $\mu\text{g}/\text{ml}$ of recombinant laforin at 37°C for 2 hours. For glucosidase treatment, glycogen was incubated with or without 0.3 mg/ml of both α -amylase and amyloglucosidase at 42°C for 2 hours. Reactions were terminated by heating in a boiling water bath for 5 minutes, cooled on ice and centrifuged to collect condensation. For analysis of $^{32}\text{P}_i$ release, ^{32}P -glycogen was purified by ethanol precipitation, treated with PiBind™ resin, described below, and subjected to gel filtration. The PiBind™ resin binds and removes free phosphate from samples. This step was added to minimize inorganic phosphate contamination of the ^{32}P -glycogen. In fact, we observed that the resin also chelated and removed UDP and UDP-glucose (data not shown).

11.2. Treatment of glycogen with PiBind™ Resin

Radio labeled glycogen was first purified by ethanol, dissolved in 120 μ l of water and treated with PiBind™ resin (Innova Biosciences, 501-0051), in order to remove contaminating $^{32}\text{P}_i$. For treatment with PiBind™ resin, 20 μ l of settled resin was washed with 200 μ l water in a 1.5 ml tube by mixing and the resin was pelleted by centrifugation (1,000 x g for 1 minute at 16°C). The water was completely removed with an insulin syringe. 120 μ l of water was added to the tubes, with and without PiBind™ resin. The dissolved glycogen was added to the tubes (75 μ l) and incubated at room temperature, 25°C with rocking on a Nutator for 1 hour. Samples were then transferred to a spin column and centrifuged for 2 minutes at 1,000 x g at 4°C and the flow through was collected in a new tube. The flow through was then dried using a Speed Vac and the glycogen was dissolved in buffer or water for further treatment or TLC analysis.

11.3. Spin Column and Gel Filtration

Glycogen synthase reactions were carried out as previously described to obtain the ^{14}C and ^{32}P labeled glycogen, and a sample was taken for TLC analysis. An equal volume of water was added and LiCl and Na_2SO_4 were added and glycogen was precipitated with ethanol, as described above. The samples were incubated at -20°C for a minimum of 4 hours, heated in a boiling water bath for 2 minutes, cooled on ice for 10 minutes and centrifuged at 15,000 x g for 30 minutes at 4°C. The supernatant was removed and the pellet was dissolved in H_2O 2X the original volume, LiCl was added for a final 6 mM and the sample was again precipitated with cold ethanol and incubated at -20°C for a minimum of 4 hours. The samples were again heated in a boiling water bath, cooled on ice, centrifuged and the supernatant was removed. The glycogen pellet was dried in a Speed Vac and dissolved in 150 – 160 μ l of 10 mM Tris-HCl pH 7.5.

Once the glycogen was completely dissolved, the sample was split and 70 μ l was transferred to a tube as a “before column” sample and 70 μ l was added to a spin column (Promega) containing ~1 ml of packed Sephadex G50 (Sigma), which had been equilibrated with 10 mM Tris-HCl pH 7.5. Prior to adding the

sample to the spin column, excess buffer was removed by centrifuging the column at 1,000 x g for 1 minute at 16°C. The sample was loaded onto the G50 resin, centrifuged at 1,000 x g for 1 minute at 16°C and the flow through collected, and referred to as the "after column" sample. Both the samples before and after column were dried in a Speed Vac and dissolved in 25 µl of 10 mM Tris-HCl pH 7.5. Once the glycogen was dissolved 20 µl of the sample was taken and 5 µl of 5X SDS loading buffer was added, heated in a boiling water bath for 5 minutes, and 275 – 375 µg of glycogen was loaded on a SDS page gel. The gel was then dried, using a gel dryer and imaged with a phosphorimager. The remaining 5 µl of sample was used for TLC analysis and scintillation counting.

11.4. Hydrolysis of UDP with Recombinant Human Soluble Calcium-Activated Nucleotidase (hSCAN-1)

hSCAN-1 is a nucleotidase that converts UDP to UMP but does not act on UMP (248,249) or UDP-glucose and glucose-6-P (data not shown). ³²P- and ¹⁴C-labeled glycogen was purified by three ethanol precipitations. After the last precipitation, the glycogen pellet was dried in a SpeedVac and dissolved in 50 mM Tris-HCl pH 7.5, 0.05% (v/v) Tween-20, and incubated at 37°C for 30 min with or without 1.2 µg/ml hSCAN-1 plus 2 mM CaCl₂. The reactions were terminated by boiling and processed for SDS-PAGE as described above. In other experiments, the glycogen synthase reactions were terminated by boiling, 2 mM UDP was added and the samples incubated at 37°C for 30 min with or without 1.2 µg/ml hSCAN-1 plus 2 mM CaCl₂ in excess of the EDTA concentration, final 7 mM CaCl₂. Samples were then analyzed by TLC and/or SDS-PAGE.

11.5 Competition with Unlabeled UDP

³²P- and ¹⁴C-labeled glycogen was purified with three cycles of ethanol precipitation and dissolved in 50 mM Tris-HCl pH 7.5, 0.05% (v/v) Tween-20. Once the glycogen was completely dissolved, 2 mM UDP was added, 1000-fold excess compared to labeled UDP-glucose, and incubated at room temperature

for 30 min. In other experiments, the UDP was added prior to ethanol precipitation. Samples were then processed and analyzed by SDS-PAGE.

11.6 Binding of ^{32}P -UDP to glycogen

Rabbit skeletal muscle glycogen at 6.7 mg/ml was incubated in 50 mM Tris-HCl pH 7.8, 5 mM EDTA, 7.2 mM glucose-6-P, 1 μM UDP-[U- ^{14}C]glucose (specific activity ~ 450 cpm/pmol), with or without 4 μM [α - ^{32}P]UDP (specific activity of $\sim 100,000$ cpm/pmol), the reaction was started by adding recombinant yeast glycogen synthase (10 $\mu\text{g}/\text{ml}$) or buffer as a control and incubated for 60 min at 30°C . The reactions were then terminated by boiling for 5 min, cooled on ice, and the glycogen precipitated with ethanol as described above. The glycogen was dried in a Speed Vac and dissolved in 48 μl of water, 5 mM UDP or 20 mM NaOAc pH 4.8 for glucosidase digestion. Amyloglucosidase and α -amylase, each at 60 $\mu\text{g}/\text{ml}$, were added and incubated overnight at 40°C , other samples were kept at -20°C during the overnight digestion. All samples were boiled for 5 min, cooled on ice and analyzed by SDS-PAGE.

12. Thin Layer Chromatography

High-performance thin layer chromatography (HPTLC) plates (Merk, Silica gel 60 F₂₅₄) were used for TLC analysis of hSCAN-1 action towards nucleotides. One or two μl of sample was spotted on the plate which was developed by ascending chromatography with n-propanol:ethyl acetate:water (7:1:4). Plates were laid flat and allowed to air dry at room temperature. Visualization of radioactivity was achieved by using a phosphorimager or by exposing the plates to X-ray film. For visualization of UV signal, TLC plates were placed under a UV lamp ($\lambda = 254$ nm), the UV absorbing areas, where nucleotides are present were marked, and the plates were photographed. $^{32}\text{P}_i$ release from ^{32}P -glycogen by laforin was analyzed using polyethyleneimine (PEI) cellulose plates (Merck, 1.05725.0001) and developed by ascending chromatography with 1M acetic acid: 3M LiCl (9:1). Plates were air dried and imaged as described above.

13. Recombinant Laforin Purification and Reactions

13.1 Purification of Recombinant His-Tagged Laforin

Recombinant His-tagged laforin, wild type or C266S mutant, was expressed in *Escherichia Coli* and purified by affinity chromatography using Ni-NTA agarose essentially as previously described by Wang and Roach (178). *E. Coli* transformed with a N-terminal His-tagged recombinant laforin was grown in a starter culture, 10 ml of Luria broth (LB) containing 50 µg/ml of kanamycin, overnight at 37°C with shaking. The starter culture was then added to 1 L of LB broth with 50 µg/ml of kanamycin and grown to an OD_{600nm} of ~0.500 at 37°C. Once the OD was reached, the culture was induced with 2 mM isopropyl β-D-1 thiogalactopyranoside (IPTG) and incubated overnight at 18°C to induce protein production. The cells were collected by centrifugation at 10,000 x g for 10 minutes at 4°C, the supernatant was decanted, the cell pellet washed by resuspending in PBS, re-centrifugation and the PBS was decanted. The cell pellet was then snap frozen in liquid nitrogen and stored at -80°C. Buffers used were as follows: 1) Lysis buffer consisted of 50 mM Tris – HCL pH 8.0, 300 mM NaCl, 20 mM imidazole, 1 mM benzamide, 1 mM PMSF, 1 µg/ml aprotinin, 1 µg/ml leupeptin, 1 µg/ml pepstatin and 0.05% β-mercaptoethanol. 2) Imidazole wash buffer, 50 mM Tris – HCL pH 8.0, 300 mM NaCl and 50 mM imidazole. 3) Elution buffer, 50 mM Tris – HCL pH 8.0, 300 mM NaCl and 250 mM imidazole. Ni-NTA agarose beads were equilibrated by washing 3 ml of packed beads with 10 ml of ice cold water 3 x followed by one 10 ml wash with the lysis buffer minus the protease inhibitors. After the wash with the lysis buffer, the beads were maintained in lysis buffer.

The frozen cell pellets were re-suspended in 20 ml lysis buffer and passed through a French press three times or until the lysate was fluid, then Triton X-100 was added for a final 0.5% (v/v) concentration and the lysate was incubated on ice for 5 minutes. The lysate was clarified by centrifugation at 20,000 x g for 20 minutes at 4°C and the supernatant was removed and placed in a column containing equilibrated Ni-NTA agarose and was rocked on a Nutator at 4°C for 2

hours. The lysate was allowed to flow out of the column and collected. The beads were washed 2-times with lysis buffer containing 0.5% (v/v) Triton X-100 without protease inhibitors and once with the imidazole wash buffer. All washes used 10 ml of the given solution with a flow rate of 1 ml/minute. Elution of the His-tagged laforin was achieved by applying 10 ml of the elution buffer to the column and after one ml of liquid had exited the column, it was clamped to allow the beads to equilibrate with the elution buffer for 5 minutes after which the clamp was removed and 1 ml fractions were collected at a flow rate of 0.5 ml/min. Each fraction was then transferred to 12-14,000 MW cutoff dialysis tubing and dialyzed at 4°C against 4 L of dialysis buffer consisting of 50 mM Tris – HCL pH 8.0 with 2 mM DTT and dialyzed overnight with constant stirring. Samples were then analyzed by SDS-PAGE gel, stained with Coomassie blue, destained and dried to estimate protein purity. The fractions, which contained purified laforin and had activity toward *pNPP*, were pooled and concentrated using an Amicon Ultra centrifugal filter with a 10,000 molecular weight cutoff and centrifuged for 5 minutes at 3,000 x g at 4°C. Protein concentration was determined by the Bradford assay and activity was measured against *pNPP* and purified oligosaccharides, described below.

13.2 Laforin Phosphatase Activity using *pNPP* as a Substrate

Hydrolysis of *p*-nitrophenylphosphate (*pNPP*) was performed in a 100 µL reaction volume containing phosphatase buffer, 500 mM NaOAc, 250 mM Bis-Tris, 250 mM Tris - HCL pH 6.5, with 15 µg/mL recombinant laforin and varying amounts of *pNPP*, 0 – 30 mM. Reactions were incubated at 37°C for 5 minutes and terminated by adding 400 µl of 0.25 M NaOH. An additional 500 µl of water was added and the absorbance was read at 410 nm. Activity was measured by the extinction coefficient of *pNPP* as 18.3 mM⁻¹cm⁻¹.

13.3 Dephosphorylation of Phospho-oligosaccharides with Laforin and HPAEC Analysis

Phospho-oligosaccharides purified from either rabbit skeletal muscle or from amylopectin were used as substrates for laforin, similarly to what was described by Tagliabracci et al. (16). The reaction consisted of phosphatase buffer or of 100 mM NaOAc pH4.8, with 10 – 100 μ M of phospho-oligosaccharides, based on phosphate content. The reactions were started by the addition of recombinant laforin, either wild type or C226S catalytically inactive, at 25 – 50 μ g/ml and incubated in a 37°C for a minimum of one hour, terminated by heating in a boiling water bath for 5 minutes and cooled on ice. Denatured protein was pelleted by centrifugation at 17,500 x g for 10 minutes at 4°C. The supernatant was then filtered through a Costar SpinX column. Phosphorylated oligosaccharides, 0.25 – 2.5 nmols, from rabbit skeletal muscle glycogen and amylopectin were analyzed by high performance anionic chromatography (HPAEC) using a Dionex ICS3000 with a PA200 column and detected by pulse amperometric detection. Phospho-oligosaccharides were loaded based on phosphate concentration and 2.5 nmol were analyzed. Standards, 2.5 nmol, of glucose, maltose, maltotriose, maltotetraose, maltopentaose, maltohexaose, maltoheptaose, and maltooctaose were also analyzed using the HPAEC. All samples and standards were filtered through a Costar Spin-X spin filter (Coastar Spin-X, 8160) prior to being loaded into a 25 μ l injection loop. Eluent A consisted of 100 mM NaOH and eluent B consisted of 100 mM NaOH and 1 M NaOAc. Phospho-oligosaccharides and standards were eluted off the PA200 column using a continuous gradient of eluent B from 0-50% over 60 minutes with a flow rate of 0.350 ml/min.

13.4 Assay of Potential Laforin substrates by HPAEC Analysis

Uridine diphosphate and UDP-glucose were treated with laforin to determine whether laforin is capable of hydrolyzing the phosphate ester bonds in these compounds. Reaction mixtures with recombinant WT laforin or C226S laforin contained 25 μ g/ml of each enzyme, 20 mM NaOAc pH 4.8 and 2.5 mM of

either UDP or UDP-glucose. The reactions were incubated at 37°C for 2 hours and were terminated by heating in a boiling water bath for 5 minutes. A sample of the reaction was taken and diluted to 50 μ M of either UDP or UDP-glucose. The samples were then passed through a centrifuge filter (Coastar Spin-X, 8160) and the sample was loaded on to a Dionex high-performance anion exchange chromatography (HPAEC) ICS 3000 and 25 μ l of the sample was loaded onto a PA200 column. The mobile phase, eluent A, consisted of 100 μ M NaOH and the nucleotides were eluted off the column with Eluent B, 100 μ M NaOH/1M NaOAc, with a gradient set at 20 – 50% from 0 – 10 minutes, 55 – 85% from 10 – 35 minutes and from 85 – 100% from 35 – 40 minutes and flow rate of 0.30 ml/min. The nucleotides were detected by UV absorption at 262nm.

14. Phosphooligosaccharide Purification and Analysis

The procedure was as previously reported by Tagliabracci et al (16). Rabbit skeletal muscle, purified by the TCA method and KOH method, or amylopectin was extensively digested with α -amylase and amyloglucosidase. Rabbit skeletal muscle glycogen, approximately 250 mg, was first dissolved in 2.4 ml of water then CaCl_2 and a mixture of α -amylase and amyloglucosidase was added for a final volume of 3 ml with final concentrations of 1 mM CaCl_2 and 300 μ g/ml of each enzyme in 10 mM NaOAc pH 4.8. For amylopectin, approximately 250 mg was dissolved in 2.4 ml of 1.25% DMSO and CaCl_2 , α -amylase and amyloglucosidase, and NaOAc were added to a final volume of 3 ml with equal concentrations as described above. The reaction was incubated overnight at 42°C, centrifuged at 10,000 x g for 5 minutes to remove any insoluble material and the supernatant was transferred to 2 ml screw cap tubes. The supernatant was then placed in a boiling water bath for 5 minutes, cooled on ice and centrifuged for 10 minutes, 15,500 x g at 4°C. The supernatant was added to 2 ml (bed volume) DEAE Sepharose that had been extensively washed with ice cold H_2O , equilibrated with 10 mM NaOAc pH 4.8 and placed on a Nutator at 4°C overnight. The DEAE Sepharose resin mixture was transferred to a 3 ml column, washed with 40 ml of H_2O , and the flow rate was adjusted to 0.5

ml/minute. Phosphorylated species were eluted stepwise, collecting 1 ml fractions, with 4 ml of 10 mM, 50 mM, 100 mM, 500 mM and 1 M of NH_4HCO_3 . From each fraction an aliquot of 75-100 μl was taken for phosphate determination. Briefly, 25-30 μl of the aliquot taken from each fraction was transferred to borosilicate glass tubes in triplicate, one non-hydrolyzed and two hydrolyzed, which were then dried in a Speed Vac. For hydrolysis, 40 μl of a 3:1 solution of 60% HClO_4 :10N H_2SO_4 was added to the glass tubes and incubated at 190°C for 2 hours. Phosphate amounts were determined using the Malachite green assay described above. Fractions containing phosphate were pooled, dried in a Speed Vac and re-suspended in water for a final concentration of 1 mM of phosphate for NMR analysis. Figure 12 shows the phosphate content of each elution.

14.1 HPAEC Analysis of Phospho-Oligosaccharides

phosphorylated oligosaccharides, 2.5 nmol based on phosphate concentration, from rabbit skeletal muscle glycogen and amylopectin were analyzed by HPAEC using a Dionex ICS3000 with a PA200 column and detected by pulse pulsed amperometric detection. All samples were filtered through a spin filter before loading into a 25- μl injection loop. Eluent A consisted of 100 mM NaOH, and eluent B consisted of 100 mM NaOH and 1 M NaOAc. Phospho-oligosaccharides and standards were eluted from the PA200 column using a continuous gradient of eluent B from 0-to 50% over 60 min at a flow rate of 0.35 ml/min. Polyglucose standards from glucose up to maltooctaose were also analyzed at 0.25 nmol of each.

14.2 Analysis of Phospho-oligosaccharides by Mass Spectrometry

MALDI-TOF-MS analysis was performed by the Complex Carbohydrate Research Center, The University of Georgia essentially as previously describe (16). Briefly, 1 μL of 1 mM phosphate of purified phosphorylated oligosaccharides was mixed with the same volume of matrix solution containing 2,4,6-

trihydroxyacetophenone and spotted onto a MALDI plate. The analysis was performed in reflector negative ion mode. All spectra were obtained using a Microflex LRF (Bruker).

14.3 Analysis of Phospho-oligosaccharides by NMR Spectroscopy

NMR analysis was performed by the Complex Carbohydrate Research Center, The University of Georgia essentially as previously described (16). Phospho-oligosaccharides from glycogen and from amylopectin were lyophilized and deuterium-exchanged by lyophilization from D₂O (99.9% deuterium; Sigma), dissolved in D₂O (99.96% deuterium, Cambridge Isotope), and transferred to a 5-mm NMR tube with magnetic susceptibility plugs matched to D₂O (Shigemi). Proton-proton (correlation spectroscopy (gCOSY), total correlation spectroscopy (zTOCSY), rotating frame nuclear overhauser effect spectroscopy (ROESY)) and proton-carbon (gHSQC) correlated spectra were acquired on a Varian Inova 600-MHz spectrometer equipped with a 5-mm cryoprobe, and proton-phosphorus-correlated spectra were acquired on a Varian Inova 500 MHz spectrometer equipped with an 8-mm XH room temperature probe. All spectra were taken at 25 °C. Proton chemical shifts were referenced to internal acetone ($\delta = 2.218$ ppm) (250). Carbon and phosphorus chemical shifts were referenced using the absolute chemical shift scale with Ξ values of 0.25144953 (¹³C) and 0.40480742 (³¹P) in MNova. All experiments except the ¹H,³¹P-correlated spectra were acquired with standard Varian pulse sequences. For ¹H,³¹P-correlated experiments, the regular HMQC and HMQC-TOCSY experiments were modified for ³¹P in the X channel, with a π pulse of 13.5 μ s at a level of 60 db and a ³J_{H-P} coupling constant of 7 Hz. The spectral width was 2000 Hz in f2 and 8000 Hz in f1. 24 increments were acquired with 512 transients each. Acquisition time was 300 ms, and the mixing time in the ¹H,³¹P-HMQC-TOCSY experiment was 60 ms. The gCOSY experiment was acquired in 8 transients and 400 increments, with an acquisition time of 150 ms. The zTOCSY experiment was acquired in 16 transients and 128 increments, with an acquisition time of 150 ms and a mixing time of 80 ms. The ROESY experiment was acquired in 16 transients and 128

increments, with an acquisition time of 150 ms and a mixing time of 200 ms. For the $^{13}\text{C}, ^1\text{H}$ gHSQC with adiabatic 180-degree carbon pulses experiment, the spectral width was 3378 Hz in f2 and 10555 Hz in f1. 64 increments were acquired with 200 transients each. The acquisition time was 150 ms, and the 1-bond C-FIGURE coupling constant was set to 140 Hz. The sample was 280 ml of a solution 2 mM with respect to phosphate. The raw data were processed in MNova using a 7-Hz gaussian function in f2 and a 90° -sine² function in f1 ($^1\text{H}, ^{31}\text{P}$ spectra) and 7- and 80-Hz Gaussian functions in f2 and f1 ($^{13}\text{C}, ^1\text{H}$ spectra), respectively, as well as linear prediction in f1.

15. Recombinant Glycogen Branching Enzyme Purification

Purification of mammalian N-terminally glutathione S-transferase (GST) tagged human glycogen branching enzyme (GST-GBE) was as follows. The procedure typically yielded approximately one milligram of purified enzyme from one liter of bacterial culture. *E. Coli* transformed with the GST-GBE were grown in a 10 ml starter culture overnight at 30°C in Luria Broth (LB) with 100 µg/ml of ampicillin. The starter culture was then added to 1 L of Terrific Luria Broth (TLB) with ampicillin, 100 µg/ml and grown at 30° C with shaking until the OD₆₀₀ reached 0.600. At this time, the bacteria culture was placed on ice for 20 minutes to stop growth. The culture was then placed back into the 30° C incubator with shaking and allowed to grow over night, approximately 16 hours. Optimal expression of the GST-GBE was obtained under non-induced, no IPTG, conditions using the TLB media. Cells were collected by centrifugation, 5,000 x g for 10 minutes, washed with PBS and then either immediately lysed or snap frozen and stored at -80° C. The lysis buffer consisted of PBS with protease inhibitors (200 mM PMSF, 1 mM benzamine, 1 µg/ml leupeptin, 1 µg/ml pepstatin, 1 µg/ml aprotonin). The cell pellet was resuspended in 35 ml of lysis buffer, freshly prepared lysozyme was added for a 1 mg/ml concentration and incubated on ice for 2 hours. Cells were then lysed using a French press, and passed through three times. The lysate was then clarified by centrifugation at 10,000 x g for 15 minutes at 4°C, if lysate remained cloudy after initial centrifugation the

sample was centrifuged at 20,000 x g for 30 minutes. The supernatant was then passed over 2 layers of Miracloth, transferred to a 50 ml screw cap tube, 44 mg of swollen GST-Agarose beads, previously washed with water and equilibrated with the lysis buffer, were added to the lysate supernatant and incubated on a Nutator for 1 hour at 4°C. Agarose beads were collected by centrifugation, 10,000 x g for 2 minutes at 4°C. The beads were washed 3 times by resuspending in 10 ml of the wash buffer (50 mM Tris-HCl pH 7.6, 100 mM NaCl, 0.2% Triton X-100, and protease inhibitors), After each wash the beads were collected by centrifugation, 10,000 x g for 2 minutes at 4°C, and the supernatant was transferred to a new tube until the purification process was complete. After the last wash the beads were collected and transferred to a 1.5 ml tube and quickly centrifuged to collect any remaining wash buffer, which was removed. Elution buffer (500 µl), 50 mM Tris-HCl and 200 mM glutathione, was added to the beads, mixed and incubated on a Nutator for 10 minutes at 4°C. The beads were pelleted by centrifugation, the eluted material was transferred to a new tube and the beads were eluted again with 500 µl elution buffer. The eluates were combined and dialyzed using Spectra/Por (Spectrum) 10 mm diameter, 12-14,000 MW cutoff dialysis tubing at 4°C against 50 mM Tris – HCL pH 8.0, 100 mM NaCl and 2 mM DTT. Following dialysis protein concentration was measured and the samples were snap frozen with liquid nitrogen and stored at -80°C

16. Branching Enzyme Activity

16.1 Indirect Branching Enzyme Activity

The glycogen branching enzyme activity was measured indirectly by monitoring the incorporation of [U¹⁴C]-glucose by the actions of either glycogen phosphorylase or glycogen synthase similar to the procedure described by Hawker et al. (251). Phosphorylase b, purified from rabbit skeletal muscle (224), and recombinant yeast glycogen synthase were used to monitor the incorporation of [U¹⁴C]-glucose into glycogen from either [U¹⁴C]-glucose-1-phosphate or from UDP-[U¹⁴C]-glucose for the respective enzymes. As the GBE

introduces branch points, there will be new non-reducing ends for phosphorylase or glycogen synthase to incorporate a new glucose molecule that allows monitoring of the GBE activity indirectly. When using phosphorylase b, a reaction mixture was made at 1.25 x the final concentration and consisted of 125 mM sodium citrate pH 7.0, rabbit skeletal muscle glycogen 1.25 mg/ml, 12.5 mM AMP, 62.5 mM glucose-1-phosphate with a specific activity ~75 cpm/pmol [^{14}C]-glucose-1-phosphate in 500 – 700 μl . The reactions were started by adding a 5 x solution containing 50 mM citrate, 250 $\mu\text{g/ml}$ of GBE and 0.5 mg/ml phosphorylase b. The final reaction mix consisted of 100 mM citrate pH 7.0, rabbit skeletal muscle glycogen 1.0 $\mu\text{g/ml}$, 10 mM AMP, 50 mM glucose-1-phosphate with a specific activity ~60 cpm/pmol [^{14}C]-glucose-1-phosphate, 100 $\mu\text{g/ml}$ phosphorylase b and 50 $\mu\text{g/ml}$ GBE. Reactions using glycogen synthase were prepared similarly and the final reaction conditions consisted of 25 mM Tris-HCl pH 7.6, 5 mM EDTA, 50 mM UDP-glucose, UDP- ^{14}C -glucose specific activity of ~15 cpm/pmol, rabbit skeletal muscle glycogen 100 $\mu\text{g/ml}$, 26 $\mu\text{g/ml}$ recombinant yeast glycogen synthase and 26 - 50 $\mu\text{g/ml}$ GBE in 500 -700 μl . At given time points, 20 μl of the reaction was spotted, in duplicate, on ET3 filter paper and placed in cold, -20°C , 66% (v/v) ethanol to terminate the reaction and wash off any unreacted [^{14}C]-glucose-1-phosphate or UDP- ^{14}C -glucose. The filter papers were washed a total of 3 times, 15 min per wash, in 66% (v/v) ethanol, the first wash at -20°C , 66% (v/v) ethanol and the others at room temperature. A magnetic stirring bar stirred the ethanol. The filter papers were finally washed with acetone for 5 minutes and dried under a heat lamp. [^{14}C]-Glucose incorporation was determined by measuring the radioactivity at the given time points. Figure 13 shows the activity of the GBE using either phosphorylase b or recombinant yeast glycogen synthase.

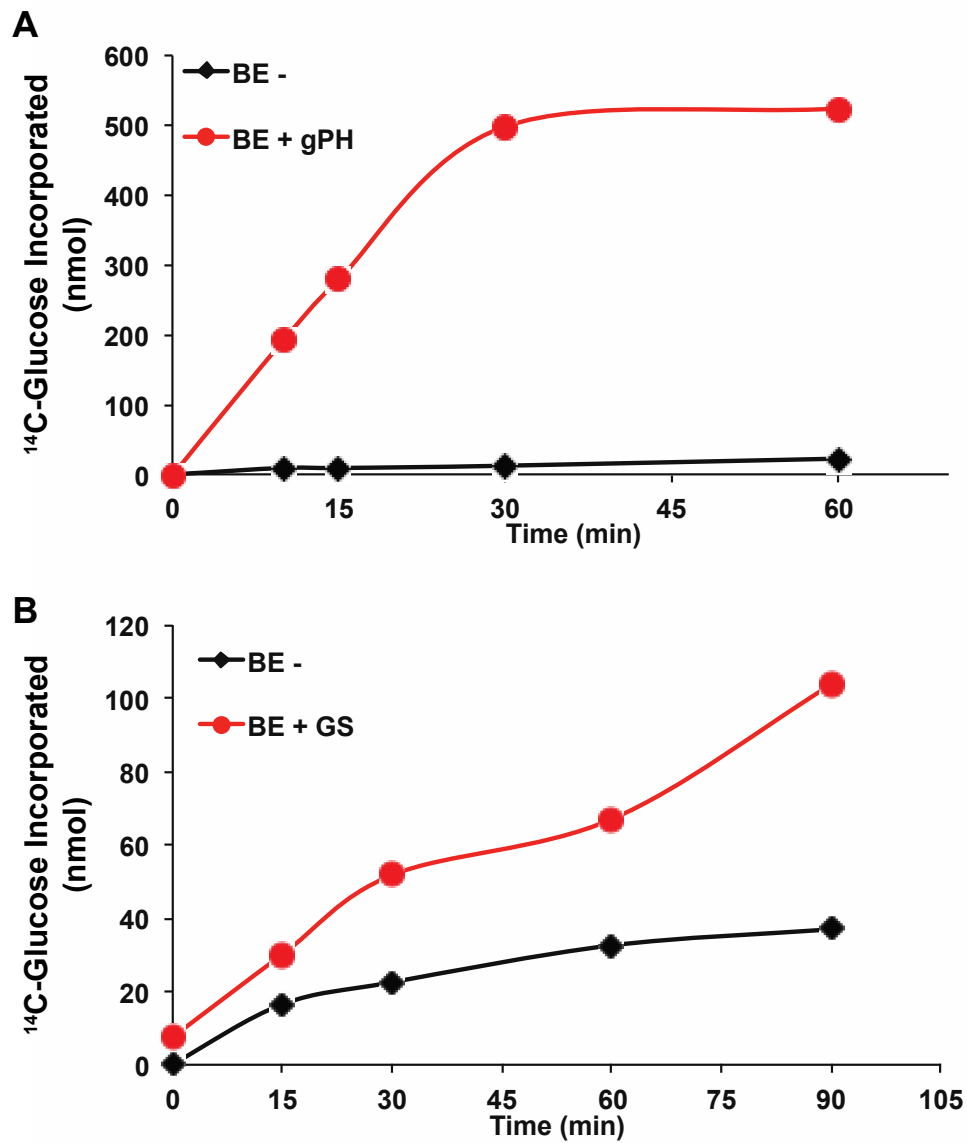


Figure 13. Branching enzyme activity. Branching enzyme activity determined by monitoring the incorporation of ^{14}C -glucose by either glycogen phosphorylase (A) or glycogen synthase (B).

16.2 Branching Enzyme Activity Using Amylose and HPAEC

Monitoring the changes in oligosaccharide chain length with HPAEC analysis provides a means to monitor the activity and determine the chain length. The procedure was similar to that described by Devillers et al (252). Reactions could either be set up to monitor the action of the GBE as a function of time, enzyme concentration or substrate concentration. The reaction mixtures were prepared in 50 mM Tris-HCl pH 7.6, 1 – 5 mg/ml amylose and started by adding the GBE for a final 70 $\mu\text{g/ml}$, which could also vary depending on the experiment, in 100 μl . The amylose used in the experiments was dissolved in a 1 N NaOH solution at 50 mg/ml, which was diluted to 10 mg/ml with 50 mM Tris – HCL pH 7.6 and was neutralized with 1 N HCl to pH 7.6. After neutralization the amylose was added to the GBE reaction. At given time points, samples were removed and heated in a boiling water bath for 5 minutes to terminate the reaction, cooled on ice and quickly centrifuged to collect condensate. Debranching by isoamylase was carried out by adding one volume, typically 50 μl , of isoamylase in NaOAc buffer for a final of 200 mM NaOAc pH 3.5 with 20 $\mu\text{g/ml}$ isoamylase, which was incubated at 40°C overnight. Reactions were terminated by heating in a boiling water bath for 5 minutes, cooled on ice and centrifuged, 15,500 x g for 10 minutes at 4°C to collect condensate and pellet denatured proteins. The supernatant was transferred to a new tube and diluted to 0.1 mg/ml of initial amylose concentration, filtered through a Coastar SpinX spin column and 25 μl of the resulting glucose polymers were loaded onto a PA1 or a PA-200 column and separated by high-performance anion exchange chromatography (HPAEC) using a Dionex ICS3000 with pulsed amperometric detection. For standards, from monomeric glucose to maltooctose, 25 μl of a 0 – 10 μM solution was loaded on to the column for quantitation. Eluent A consisted of 100 mM NaOH and eluent B 100 mM NaOH with 1M NaOAc. The samples were eluted with a continuous gradient from 0%–50% of Eluent B over 60 min with a flow rate of 0.3 ml/min. Data was expressed as the sum of the integral of a given polymer length divided by the sum of all polymer signals, shown as a relative peak area. Additionally, the

relative peak area can be plotted as a change in a given peak area by normalizing to a control sample that did not contain the GBE.

17. Measuring Reducing Ends of Carbohydrates

Reducing ends of carbohydrates can be used to determine the amount of reducing carbohydrates present in a heterogenous mixture or to analyze the production of new reducing ends. To measure the reducing ends a procedure similar to that described in Waffenschmidt and Jaenicke (253) was used. Two solutions were prepared; solution A consisted of 5 mM bicinchoninic acid (BCA), 512 mM sodium carbonate and 288 mM sodium bicarbonate, solution B consisted of 5 mM copper sulfate and 12 mM L-serine. Maltotriose was used to generate a standard curve, which was linear up to 50 nmol. To 100 μ l of the standards 250 μ l of solution A and B were added to the tubes and incubated in a boiling water bath for 15 minutes and allowed to cool at room temperature for 20 minutes, which was then quickly centrifuged to collect condensation and 100 μ l of water was added to the reaction. The reaction produces a purple color, which has an absorbance maximum at 560nm, and a standard curve can be generated. Unknown samples were prepared similarly to the standards and the concentration of reducing ends was determined from the linear regression curve of the standards.

18. Synthesis of Glucose-1,2-Cyclic Phosphate and Glucose-3,6 and 4,6-Cyclic Phosphate

Cyclic phosphate compounds were synthesized essentially as previously described by Zmudzka and Shugar (254). Starting material, either glucose-1-phosphate, 1 g, or glucose-6-phosphate, 0.5 g, was dissolved in 5 ml of water. Glucose-1-phosphate yields the glucose-1,2-cyclic phosphate compound and glucose-6-phosphate yields a mixture of glucose-3,6-cyclic phosphate and glucose-4,6-cyclic phosphate. After dissolving the starting glucose monoester in water, it was converted to its free acid by cation exchange chromatography using Dowex 50W-X8 resin. The resin was washed with water and the free glucose

monophosphate sugar was neutralized immediately with pyridine, and concentrated in borosilicate glass tubes with a Speed Vac to a volume of approximately 10 ml. For glucose-1-phosphate, 30 ml of pyridine and 3 g of dicyclohexylcarbodiimide (DCC) was added, mixed and incubated at 0°C for 48 hours. Glucose-6-phosphate received 10 ml of pyridine and 1.5 g of DCC and was incubated at room temperature, ~25°C, for 72 hours. After the DCC reaction was complete 10 ml of water was added and precipitated cyclohexylurea was filtered away by vacuum filtration. The filtrate was extracted 3 times with an equal volume of diethyl ether, the aqueous phase was collected and concentrated with a Speed Vac to about 5 ml in borosilicate glass tubes. Any insoluble material present was removed by vacuum filtration and the filtrate was passed over a Dowex cation exchange resin and rapidly neutralized with a saturated solution of barium hydroxide to pH 8.0. The solution was concentrated in borosilicate glass tubes using a Speed Vac to ~1ml, centrifuged at 5,000 x g for 5 minutes to clarify the solution. The barium salt of the glucose cyclic phosphate was precipitated with 3 ml of acetone and centrifuged for 5 minutes at 5,000 x g to pellet the precipitate. The cyclic phosphate was washed 3 times with 10 ml of -20°C 100% ethanol by mixing well and centrifugation at 5,000 x g for 5 minutes followed by 3 washed with and equal volume of acetone. The barium salt of the glucose cyclic phosphate was dried using a Speed Vac and stored at -20°C until use.

19. Synthesis of Glucose-2-Phosphate

Acid hydrolysis of glucose-1,2-cyclic phosphate was used to produce glucose-2-phosphate and purified as the barium salt (255,256). The acid hydrolysis was performed under conditions that would open the ring, hydrolyze glucose-1-phosphate but not hydrolyze the phosphate from glucose-2-phosphate (256). To produce glucose-2-phosphate 100 μ moles of glucose-1,2-cyclic phosphate was dissolved in water (9 ml) and HCL was added for a final 1 N concentration. The solution was then incubated in a boiling water bath for 5 minutes and cooled on ice. A saturated solution of barium hydroxide was used to adjust the pH between 9-10 and kept on ice to allow for barium phosphate to

form and precipitate out of solution, which was collected by centrifugation at 10,000 x g for 10 minutes at 4°C and the supernatant was transferred and saved in a different tube. The precipitate was redissolved in 0.1 N HCl and the pH adjusted between 9-10 with a saturated barium hydroxide solution, cooled on ice, the precipitate collected by centrifugation and the supernatant transferred. This process was repeated once more and the supernatants were combined. The barium salt of glucose-2-phosphate was precipitated by adding and 3 volumes of 100% ethanol to the combined supernatants and was incubated at 4°C overnight. The precipitate was collected by centrifugation, washed with 100% ethanol, dried with a Speed Vac and stored at -20°C until use.

20. Mouse Exercise Protocol

Mice were exercised to exhaustion on a treadmill (Exer6M, Columbus Instruments) following a procedure similar to that described previously (140). Briefly, 11.5— 12.8 month-old (will be referred to as 12 month old) male wild type, *laforin*^{-/-} and *malin*^{-/-} mice were trained and acclimated to the treadmill and the exercise to exhaustion was conducted essentially as described (140) except that on the last day of training the incline was kept at 15 degrees and the speed did not exceed 25.2 m/min. The mice were placed on the treadmill and the incline was set at 15 degrees. The speed was increased as described previously but did not exceed 25.2 m/min. Once the mice could no longer remain on the treadmill belt, they were removed, body weight and blood glucose levels were measured. Mice in one group were given a bolus of glucose (3.6 g of glucose/kg of body weight) by oral gavage and placed in a cage with food and water. Mice were sacrificed at different times post-exercise by cervical dislocation and tissues were harvested and immediately frozen in liquid nitrogen and stored at -80 °C for analysis of glycogen, glycogen phosphate content and Western Blotting. Blood glucose was measured using a *Breeze 2* glucometer (Bayer) pre- and post-exercise.

21. Tissue Staining

Visualization of Lafora bodies in quadriceps from mice was performed as previously described (189). Briefly, quadriceps were fixed in 10% formalin and embedded in paraffin. Slices, 5 μm , were deparaffinized and treated with a solution containing 0.1% Diastase in 20mM NaOAc (pH 6.0) for 1 hour at 40 °C, which effectively degrades normal glycogen. Sections were then oxidized with 0.5% periodic acid for 5 minutes, stained with Schiff reagent for 15 minutes and counterstained with hematoxylin and eosin for 15 minutes. Tissues were sectioned at the Histology Core at Indiana University School of Medicine Department of Anatomy and Cell Biology.

RESEARCH OBJECTIVES

A major focus of Lafora disease research has been to identify the functions of both laforin and malin so as to understand the mechanism of the disease and thereby seek rationale strategies for its treatment. It is becoming accepted that one role of laforin is as a glycogen phosphatase (13), while the function of malin remains less clear at this time. A hallmark of Lafora disease is the appearance of Lafora bodies, which are composed of poorly branched, insoluble glycogen like material, also known as polyglucosan. Normally, glycogen contains trace amounts of phosphate. Analysis of glycogen from mouse models of Lafora disease has shown that there is an accumulation of poorly branched and hyperphosphorylated glycogen. The increase in phosphate has been associated with decreased solubility and may contribute to Lafora body formation (12,14,19). Because of the increased phosphorylation of glycogen in mouse models of Lafora disease, it is important to understand the amount and location of the phosphate in order to understand the mechanism for glycogen phosphorylation and is a part of the data presented in this thesis (Results, 1. Glycogen Phosphate). How phosphate is incorporated into glycogen has been an area of ongoing research and in this thesis I confirm that glycogen synthase is capable of incorporating phosphate into glycogen (Results, 2. Incorporation of Phosphate into Glycogen by Glycogen Synthase). Disruption of the PTG gene in a laforin^{-/-} or malin^{-/-} background alleviates Lafora body formation and I report on analyses of the amount and structure of glycogen in these double knockout mouse models. The results indicate that elevated glycogen phosphate alone may not always be sufficient to cause Lafora body formation (Results, 3. Glycogen Phosphate, Branching and Solubility) as has also been suggested recently by Nitschke et al (257). The final question I asked was whether the abnormal glycogen accumulated in Lafora disease is subject to normal metabolism. For this study, we used exercise of mouse models of Lafora disease as a means to provoke glycogen breakdown in muscle

(Results, 4. Glycogen Metabolism in Mouse Models of Lafora Disease Subjected to Exercise).

RESULTS

1. Glycogen Phosphate

1.1 Phosphate Chemistry and Abundance

Glycogen is a branched polymer of glucose but it also contains trace amounts of phosphate, about one phosphate for every 650 – 2000 glucose residues, depending on the source (18,28). In 2011 Tagliabracci et al (16) showed, by NMR analysis of phospho-oligosaccharides purified from rabbit skeletal muscle glycogen, that phosphate existed as a phosphomonoester at C2 and C3. However, Nitschke et al (15) challenged those results and concluded that C6 phosphorylation was the dominant site for phosphorylation in glycogen. This discrepancy in observations and conclusions prompted us to further investigate our initial findings. Glycogen phosphorylation had become a point of interest because of its association with Lafora disease, an early onset fatal form of juvenile epilepsy (157,209,214,258,259) as described in the Introduction. In particular, there is an association between hyper-phosphorylation and abnormal glycogen formation, such that glycogen becomes less branched and water insoluble (12). The location of phosphate in glycogen is therefore an important part of understanding how the phosphate may be affecting glycogen structure or how, mechanistically, the phosphate is introduced into glycogen. The first phase of this thesis research was therefore directed at re-evaluating the phosphorylation of glycogen in normal animals as well as in the mouse models of Lafora disease. We therefore revisited the question of the location of the phosphate in glycogen, specifically asking whether the method for glycogen purification affected the experimental results. Phosphate and other ester migration is a known phenomenon in sugar chemistry (229,231).

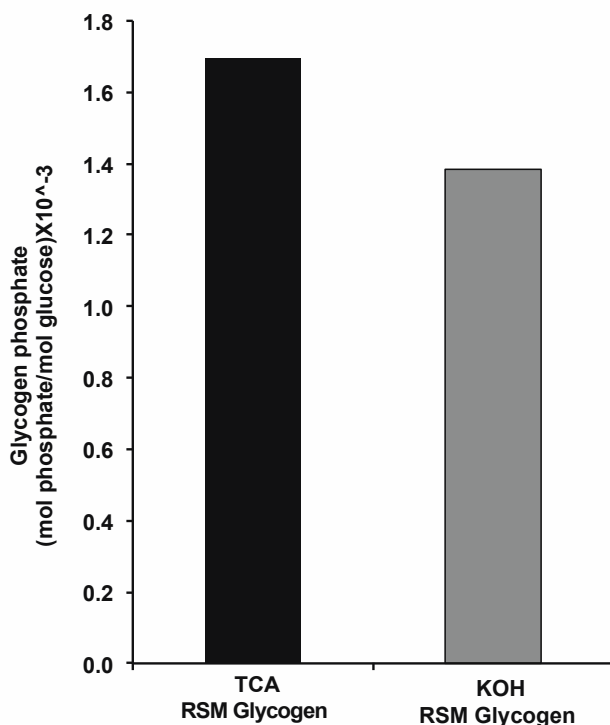


Figure 14. Rabbit skeletal muscle glycogen content. Rabbit skeletal muscle (RSM) glycogen purified by either the “TCA” or “KOH” method phosphate content. Data is the average of two measurements from the same sample of glycogen. n = 1

Phosphate ester migrations under acidic conditions have been documented, but it has also been observed under alkaline conditions (230). Because of this, glycogen from rabbit skeletal muscle was prepared using two methods to determine whether the purification procedure had any effect on the distribution of phosphate. A relatively mild procedure, where the most extreme treatment is exposing tissue homogenates to 10%(v/v) TCA at 4°C, was used, designated the “TCA” method. The second method involved subjecting skeletal muscle tissue to boiling 30%(w/v) KOH, designated the “KOH” method. Measurement of glycogen phosphate from either procedure gave a similar glycogen phosphate content (Figure 14). Rabbit skeletal muscle glycogen, purified by the procedures described above, and amylopectin, were hydrolyzed enzymatically with glucosidases to produce glucose and limit dextrin. Phospho-oligosaccharides were separated from neutral sugars by anion exchange chromatography. Phospho-oligosaccharides from potato amylopectin were processed similarly and used as a known source for phosphorylation of C6 (17,235,260). Analysis of the

phospho-glucans from glycogen by HPAEC (Figure 15, B and C) gave identical profiles for the TCA and KOH methods while the profile for amylopectin had a similar but unique profile (Figure 15, D). Mass spectroscopy analysis of the phospho-oligosaccharides gave spectra that were dominated by signals corresponding to species with one phosphate plus n hexoses, with n reaching up to around 12 hexose residues (Figure 16). Although the mixtures of phospho-oligosaccharides were complex they were similar in chemical composition, in that they were composed of glucose polymers with a covalently linked phosphate. The HPAEC and mass spectroscopy data were similar to our previous observation (16). Analysis of the phospho-oligosaccharides by two-dimensional homonuclear ^1H NMR (COSY, TOCSY and ROESY), heteronuclear $^{13}\text{C}, ^1\text{H}$ NMR (HSQC) and heteronuclear $^1\text{H}, ^{31}\text{P}$ NMR (HMQC and HMQC-TOCSY) produced chemical shifts of the signals found in the oligosaccharide mix (Table 1) and most of the signals were present in phosphooligosaccharide samples from glycogen and amylopectin. The $^{13}\text{C}, ^1\text{H}$ NMR (HSQC) spectra show that phospho-oligosaccharides from glycogen had phosphates located at C2, C3 and C6 (Figure 17, A) while amylopectin only had signals for C3 and C6 phosphate (Figure 17, D), which are indicated by circles.

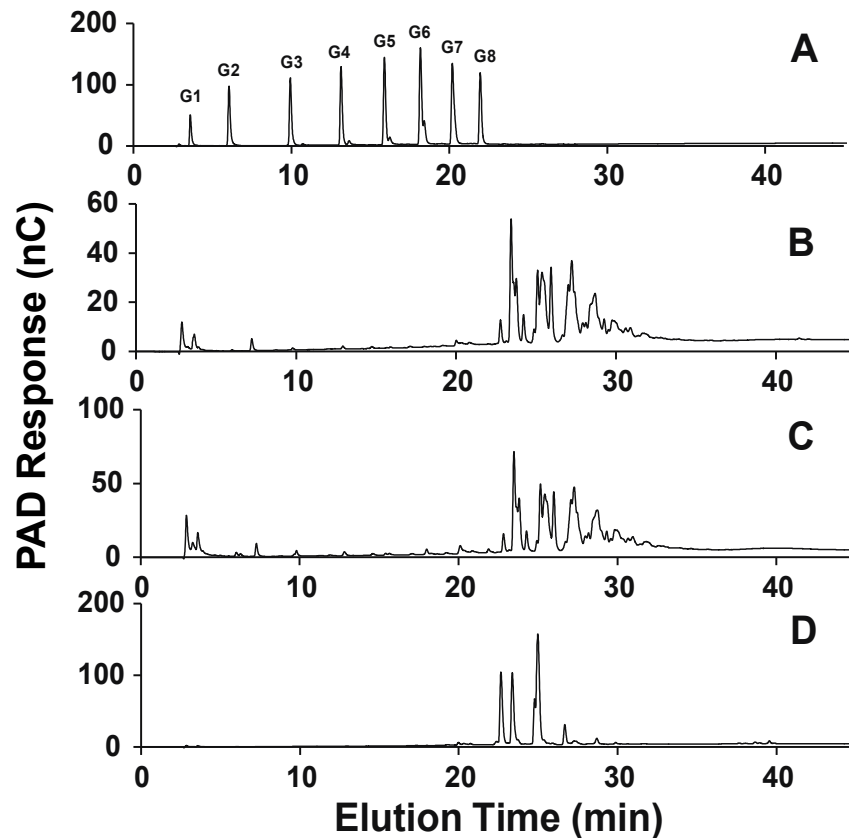


Figure 15. HPAEC analysis of phospho-oligosaccharides from glycogen and amylopectin. Oligosaccharides were separated by HPAEC using a PA200 column. A, polyglucose standards (0.25 nmol) from glucose (G1) up to moltooctaose (G8). B, phospho-oligosaccharides purified from rabbit skeletal muscle glycogen by the TCA method. C, phospho-oligosaccharides purified from rabbit skeletal muscle glycogen by the KOH method. D, phospho-oligosaccharides purified from amylopectin. nC, nanoCoulomb.

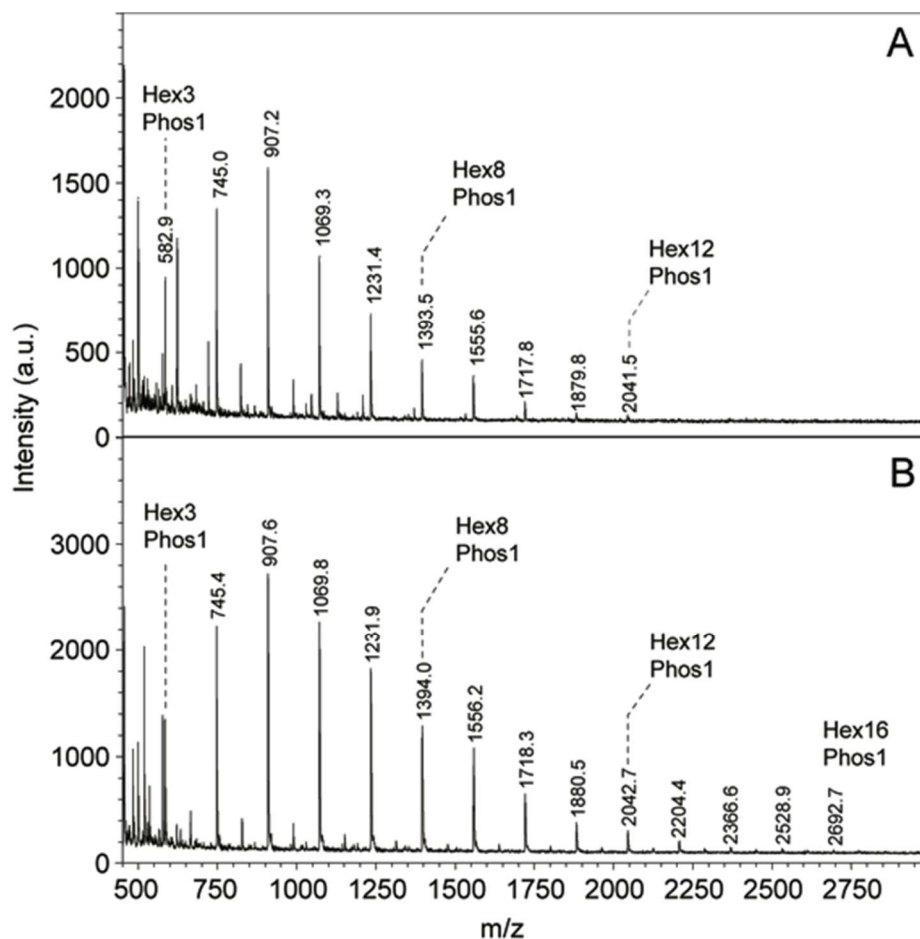


Figure 16. Analysis of phospho-oligosaccharides purified from glycogen by MALDI-TOF mass spectrometry. A 1- μ L aliquot of phospho-oligosaccharide solution (1 mM in phosphate ester), prepared by the “TCA” (A) or KOH” (B) protocol, was analyzed using THAP matrix in negative ion mode. MALDI spectra are shown in which a series of glycogen phosphate peaks from both preparations was detected. The main signals observed are series of glucose oligomers with one mole of phosphate, starting with 3 hexose units.

The glycogen samples had relatively weak C6-P signals but this was the major signal in the phospho-oligosaccharide samples from amylopectin.

To determine whether these residues were phosphorylated, $^1\text{H},^{31}\text{P}$ HMQC (Figure 17, B and E) and HMQC – TOCSY (Figure 17, C and F) spectra of both samples were obtained. The $^1\text{H},^{31}\text{P}$ HMQC spectra show peaks for protons that are at the most three bonds away from phosphorus atoms, which confirmed the assignments and showed the ^{31}P chemical shift of the different phosphate groups. The spectrum of amylopectin phospho-oligosaccharides was dominated by Glc-6-P with a small contribution from the Glc-3-P and no detectable Glc-2-P. The glycogen phospho-oligosaccharide spectrum showed similar signals Glc-2-P, Glc-3-P and Glc-6-P. The $^1\text{H},^{31}\text{P}$ HMQC – TOCSY experiments were acquired to provide a reliable assignment of the signals found in the $^1\text{H},^{31}\text{P}$ HMQC spectra, and was able to show protons up to four bonds away from phosphorus atoms. $^1\text{H},^{31}\text{P}$ HMQC – TOCSY spectra gave the following signals, Glc-2P gave cross peaks between ^{31}P and H-1 and H-2, Glc-3-P showed correlations between ^{32}P and H-2, H-3 and H-6. All assignments derived from COSY, TOCSY, $^{13}\text{C},^1\text{H}$ HSQC and $^1\text{H},^{31}\text{P}$ HMQC – TOCSY were in agreement between the spectra (Table 1). An approximate quantitation of the NMR signals for the glycogen phospho-oligosaccharides (Table 2) showed roughly equal proportions of C2, C3 and C6 phosphate for the TCA and KOH prepared samples. However, the previous TCA (16) sample had a lower level of C6 phosphate. Additionally, C6 phosphate in amylopectin was the dominant location for phosphate, ~85% of the total, which would be expected from previous reports. These data suggest, that use of KOH to purify glycogen does not influence the phosphate distribution as determined by NMR. Why the 2010 sample had ~19% of the phosphate at C6 versus ~30% in the 2013 remains an unknown. However, the average of the two samples is ~24%, which is in line with the enzymatic quantitation for C6 phosphorylation, as discussed in the next section (Figure 18).

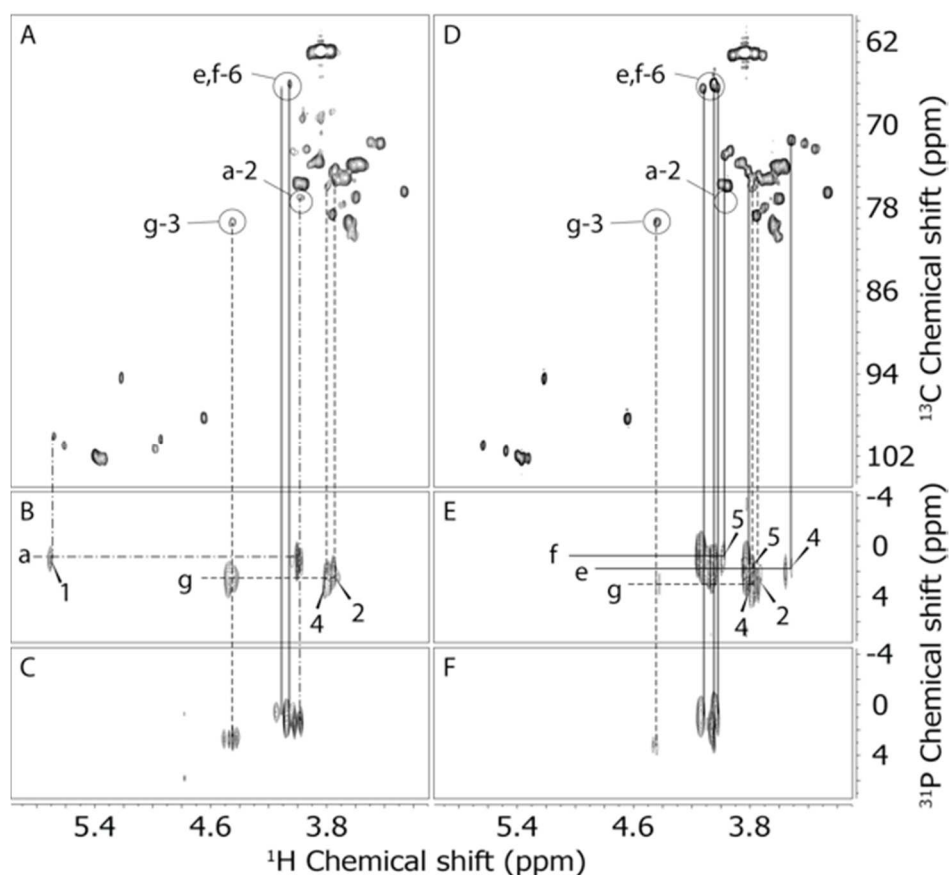


Figure 17. Analysis of phospho-oligosaccharides purified from glycogen and amylopectin by NMR.

Two-dimensional heteronuclear NMR spectra were acquired as described in “Experimental Procedures” with D₂O as solvent from samples 2 mM with respect to phosphate. **A.** ¹H-¹³C-gHSQC spectrum of purified glycogen phospho-oligosaccharides, prepared by the “KOH” protocol. The signals from H/C pairs of phosphorylated positions are circled and labeled. The contribution of each isomer was estimated by measuring the peak volumes of the labeled signals; **B.** ¹H-³¹P-HMQC-TOCSY spectrum of purified glycogen phospho-oligosaccharides, showing phosphorus correlations to H-1 and H-2 of Glc-2-P and to H-2, H-3, and H-4 of Glc-3-P; **C.** ¹H-³¹P-HMQC spectrum of purified glycogen phospho-oligosaccharides, showing phosphorus correlations to H-2 of Glc-2-P, H-3 of Glc-3-P, and H-6 of Glc-6-P; **D.** gHSQC spectrum of purified amylopectin phospho-oligosaccharides. The same areas as in Panel A are circled although no C2 phosphate was detected in amylopectin. The contribution of each isomer was estimated by measuring the peak volumes of the labeled signals; **E.** ¹H-³¹P-HMQC-TOCSY spectrum of purified amylopectin phospho-oligosaccharides, showing phosphorus correlations to H-5 and H-6 of 4-Glc-6-P, to H-4, H-5, and H-6 of t-Glc-6-P, and to H-2, H-3, and H-4 of Glc-3-P; **F.** ¹H-³¹P-HMQC spectrum of purified glycogen phospho-oligosaccharides, showing phosphorus correlations to H-3 of Glc-3-P and H-6 of Glc-6-P. The lines connecting the signals are coded to the different phosphorylated glucose residues; e and f: solid, g: dashed, a: dash-dot lines.

Table 1. Proton, carbon, and phosphorus chemical shifts (in ppm) of phosphorylated amylopectin and glycogen oligosaccharides

Residue		1	2	3	4	5	6	
a ¹	t- α -Glc-2-P-(1 \rightarrow)	¹ H	5.67	3.98	3.76	3.49	3.70	3.83/3.77
		¹³ C	100.0	77.3	74.7	71.8	75.3	63.3
		³¹ P		1.12				
b	t- α -Glc-(1 \rightarrow 4)	¹ H	5.60	3.57	3.66	3.43	3.66	3.83/3.77
		¹³ C	101.1	74.0	75.4	72.1	75.4	63.3
c ²	t- α -Glc-(1 \rightarrow 4-Glc-6-P)	¹ H	5.48	3.56	3.70	3.35	n.d. ³	3.92/3.80
		¹³ C	101.6	74.1	75.4	72.4	n.d.	63.5
d	4- α -Glc-(1 \rightarrow 4)	¹ H	5.39	3.59	3.97	3.64	3.84	3.83/3.77
		¹³ C	102.2	74.1	76.0	79.7	73.8	63.3
e	t- α -Glc-6-P	¹ H	5.38	3.61	3.68	3.51	3.81	4.05/4.05
		¹³ C	102.4	74.1	75.4	71.5	74.5	66.2
		³¹ P						2.07
f	4- α -Glc-6-P	¹ H	5.37	3.63	n.d.	3.71	3.98	4.12/4.03
		¹³ C	102.2	74.1	n.d.	78.1	73.0	66.6
		³¹ P						1.02
g	4- α -Glc-3-P	¹ H	5.35	3.75	4.46	3.81	3.87	n.d.
		¹³ C	102.4	74.6	79.9	76.4	73.8	n.d.
		³¹ P			2.81			
h	4- α -Glc _{red}	¹ H	5.21	3.56	3.95	3.64	n.d.	n.d.
		¹³ C	94.5	74.0	76.0	79.7	n.d.	n.d.
i	4- β -Glc _{red}	¹ H	4.64	3.27	3.75	3.64	n.d.	n.d.
		¹³ C	98.5	76.6	78.8	79.7	n.d.	n.d.
j ¹	4,6- α -Glc _{red}	¹ H	5.22	3.55	3.96	3.64	3.93	3.98/3.83
		¹³ C	94.6	74.2	76.0	79.7	72.7	69.7
k ¹	t- α -Glc-(1 \rightarrow 6)	¹ H	4.99	3.54	3.74	3.44	3.86	n.d.
		¹³ C	101.5	74.7	74.2	72.1	73.8	n.d.
l ¹	4- α -Glc-(1 \rightarrow 6)	¹ H	4.95	3.59	4.01	3.63	3.85	n.d.
		¹³ C	100.7	74.1	73.0	80.6	74.0	n.d.
m ¹	4,6- β -Glc _{red}	¹ H	4.65	3.25	3.77	3.62	3.60	3.97/3.73
		¹³ C	98.5	76.7	78.9	80.6	77.3	68.8

¹only observed in glycogen phospho-oligosaccharides

²only observed in amylopectin phospho-oligosaccharides

³n.d.=not determined

Table 2. Phosphomonester distribution in phospho-oligosaccharides from glycogen and amylopectin based on NMR analyses.

Sample	C2 phosphate (%)	C3 phosphate (%)	C6 phosphate (%)
Glycogen			
TCA (2010)	28	53	19
TCA (2013)	30	39	31
KOH	29	37	34
Amylopectin	0	13	87

The relative proportions of C2, C3 and C6 phosphorylation were estimated by integrating the corresponding signals in NMR experiments such as shown in Fig. 17. Samples were oligosaccharides prepared from the indicated source as described under "Methods". In the case of the glycogen "TCA" samples, the data refer to re-evaluation of a previous sample as well as a new sample analyzed in the present study.

1.2 Phosphorylation of Glycogen at C6 in Mouse and Rabbit Muscle Glycogen

The data obtained by NMR is a powerful means to determine phosphate location on specific glucose carbon atoms in the phospho-oligosaccharides however, it requires a significant amount of material and is limited in its quantitative measurements. Because of this, Dr. DePaoli-Roach in the laboratory developed a sensitive enzymatic fluorescence-based assay for glucose-6-phosphate in hydrolysates of purified glycogen samples, described in the "Methods section." This highly sensitive assay allows for the measurement of glucose-6-phosphate in small glycogen sample. Additionally, because the enzymatic assay requires less time and sample material it is possible to obtain measurements from multiple samples and obtain reliable statistics, unlike the NMR analysis. We were able to couple the measurements of total glycogen phosphate, measured by the malachite green protocol (12,14,243), with the amount of glucose-6-phosphate from individual samples for direct comparison. The measured total phosphate content of mouse skeletal muscle is significantly

lower than that of rabbit muscle glycogen, similar to what has been previously observed (12,13). Additionally, when using the malachite green assay to measure glycogen phosphate, there is undetectable phosphate in un-hydrolyzed samples, indicating the purity of the glycogen and lack of phosphate contamination. Measurements of glucose-6-phosphate, in our hands, were similar to those reported by Nitschke *et al* (15). Interestingly, mouse and rabbit skeletal muscle glycogen contained similar proportions of glucose-6-phosphate, ~20% (Figure 18). For rabbit skeletal muscle, the levels of glucose-6-phosphate measured were in agreement with the values obtained from the NMR analysis (Table 2). Similar analyses of amylopectin indicated that C6-phosphate is the dominant phospho-monoester at ~75% of the total, again in agreement with the NMR data.

1.3 C6 Phosphorylation of Glycogen from Mouse Models of Lafora Disease

There are several reports that glycogen phosphate levels are elevated in mouse models of Lafora disease (13,14,18,19). The increase in glycogen phosphate content has also been shown to increase with age along with decreased branching (12). Nitschke *et al* (15) had proposed that C6 is the most important site of phosphorylation in glycogen in mouse models of Lafora disease and this could possibly lead to decreased branching and abnormal glycogen formation. Therefore, it was of interest to determine whether there is a specific increase in C6 relative to C2/C3 phosphate. In 9-10 month-old *laforin*^{-/-} and *malin*^{-/-} mice total skeletal muscle glycogen phosphate increased 7.5 and 4.3 fold, respectively, over that of wild type mice. The lesser elevation in glycogen phosphate content in the *malin*^{-/-}, compared to *laforin*^{-/-} mice is consistent with other reports (19). The absolute amounts of C6 phosphate in the knockouts were increased to 4.0 and 9.2 fold over the wild type animals (Table 3). However, considering the proportion of C6 phosphate to the total phosphate content, the increase of C6 phosphate was in strict proportion, ~20%. Therefore, we cannot

assess whether C6 or C2/C3 phosphate contributes more to the formation of abnormal glycogen.

Table 3. Determination of total phosphate and glucose-6-P in glycogen and amylopectin

Source ^a	Glycogen phosphate (mol/mol) x 10 ⁻³		% C6 phosphate	Glucose residues per		Fold increase over WT	
	Total	C6		Total P	C6 P	Total P	C6 P
WT (4)	0.371 ± 0.03	0.063 ± 0.007	17	2700	15800	1	1
Malin^{-/-} (5)	1.612 ± 0.19	0.263 ± 0.015	16	620	3800	4.3	4.0
Laforin^{-/-} (4)	2.785 ± 0.09	0.582 ± 0.021	21	360	1720	7.5	9.2
Rabbit (5-11)	1.525 ± 0.10	0.324 ± 0.001	21	650	3090	NA ^b	NA
Amylo- pectin (4)	4.403 ± 0.18	3.307 ± 0.034	76	227	300	NA	NA

^aFor the analyses of muscle glycogen from wild type (WT), malin^{-/-} and laforin^{-/-} mice, the numbers in parentheses refer to the number of samples, each from a separate mouse, that were analyzed. For the analyses of rabbit muscle glycogen and amylopectin, the numbers in parentheses refer to the number of independent, replicate analyses made from the same starting material.

^bNA, not applicable

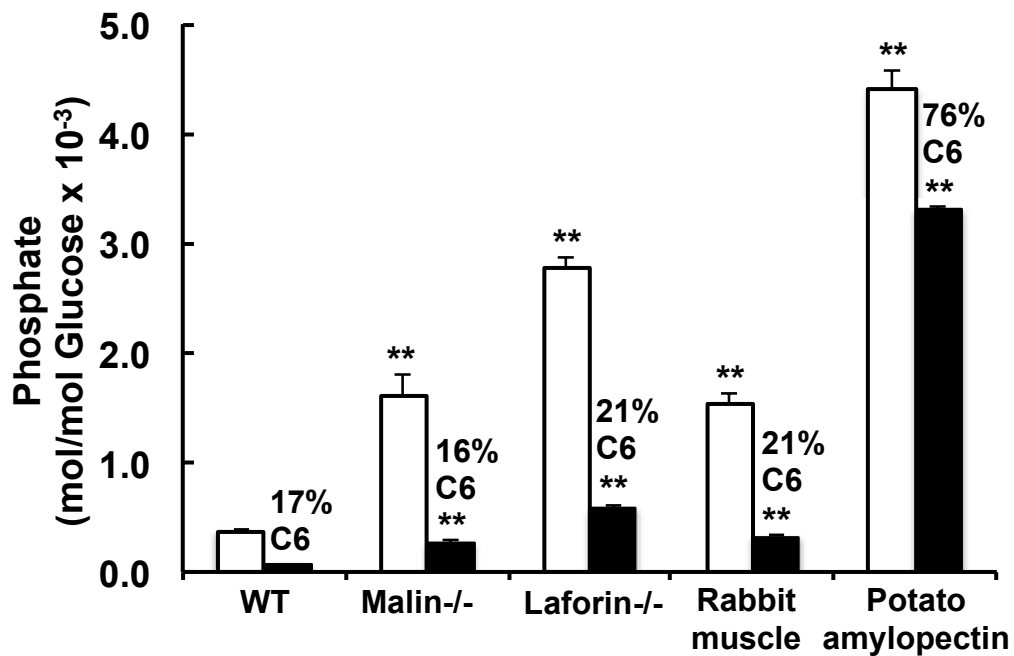


Figure 18. Total phosphate and C6 phosphate content of rabbit and mouse glycogen and amylopectin. The total inorganic phosphate (open bars) and glucose-6-P (filled bars) in hydrolysates of glycogen or amylopectin were measured as described under " Experimental Procedures". Shown are analyses of glycogen purified from wild type (4), malin^{-/-} (5) and laforin^{-/-} (4) mouse muscle, where the numbers in parentheses denote the number of animals analyzed. For rabbit muscle glycogen (5-11) and potato amylopectin (4), the number of replicate analyses is indicated. The percentage of C6 phosphorylation is shown above the filled bars. The error bars indicate the standard error of the mean; asterisks denote $p \leq 0.01$ with respect to wild type mouse glycogen phosphate.

2. Incorporation of Phosphate into Glycogen by Glycogen Synthase

It was originally proposed that an enzyme other than glycogen synthase was responsible for the incorporation of phosphate into glycogen (261). In an attempt to find such an enzyme, our laboratory discovered that glycogen synthase was capable of incorporating phosphate into glycogen as a minor side reaction and we proposed a mechanism for the phosphate addition (16). However, our findings were challenged by Nitschke (15) et al. who concluded that glycogen synthase does not incorporate phosphate but rather that our observations were the result of ^{32}P -labeled UDP, a product of the normal reaction, binding to glycogen. Because of this discrepancy in results, we therefore re-evaluated our initial findings to verify that glycogen synthase can incorporate phosphate and that our observations were not the result of nonspecific binding of UDP to glycogen.

2.1 Assay for monitoring incorporation of the β -phosphate of UDP glucose into glycogen

The assay for monitoring phosphate incorporation into glycogen is based on a procedure developed for measuring the activity of glucose-1-phosphotransferase, which is involved in glycoprotein synthesis (262). Glycogen synthase activity, traditionally, is measured by the incorporation of $[\text{U}^{14}\text{C}]$ -glucose from UDP- $[\text{U}^{14}\text{C}]$ -glucose using a filter paper assay. With a similar approach but using $[\beta\text{-}^{32}\text{P}]\text{UDP}$ -glucose as a substrate, we can monitor the incorporation of the β -phosphate into glycogen (16). Tagliabracci et al determined that only ~ 1 phosphate for every 10,000 catalytic cycles resulted in the transfer of the $\beta\text{-}^{32}\text{P}$ into glycogen (16). However, measuring the phosphate when $[\beta\text{-}^{32}\text{P}]\text{UDP}$ -glucose is the substrate is technically challenging, due to the fact that $[\beta\text{-}^{32}\text{P}]\text{UDP}$ formed by the normal glycogen synthase reaction can bind to the filter paper.

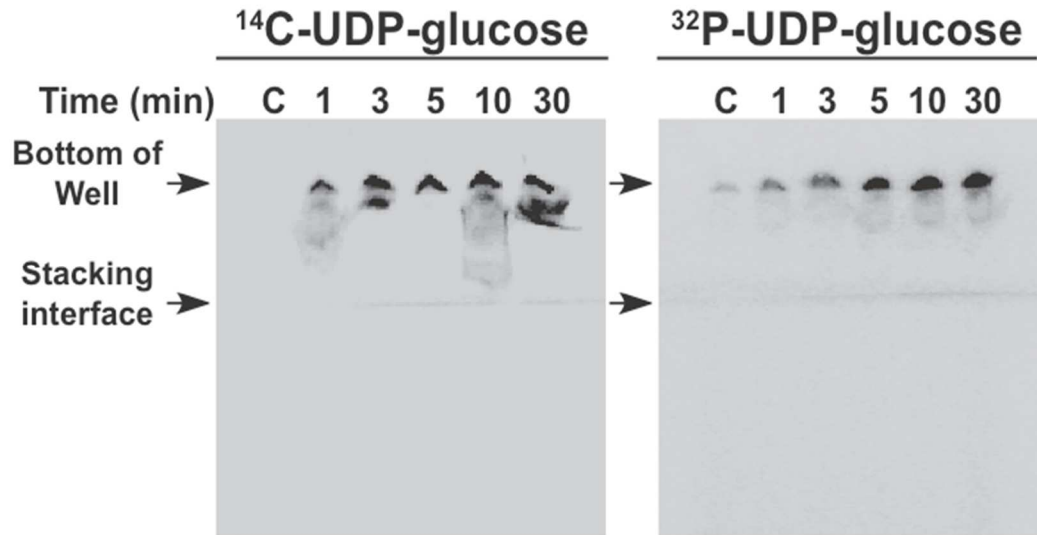


Figure 19. Time-dependent incorporation of ^{32}P into synthesized glycogen by glycogen synthas. Glycogen synthase (yeast Gsy2p, 5 $\mu\text{g}/\text{ml}$) was incubated with glycogen, and 2 μM [β - ^{32}P]UDP-glucose or UDP-[U- ^{14}C]glucose, aliquots were removed at the indicated times, precipitated with ethanol and analyzed by SDS-PAGE (see Materials and Methods). C indicates a control reaction that lacking enzyme. Dried gels were analyzed by a Phosphorimager. The bottom of the gel wells and the stacking/separating gel interfaces are indicated with arrows.

Therefore, the [β - ^{32}P]UDP needs to be removed from the reaction mixture by precipitation of glycogen with ethanol followed by re-dissolving in aqueous solution (once or multiple times) and/or by SDS-PAGE. Tagliabracci et al (16) had demonstrated that these methods were effective at removing the [β - ^{32}P]UDP from glycogen and was able to obtain the rate of phosphate incorporation mentioned above using SDS-PAGE as the final assay. However, Nitschke et al. (15) challenged those findings and suggested that glycogen synthase was not incorporating ^{32}P into glycogen from [β - ^{32}P]UDP-glucose. Rather, Nitschke et al. (15) claimed that the ^{32}P signal that we had observed associated with glycogen was simply [β - ^{32}P]UDP, produced during the glycogen synthase reaction, tightly bound to glycogen. We therefore performed several experiments to address whether or not the ^{32}P -glycogen signal was due to covalent phosphorylation or not.

The first goal was to repeat our initial experiment, which involved labeling glycogen with either [U¹⁴C]-glucose or ³²P with purified recombinant yeast glycogen synthase and visualizing the labeled glycogen after SDS-PAGE, as reported previously (16). Our observations were consistent and we observed, by phosphorimaging of SDS-PAGE, a time dependent increase of either ¹⁴C or ³²P glycogen labeling when glycogen synthase was incubated with UDP-[U¹⁴C]-glucose or [β-³²P]UDP-glucose (Figure 19). High molecular weight glycogen is typically retained at the bottom of the SDS-PAGE well, but presumably smaller molecular weight polysaccharides, give signals that extend into the stacking gel and sometimes accumulate at the stacking-separating gel interface. Negatively charged, small molecules such as nucleotides would be expected to migrate through the separating gel, which had no detectable radioactivity (Figure 19). A noticeable amount of signal is observed at the bottom of the well of control samples lacking enzyme when [β-³²P]UDP-glucose is present and to a much lesser extent with UDP-[U¹⁴C]-glucose. We consider the signal observed in the control wells to be a background signal.

2.2 Evidence that Phosphate Incorporated by Glycogen Synthase is Associated with Glycogen

2.2.1 Gel Filtration

Nitschke et al. (15) had observed similar results regarding ¹⁴C and ³²P incorporation from UDP-glucose. However, when Nitschke et al (15) subjected the glycogen synthase reaction to gel filtration, a common means to remove small molecules from macromolecules, prior to SDS-PAGE analysis, they reported that the ¹⁴C labeled glycogen was unaffected but that the ³²P signal was lost. Based on this observation, Nitschke et al (15) concluded that the ³²P signal was due to non-specific binding of [β-³²P]UDP to glycogen.

To test whether the observed radioactive ³²P signal could be eliminated by gel filtration we applied this technique to analyze elongated glycogen by incubating recombinant yeast (Figure 20, A) and human glycogen synthase (Figure 20, B) with UDP-[U¹⁴C]-glucose or [β-³²P]UDP-glucose. Following glycogen synthase reactions the glycogen was precipitated with ethanol, to remove the glycogen

from the reaction mixture, and dissolved in an aqueous solution and split into two samples, one for gel filtration and one as a control. One set of samples was then passed through Sephadex G50 prior to SDS-PAGE. After gel filtration, a small sample of the ^{14}C sample was taken for quantitation and we determined a recovery of >95% of the input (data not shown), indicating that the labeled glycogen passed freely through the Sephadex G50. The samples both before column and after gel filtration were dried in a Speed Vac and redissolved in an equal amount of buffer and subjected to SDS-PAGE. In our hands, both ^{32}P and ^{14}C labeling was minimally influenced by gel filtration. We observed the expected time-dependent incorporation of both ^{14}C and ^{32}P signals. Note that in control lanes (lanes "C"), incubations with $[\beta\text{-}^{32}\text{P}]\text{UDP-glucose}$ present but lacking glycogen synthase, there was a background signal that was reduced after gel filtration but still detectable. Therefore, we conclude that the majority of the ^{32}P and ^{14}C radioactivity associated with the glycogen in SDS-PAGE is not removed by gel filtration.

2.2.2 Laforin Removal of ^{32}P from Glycogen and UDP

Hydrolysis

To confirm that glycogen synthase was incorporating phosphate into glycogen, we tested the ability of laforin to remove the incorporated label. Catalytically active wild type laforin can remove ^{32}P introduced into glycogen by glycogen synthase (16). When we incubated glycogen, labeled with either ^{14}C or ^{32}P , with wild type, catalytically active laforin, the signal from the ^{32}P labeled glycogen was reduced to background levels while the ^{14}C signal was unchanged (Figure 21, A). There was no change in the signal of the ^{14}C or ^{32}P

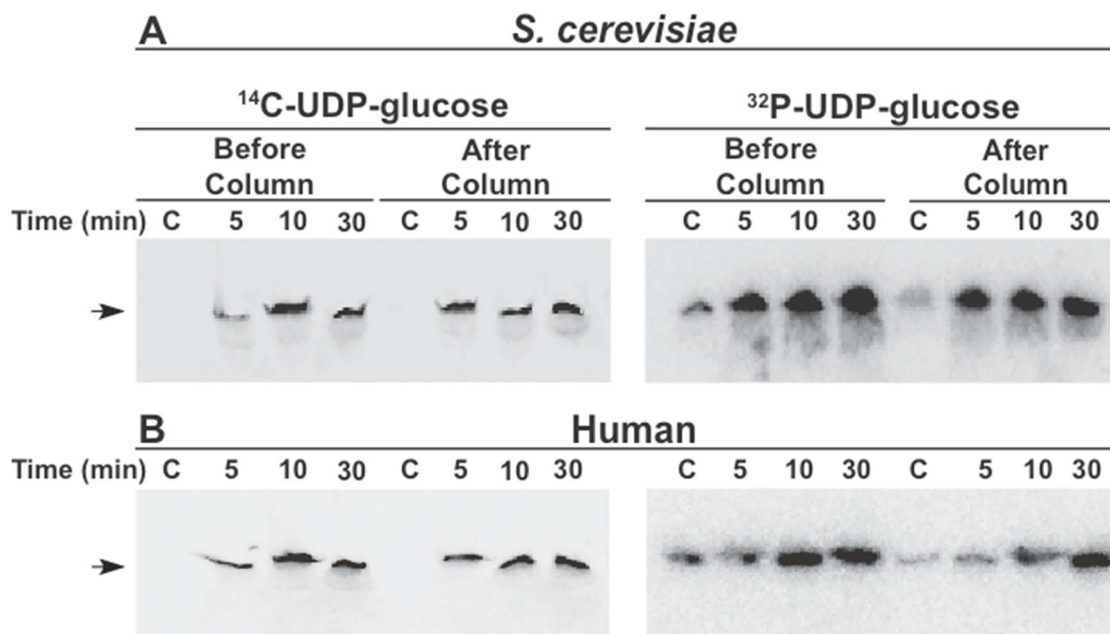


Figure 20. Effect of gel filtration on ³²P-labeled glycogen. Reactions with 2 μM [β-³²P]UDP-glucose (right panels) or [U-¹⁴C]glucose (left panels), glycogen and yeast (**A**) or human (**B**) glycogen synthase (2 μg/ml) were sampled at the indicated times, aliquots precipitated with ethanol two times, and treated or not by gel filtration over Sephadex G50 and analyzed by SDS-PAGE (see Materials and Methods). C indicates a control reaction lacking enzyme. Dried gels were analyzed by a Phosphorimager.

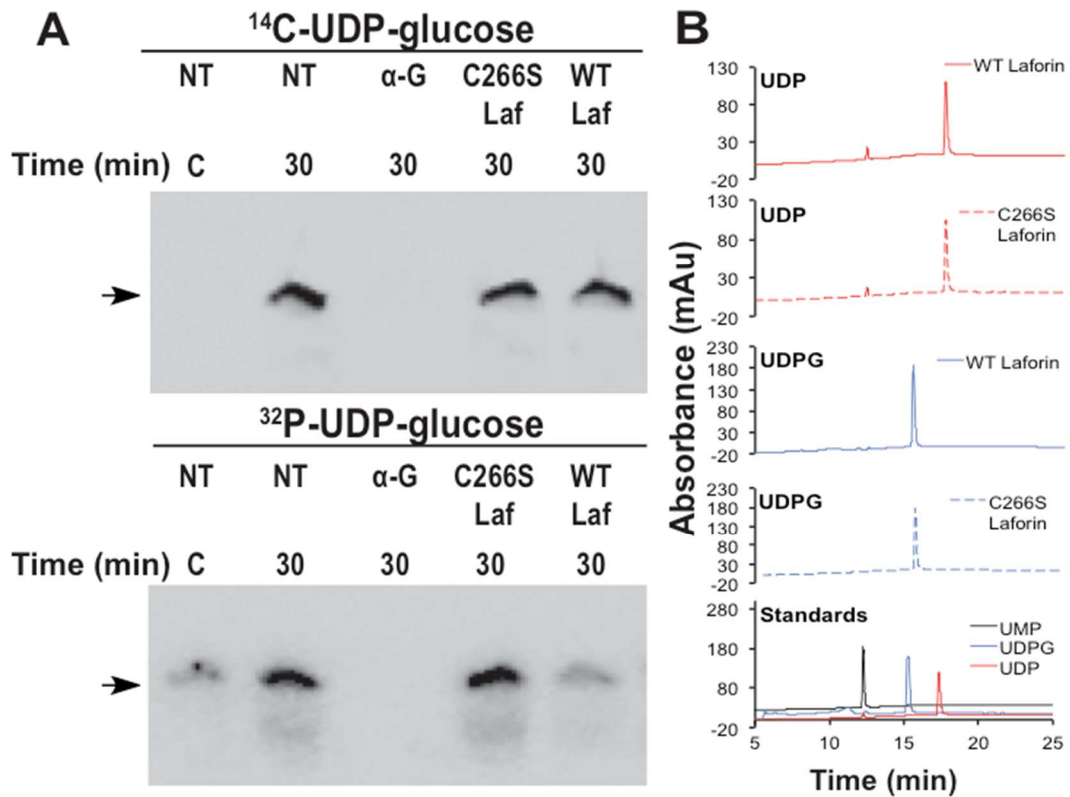


Figure 21. Effect of treating ³²P-labeled glycogen with laforin or glucosidases. **A** Glycogen was labeled by incubation with 5 μM [^β-³²P]UDP-glucose (lower panel) or [U-¹⁴C]glucose (upper panel) and yeast glycogen synthase (2 μg/ml) for 30 min. Glycogen was precipitated with ethanol, dissolved in buffer and treated with α-glucosidases (α-amylase and amyloglucosidase) (α-G), inactive mutant laforin (C266S Laf) or wild type laforin (WT Laf) as indicated, and analyzed by SDS-Page (see Materials and Methods). Dried gels were analyzed by a Phosphorimager. C, control reaction lacking glycogen synthase; NT, not treated. **B** UDP-glucose and UDP were incubated with active (WT) or inactive (C266S) laforin as indicated and analyzed by HPAEC. Chromatograms of UDP, UMP and UDP-glucose standards are shown in the lowermost panel.

labeled glycogen when incubated with the catalytically inactive C266S laforin mutant. Incubation of the labeled glycogen with glucosidase enzymes, α -amylase and amyloglucosidase, resulted in the elimination of both the ^{14}C and ^{32}P signals, which is expected as the enzymes hydrolyze the polysaccharides. These data were similar to our previous observations (16).

The argument was made that laforin might be removing the β -phosphate from $[\beta\text{-}^{32}\text{P}]\text{UDP}$ that is bound to glycogen (15). Therefore, we tested whether the laforin can hydrolyze UDP and UDP-glucose. UDP and UDP-glucose were incubated with either wild type or catalytically inactive C266S laforin and the reaction analyzed by HPAEC, monitoring the UV absorbance (Figure 21, B). We observed that even commercially available UDP with high purity (99.2%) had detectable trace amounts of UMP by this analysis (Figure 21, B). However, incubation of UDP with either wild type or C266S laforin caused no decrease in UDP nor any increase in UMP. Similarly, there was no observed decrease or hydrolysis of UDP-glucose by laforin. These data suggest that UDP and UDP-glucose are not substrates for laforin and that our observations of decreased ^{32}P signal from labeled glycogen were due to laforin hydrolyzing phospho-monoesters from glycogen.

In other experiments, we showed that laforin is capable of releasing inorganic phosphate ($^{32}\text{P}_i$) from ^{32}P labeled glycogen (Figure 22). Similar to previous experiments recombinant laforin was utilized to release incorporated phosphate from glycogen. However, when using SDS-PAGE to analyze glycogen we are only able to observe a reduced signal after laforin treatment. Therefore, we utilized thin layer chromatography (TLC) to separate the released ^{32}P phosphate, which was incorporated by glycogen synthase. The ^{32}P -glycogen for this experiment was purified by ethanol precipitation, gel filtration and treated with PiBindTM resin to eliminate phosphate and to remove any $[\beta\text{-}^{32}\text{P}]\text{UDP}$ from the glycogen synthase reaction. Thin layer chromatography (TLC) was used to analyze the reaction products using PEI-cellulose plates. Labeled glycogen was concentrated at the origin and migrated through the matrix giving a “comet trail” like appearance (Figure 22). After incubation with active laforin there was a

reduction in the ^{32}P -glycogen signal and a ^{32}P signal with the mobility of inorganic phosphate was produced (Figure 22 A). The ^{14}C -glycogen signal was unchanged (Figure 22, B). When laforin was absent (“C”) or when it was heat inactivated (“HI”), no ^{32}P signal was observed. Therefore, we conclude that ^{32}P , introduced by glycogen synthase, is covalently attached to glucose residues of glycogen by phospho-monoester linkages and that laforin is capable of hydrolyzing and releasing inorganic phosphate from glycogen.

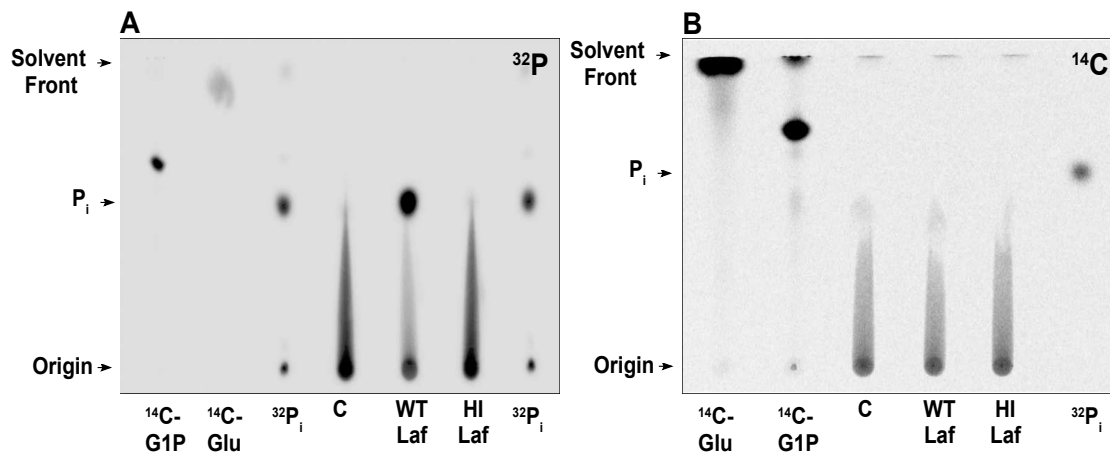


Figure 22. Release of $^{32}\text{P}_i$ from ^{32}P -glycogen by laforin. Glycogen was labeled by incubation with $5\ \mu\text{M}$ [β - ^{32}P]UDP-glucose (A) or [^{14}C]glucose (B) and yeast glycogen synthase ($5\ \mu\text{g}/\text{ml}$) for 30 min. Glycogen was precipitated 3 times with ethanol, treated with PiBind™ resin, purified by gel filtration and dissolved in buffer. The glycogen was incubated for 2 hours with $50\ \mu\text{g}/\text{ml}$ laforin (WT Laf) or laforin inactivated by boiling for 5 min (HI Laf). A control (C) lacked laforin. The reaction mixtures were analyzed by TLC using PEI-cellulose plates. Standards of ^{14}C -glucose-1-P (^{14}C -G1P), ^{14}C -glucose (^{14}C -Glu) and inorganic phosphate (P_i), labeled with the indicated isotope, were also analyzed.

2.2.3 Further Investigations of Potential [β - ^{32}P]UDP Binding to Glycogen

To further address the possibility that [β - ^{32}P]UDP could bind to glycogen, we conducted three other types of experiment. The first was an attempt to compete ^{32}P associated with glycogen by adding unlabeled UDP. We added a 1,000-fold molar excess of unlabeled UDP after the glycogen synthase reactions but before SDS-PAGE (Figure 23). If [β - ^{32}P]UDP was binding to glycogen non-specifically, then we would expect that diluting with unlabeled UDP would compete and the ^{32}P signal should be reduced. However, this was not what we observed (Figure 23). Additionally, as expected the excess unlabeled UDP had no effect on the ^{14}C signal (Figure 23).

The second approach took advantage of the action of hSCAN-1 enzyme, a UDPase that can hydrolyze UDP but has no action towards UDP-glucose or UMP (248,249). Glycogen was labeled either with ^{14}C or ^{32}P , samples were removed at given time points and the reaction terminated by boiling for 5 minutes before being incubated with hSCAN-1. The reaction products were analyzed by TLC, visualized under UV light and quantitated with a phosphorimager (Figure 24). During the time course, we observed a time dependent consumption of UDP-glucose, both ^{14}C and ^{32}P , along with the generation of [β - ^{32}P]UDP (Figure 24, A). Once reactions were terminated, unlabeled UDP was added to each reaction for a final 1 mM concentration, to give a sufficient amount for analysis by

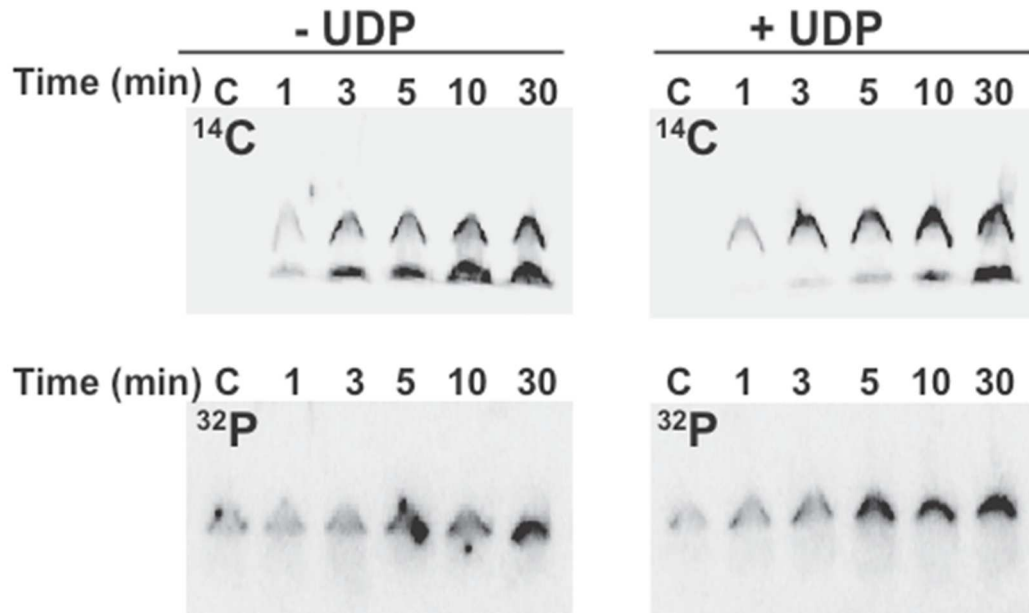


Figure 23. Effect of unlabeled UDP on ^{32}P -labeling of glycogen. Glycogen was labeled by incubation with $2\ \mu\text{M}$ [β - ^{32}P]UDP-glucose (lower panel) or [^{14}C]glucose (upper panel) and yeast glycogen synthase ($5\ \mu\text{g}/\text{ml}$) for the indicated times. Unlabeled UDP ($2\ \text{mM}$, a 1000-fold excess of UDP-glucose) was added prior to SDS-PAGE (see Methods). C, control reaction lacking glycogen synthase.

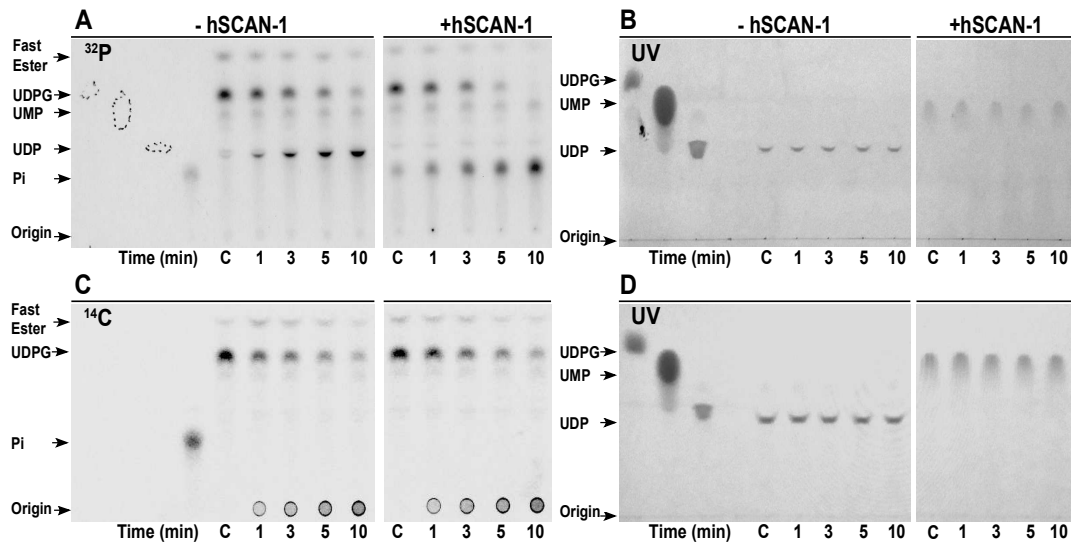


Figure 24. Analysis of the progress of glycogen synthesis by glycogen synthase. Glycogen was synthesized by incubation with 2 μ M [β - 32 P]UDP-glucose (**A,B**) or [U- 14 C]glucose (**C,D**) and yeast glycogen synthase (5 μ g/ml), and aliquots removed at the indicated times. C corresponds to reactions lacking glycogen synthase. After addition of 2 mM mM UDP, the aliquots were analyzed by TLC and visualized either by Phosphorimager (**A,C**) or UV (**B, D**). Standards of UDP-glucose, UMP, UDP and [32 P] phosphate were run in the left most tracks and their migrations indicated. Prior to chromatography, the aliquots were treated or not with the UDPase SCAN for 30 min, as indicated (see Methods).

UV. Incubation with hSCAN-1 clearly converted UDP to UMP as judged by the UV signal (Figure 24, B). As the [β - 32 P]UDP decreased, a corresponding 32 Pi signal was generated. We did not observe any change in the migration of UDP-glucose, indicating that hSCAN-1 did not have any activity towards UDP-glucose. When the glycogen from the glycogen synthase reaction, followed by hSCAN-1 treatment, was analyzed by SDS-PAGE (Figure 25) we did not see any decrease in the 32 P signal. Since hSCAN-1 was active and able to hydrolyze UDP to UMP, but did not have any effect on the 32 P glycogen signal, it suggests that the observed 32 P signal is not due to [β - 32 P]UDP hydrolysis.

Our third experimental approach tested whether binding of 32 P-UDP to glycogen could be detected after SDS-PAGE. For these experiments, we used

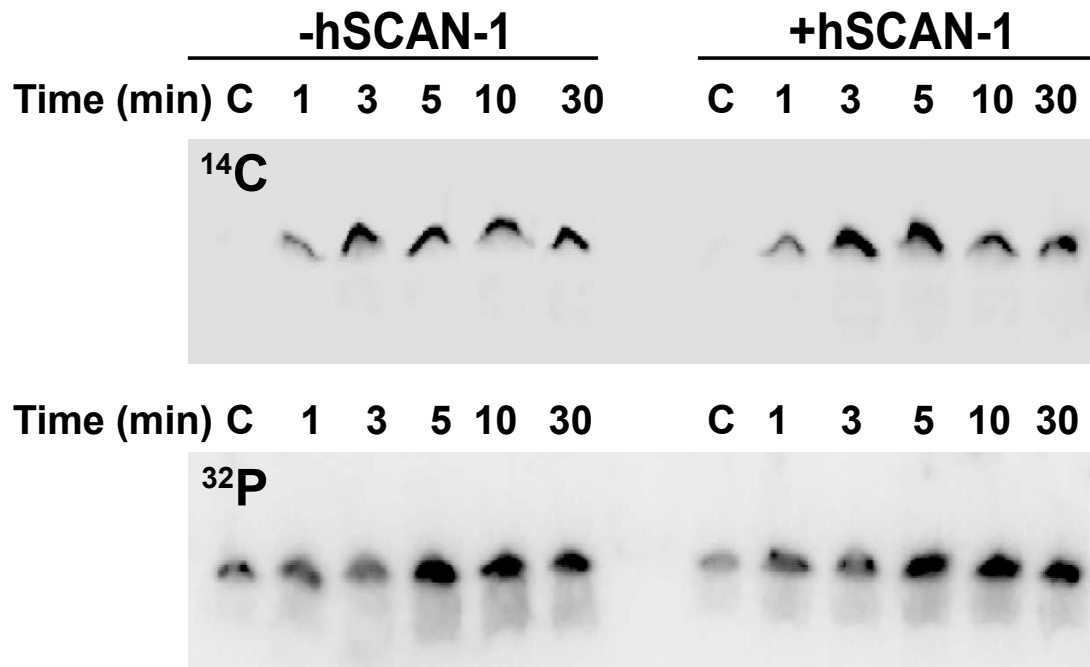


Figure 25. Effect of hSCAN-1 treatment on ³²P-labeling of glycogen.

Glycogen was labeled by incubation with 2 μ M [U-¹⁴C]glucose (upper panel) or [β -³²P]UDP-glucose (lower panel) and yeast glycogen synthase (5 μ g/ml), and aliquots removed at the indicated times. After ethanol precipitation, samples were treated with hSCAN-1(+hSCAN-1) or without (-hSCAN-1) for 30 min prior to analysis by SDS-PAGE (see Methods). C corresponds to reactions lacking glycogen synthase.

commercially available [α -³²P]UDP. The amount of radioactivity for [α -³²P]UDP was higher (~550,000 cpm/ μ l) than that of [β -³²P]UDP-glucose used in other experiments (~180,000 – 400,000 cpm/ μ l) and UDP-[U¹⁴C]-glucose was present at 400 – 1,800 cpm/ μ l for glycogen labeling. In comparison to the reaction containing only UDP-[U¹⁴C]-glucose, inclusion of [α -³²P]UDP with glycogen seemed to contribute to a slight increase in the background, which corresponded to the region where glycogen runs at the bottom of the well (Figure 26 A and B, comparing lanes 4 and 8). A faint diffuse signal was also seen above the stacking-separating gel interface and was not detected when [α -³²P]UDP was absent. The presence of a 1,000-fold molar excess of unlabeled UDP had no effect on the ³²P signal (Figure 26 B, lanes 5 and 9 to lanes 4 and 8, respectively), suggesting that the background radioactivity is associated with neither glycogen

nor UDP. To replicate the elongation of glycogen by glycogen synthase in the ^{32}P glycogen labeling experiments, $[\alpha\text{-}^{32}\text{P}]\text{UDP}$ was included in incubations where glycogen was being elongated (i.e. with glycogen synthase present). The argument is that UDP might be trapped as the glycogen is synthesized. Thus, lanes 6 in Figure 26 A and B indicates the control ^{14}C -labeling of glycogen. In the presence of $[\alpha\text{-}^{32}\text{P}]\text{UDP}$, there was no increase in ^{32}P signal (Figure 26 A and B, comparing lanes 2 and 6). The presence of unlabeled UDP also had no effect on the signal (Figure 26 B, comparing lanes 3 and 7 to lanes 2 and 6 respectively). However, treatment with glucosidases returned the signals to background levels (Figure 26 A, lanes 3 and 7).

In conclusion, based on the experiments described above, we found no evidence that ^{32}P -UDP binding to glycogen could account for the ^{32}P signal generated when $[\beta\text{-}^{32}\text{P}]\text{UDP}$ -glucose is incubated with glycogen synthase and therefore consider that our original conclusion that glycogen synthase is capable of adding phosphate to glycogen is valid.

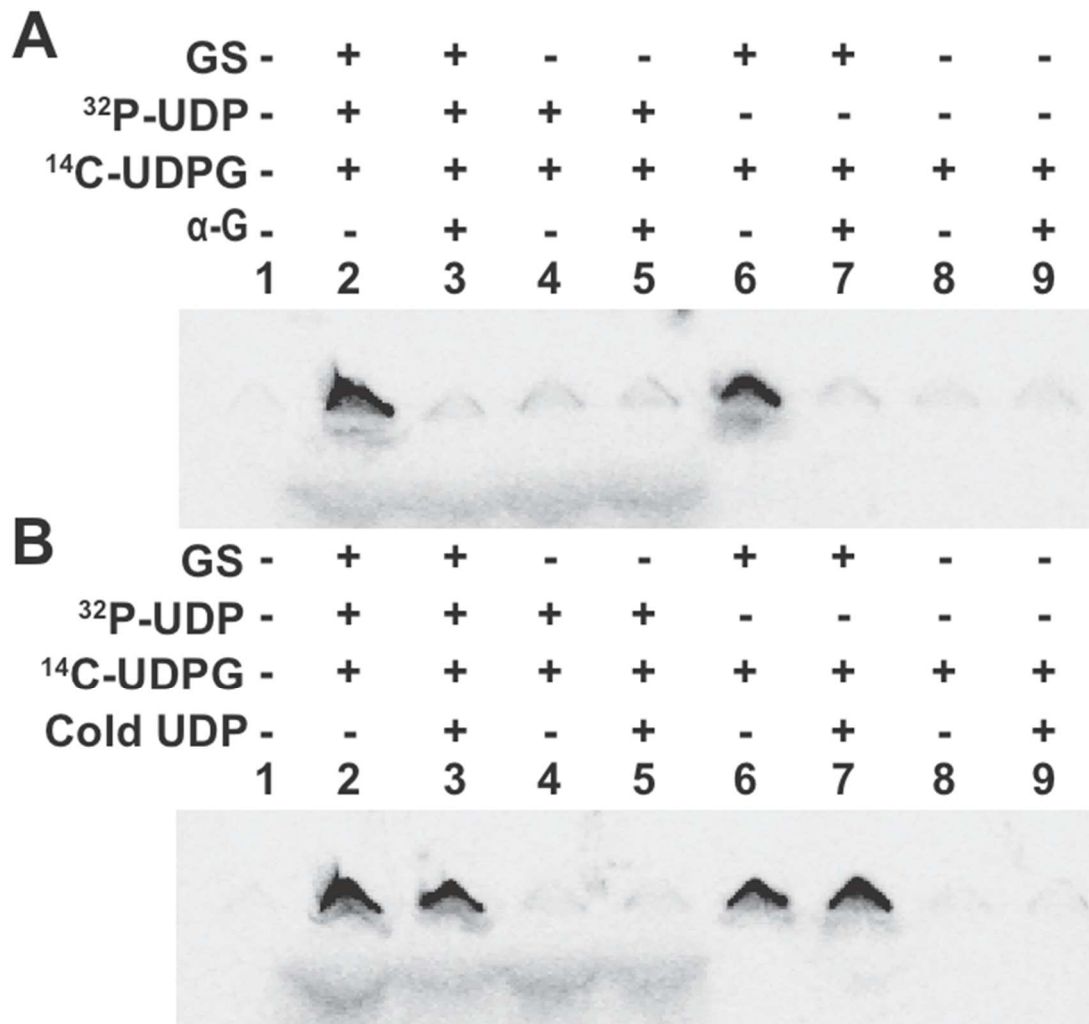


Figure 26. Test for ³²P-UDP binding to glycogen. Glycogen was incubated with [α -³²P]UDP and with (lanes 2 and 3) or without (lanes 4 and 5) glycogen synthesis by 10 μ g/ml glycogen synthase (GS) for 30 min. Samples were analyzed by SDS-PAGE and dried gels visualized with a Phosphorimager (see Methods). Controls lacked [α -³²P]UDP (lanes 6-9). In **A**, samples were treated or not with α -amylase and amyloglucosidase (α -G) and in **B**, unlabeled UDP (4 mM, a 1,000-fold excess over [α -³²P]UDP) was added to some samples prior to SDS-PAGE.

3. Glycogen Phosphate, Branching and Solubility

3.1 Analysis of Glycogen and Glycogen Phosphate from Laforin/PTG and Malin/PTG Double Knockout Mice

Laforin and malin knockout mice over-accumulate glycogen, develop Lafora bodies and have neurological defects (13,14,19,189,263-266) and thus are useful models for human Lafora disease. The targeting subunit of type 1 protein phosphatase, PTG, binds to glycogen, thus recruiting the catalytic subunit and activating glycogen synthase. Disruption of the *PTG* gene in mice results in decreased glycogen in muscle, liver and brain (241). In an attempt to suppress glycogen accumulation in mouse Lafora disease models, PTG knockout mice were crossed with laforin and malin knockout mice. The resulting double knockout mice, PTG/laforin^{-/-} or PTG/malin^{-/-} do not over-accumulate skeletal muscle or brain glycogen, have suppressed Lafora body formation and alleviated neurological symptoms (210,211). Because of the association of elevated phosphate, reduced branching and solubility of glycogen in Lafora disease, we therefore undertook a more detailed analysis of the glycogen of the double knockout mice.

3.1.1 Skeletal Muscle Glycogen Levels in WT, Single and Double Knockout Mice

First, we analyzed the amount of skeletal muscle glycogen in wild type, single PTG^{-/-}, laforin^{-/-}, malin^{-/-}, and double PTG/laforin^{-/-} and the PTG/malin^{-/-} 9-10 month old male mice (Figure 27). Similar to previous observations (241), the PTG knockouts had lower levels of skeletal muscle glycogen compared to wild type animals. The laforin^{-/-} and malin^{-/-} mice had an increase in skeletal muscle glycogen content with 1.7 and 4.5- fold increases over wild type, respectively (Figure 27, A and B), consistent with previous reports (12,14). Interestingly, when PTG was knocked out along with either malin or laforin, glycogen levels are normalized (Figure 27, A and B). Analyses of Lafora body formation in the double knockout mice, showed almost complete absence of Lafora bodies both in skeletal muscle and brain (data not shown).

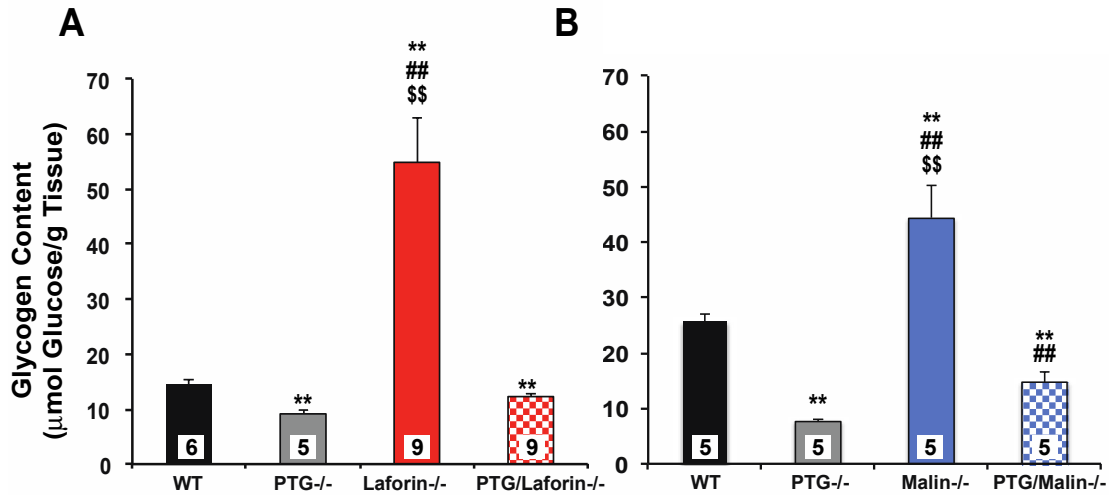


Figure 27. Skeletal muscle glycogen content. Analysis of total skeletal glycogen expressed as μmol of glucose/g of tissue. **A**, Skeletal muscle glycogen levels of wild type (WT), PTG knockout, the laforin knockout and laforin/PTG double knockout. **B**, Skeletal muscle glycogen levels of wild type (WT), PTG knockout, the laforin knockout, and PTG/malin double knockout. The error bars indicate the standard error of the mean; double symbols denote $p \leq 0.01$; * with respect to wild type mouse glycogen, # with respect to the PTG^{-/-} glycogen, \$ with respect to the double knockout, either PTG/laforin^{-/-} or PTG/malin. Numbers within bars represent the number of mice per group.

(210,211). Therefore, reducing glycogen levels prevents or reduces the amount of Lafora bodies formed, as expected.

3.1.2 Skeletal Muscle Glycogen Phosphate in WT, Single Malin or Laforin Knockout and PTG/Laforin and PTG/Malin Double Knockout Mice

In addition to the accumulation of glycogen, there is also a correlation between glycogen hyperphosphorylation, abnormal branching and Lafora body formation (12,13). Therefore, we wanted to determine the phosphate content of the glycogen from the double knockout mice. Highly purified glycogen was prepared from skeletal muscle and glycogen concentration and phosphate content was determined. The glycogen phosphate content, expressed as the molar ratio of phosphate to glucose, can be viewed as the glycogen phosphorylation density. The PTG^{-/-} mice had glycogen phosphate content similar to that of wild type animals (Figure 28, A and B). Similar to what we had previously reported (12,14), the laforin^{-/-} and malin^{-/-} mice had elevated glycogen phosphate content, with the laforin^{-/-} mice having a higher glycogen phosphate content than the malin^{-/-} mice, with 4 and 3-fold increases over the wild types, respectively (Figure 28, A and B). The PTG/laforin^{-/-} mice had similar levels of glycogen phosphate content when compared to the laforin^{-/-} mice, having an ~4 fold increase over the wild type (Figure 28, A), consistent with both lines lacking laforin. The glycogen phosphate content of the PTG/malin^{-/-} mice, however, was similar to that of the wild type levels. It has been proposed that laforin's function is dependent on malin (187,205,207,208). However, the phosphate content of the PTG/malin^{-/-} mice suggests that laforin is functioning *in vivo* and its glycogen phosphatase activity is not dependent on malin.

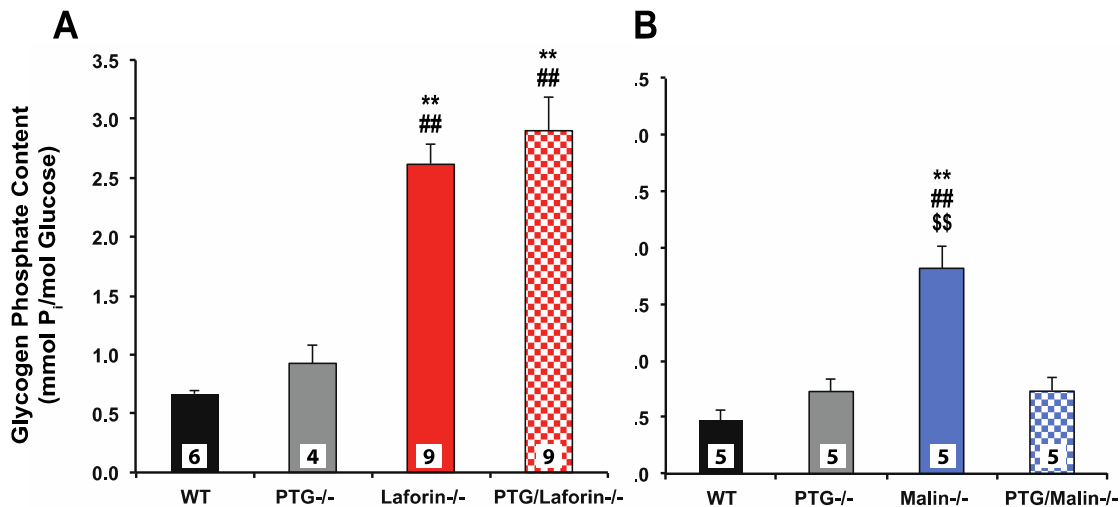


Figure 28. Skeletal muscle glycogen phosphate content. Analysis of total skeletal glycogen phosphate content expressed as $\mu\text{mol Phosphate (P}_i\text{)}/\text{mol glucose}$. **A**, skeletal muscle glycogen levels of wild type (WT), PTG knockout, the laforin knockout and laforin/PTG double knockout. **B**, Skeletal muscle glycogen levels of wild type (WT), PTG knockout, the laforin knockout, and PTG/malin double knockout. The error bars indicate the standard error of the mean; double symbols denote $p \leq 0.01$,; * with respect to wild type mouse glycogen, # with respect to the PTG^{-/-} glycogen, \$ with respect to the double knockout, either PTG/laforin^{-/-} or PTG/malin. Numbers within bars represent the number of mice per group. Numbers within bars represent the number of mice per group.

Another way to express glycogen phosphorylation is to consider the total amount of phosphate per tissue mass expressed as nmol phosphate/g tissue, which is referred to as “total glycogen phosphate” (Figure 29). The total glycogen phosphate content of the laforin^{-/-} and malin^{-/-} mice, like the total glycogen content, is elevated over the wild type, with 14 and 8-fold increases, respectively. The PTG^{-/-} mice had similar total glycogen phosphate levels as the wild type animals (Figure 29, A and B). PTG/malin^{-/-} mice have a total glycogen phosphate levels that are similar to wild type and PTG^{-/-} mice (Figure 29, B), which would be expected since both the glycogen and molar glycogen phosphate measurements were restored to wild type levels. The total glycogen phosphate of the PTG/laforin^{-/-} mice (Figure 29, A) mice was significantly less than that of the laforin^{-/-} mice but not as low as the wild type or PTG^{-/-} mice. Since the

laforin/PTG^{-/-} have normalized glycogen levels but with elevated glycogen phosphate content (mmol P_i/mol glucose) the levels of phosphate per gram of tissue should be higher than the wild type. However, there is a 70% decrease of total glycogen phosphate in the PTG/laforin^{-/-} mice compared to the laforin^{-/-} mice. These results are as expected based on the glycogen content and glycogen phosphorylation state in the different mouse models. In regard to Lafora body formation, one can propose that there needs to be an over-accumulation of glycogen as well as an increase in glycogen phosphate which may somehow contribute to the abnormal branching and solubility of glycogen associated with Lafora bodies.

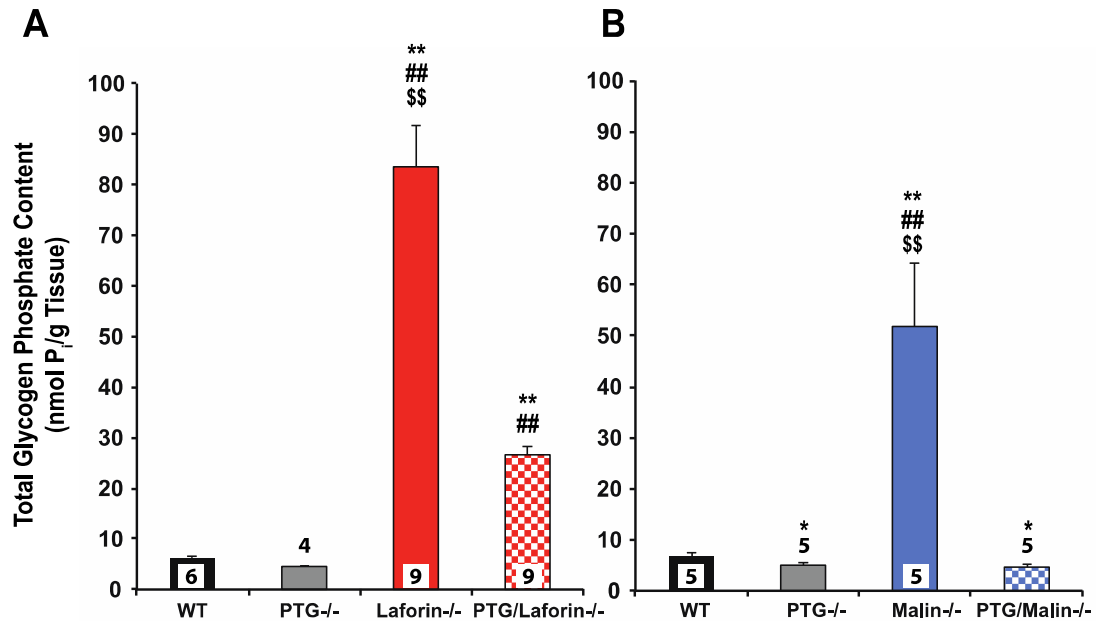


Figure 29. Total skeletal muscle glycogen phosphate. Analysis of total skeletal glycogen phosphate content represented as mmol Phosphate (Pi)/mol glucose **A**, skeletal muscle glycogen levels of wild type (WT), PTG knockout, the laforin knockout and laforin/PTG double knockout. **B**, Skeletal muscle glycogen levels of wild type (WT), PTG knockout, the laforin knockout, and PTG/malin double knockout. The error bars indicate the standard error of the mean; double symbols denote $p \leq 0.01$, ; * with respect to wild type mouse glycogen, # with respect to the PTG^{-/-} glycogen, \$ with respect to the double knockout, either PTG/laforin^{-/-} or PTG/malin^{-/-}. Numbers within bars represent the number of mice per group.

3.2 Glycogen Solubility and Branching in the Double Knockout Mice

As previously mentioned, glycogen solubility and branching seemed to be related to the phosphate content of glycogen in the laforin^{-/-} mice (12,18). Here we subjected skeletal muscle tissue extracts to low speed centrifugation to produce a low speed supernatant and pellet, and glycogen content in both were quantitated. If glycogen is normally branched and soluble, the majority of the glycogen should be in the low speed supernatant whereas if it is insoluble it would be found in the low speed pellet. Thus, abnormal insoluble glycogen generated in the Lafora disease mouse models would be expected in the low speed pellet. We also analyzed the branching pattern of glycogen from wild type,

single and double knock mice to correlate any branching abnormalities with glycogen phosphate content.

3.2.1 Skeletal Muscle Glycogen Solubility

Fractionation of skeletal muscle tissue extracts by low speed centrifugation results in a low speed pellet (LSP) and a soluble fraction, the low speed supernatant (LSS). The LSP is mainly composed of contractile proteins and other insoluble components, while the LSS contains mostly soluble proteins. Glycogen can be detected in both the LSS and LSP of mouse skeletal muscle extracts. This separation operationally defines what fraction of glycogen is soluble. Tagliabracci *et al* (12) reported that a majority of the glycogen in skeletal muscle extracts from laforin *-/-* mice was found in the LSP suggesting that it was insoluble and was poorly branched. We analyzed the glycogen distribution of the double knockout mice to determine whether their glycogen would be found in the soluble LSS fraction or in the LSP. Typically, we observe that 75 – 80% of the total glycogen from wild type muscle is present in the soluble fraction, the LSS (Figure 30), similar to previous reports (12,189). When measuring the volume of the LSS after low speed centrifugation, typically, about ~70% of the initial volume is recovered (data not shown). The PTG*-/-* mice have a glycogen distribution similar to the wild type animals, with most of the glycogen found in the soluble fraction (Figure 30). With laforin*-/-* and malin*-/-* mice, the glycogen distribution was nearly opposite of wild type, with 75 – 80% of the total glycogen being present in the LSP. This suggests that a majority of the glycogen is poorly branched and insoluble, similar to what has been previously reported (12). The laforin/PTG*-/-* and malin/PTG*-/-* mice have a distribution of glycogen between the LSS and LSP more like wild type. In the double knockout mice, the majority of the muscle glycogen is found in the soluble fraction, suggesting that it is normally branched and soluble.

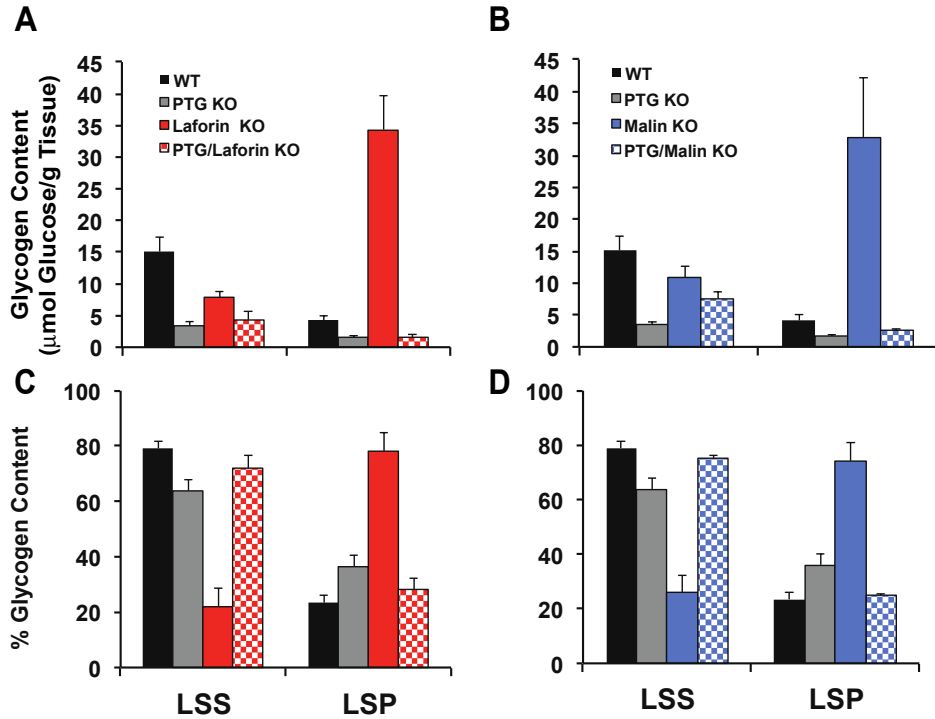


Figure 30. Low speed supernatant and pellet glycogen content. Analysis of skeletal muscle glycogen content in the low speed supernatant (LSS) or pellet (LSP) of tissue homogenates. **A and C**, Glycogen content in LSS and LSP of skeletal muscle of wild type (WT), PTG knockout, laforin knockout and Laforin/PTG double knockout mice **B and D**, Percent glycogen distribution in LSS and LSP of skeletal muscle of wild type (WT), PTG knockout, malin and Malin/PTG double knockout mice. The error bars indicate the standard error of the mean. The n for each group is 4.

The laforin/PTG^{-/-} mice had glycogen phosphate content similar to that of the laforin^{-/-} mice, on a mol P_i/mol glucose basis, which could suggest that phosphate content alone does not determine solubility. Possibly the lower glycogen synthase activity of the double knockouts allows for the branching enzyme to properly branch the glycogen.

3.2.2 Skeletal Muscle Glycogen Branching

To prove that less branched glycogen predominated in the LSP fraction, glycogen branching was analyzed by high performance anionic exchange chromatography (HPAEC) to determine the distribution of the polyglucose chain lengths of glycogen from different mouse lines. Glycogen was purified as for measurement of glycogen phosphate (described in Methods) and treated with

isoamylase to hydrolyze the α -1,6-glycosidic bonds thus producing a mixture of polymeric glucose chains. The HPAEC separates the mixture according to chain length, shorter chains eluting earlier. The eluate is monitored by amperimetric pulse detection. Figure 31, A and B, shows a branching profile for glycogen from the skeletal muscle of mice and is expressed as relative peak area, which is the percentage of the area for a given peak over the sum of all peak areas. For further analysis, data are represented as a relative change in abundance, where the data has been normalized to the wild type for each chain length. Therefore, any difference from the wild type glycogen is represented by bars above or below the x axis, a positive value meaning more representation than wild type and a negative value, less than wild type. Both laforin^{-/-} and malin^{-/-} mice have fewer short chains, from 4 – 15 glucose residues long, and more long chains, from 15 – 34 glucose residues long (Figure 31, C and D). This indicates that the glycogen in the laforin^{-/-} and malin^{-/-} mice is less branched and has an overall increase in chain length. Also, the PTG^{-/-} mice have a branching pattern that is slightly different than the wild type, with more short chains and fewer long chains. This could be due to the reduced activity of glycogen synthase resulting in shorter glucose polymer chains. Consistent with the LSS/LSP distribution (Figure 30), the double knockout mice have glycogen that is more like the PTG^{-/-}, in terms of the branching pattern. Figure 31 shows that the laforin/PTG^{-/-} or malin/PTG^{-/-} mice have a branching pattern with more shorter branches, 5 – 14 glucose residues long, and fewer long branches, 16 – 30 glucose residues. These data are consistent with the observed solubility and distribution of glycogen between the LSS and LSP (Figure 30).

The results from this section confirm that deletion of PTG in laforin^{-/-} or malin^{-/-} mice normalizes muscle glycogen levels in both models. In a malin^{-/-} background, glycogen phosphorylation is normalized but phosphorylation remains elevated in laforin^{-/-} mice. The reduced branching of glycogen was essentially restored to normal by the absence of PTG in both models. Therefore, increased glycogen phosphorylation was not always correlated with increased branching.

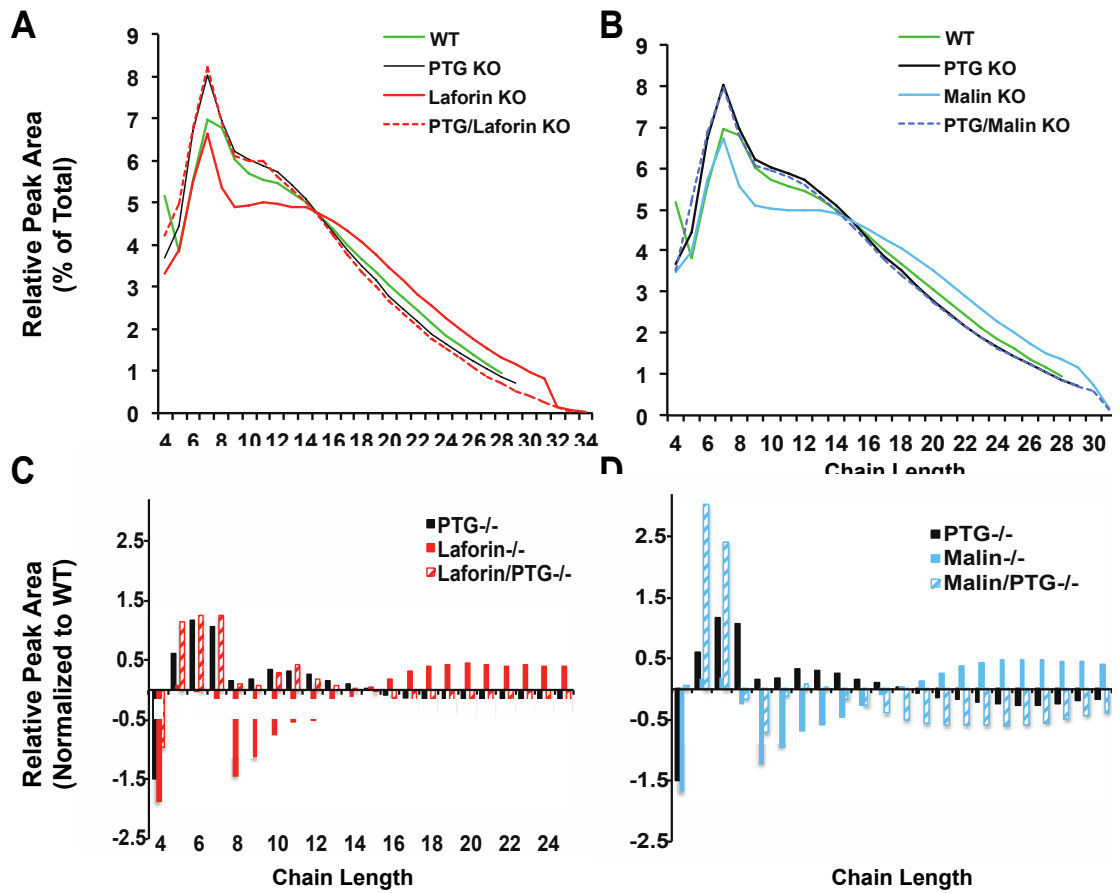


Figure 31. HPAEC analysis of skeletal muscle glycogen Analysis of purified skeletal muscle glycogen. **A and B.** HPAEC analysis of glycogen chain lengths after isoamylase treatment, represented as the percent of the total PAD signal for 4 – 25 glucose residues. **C and D.** HPAEC analysis of skeletal muscle glycogen that has been normalized to the WT glycogen.

4. Glycogen Metabolism in Mouse Models of Lafora Disease Subjected to Exercise

Lafora bodies, the hallmark of Lafora disease, are largely composed of poorly soluble glycogen and can accumulate to high levels in muscle. Two questions come immediately to mind. Can the build up of Lafora bodies affect muscle function and is the glycogen contained in Lafora bodies susceptible to normal metabolism?

4.1 Exercise Performance and Blood Glucose

Lafora bodies accumulate in the skeletal muscle of both laforin and malin knockout mice. If Lafora bodies and excess glycogen accumulation had a negative impact on muscle contraction, we might expect the knockout animals to have an impaired ability to exercise. However, older laforin and malin knockout animals displayed the same exercise capacity as wild type mice, whether judged by exercise time or work performed (Table 4), suggesting that the accumulation of Lafora bodies did not affect muscle function. The average time to reach exhaustion was ~ 45 minutes and there was no significant difference between the knockout animals and their wild type littermates (Table 4). This result is consistent with previous studies showing that young laforin^{-/-} mice, 3 month old, did not have impaired ability to exercise (238) and had no cardiac or metabolic abnormalities (240).

To test whether exercise elicited any abnormalities in glucose handling in Lafora mice, blood glucose was monitored pre- and post-exercise. Mice that were not immediately sacrificed after exercise were given an oral glucose gavage, at a dose of 3.6 g/kg of body weight, and blood glucose was monitored for up to 3 hours post exercise, during which time they had access to food and water. Both laforin^{-/-} mice and their wild type littermates had increased blood glucose following exercise; the levels further increased after receiving the oral glucose gavage (Table 5). There was no difference in glucose profiles between the laforin^{-/-} mice and wild type littermates. The glucose profiles for the malin^{-/-} mice were similar, trending to an increase in blood glucose after exercise, although the

differences did not reach statistical significance. We conclude that there was no major defect in whole body glucose handling with either knockout mouse line.

Table 4. Exercise performance

Body weights and exercise performance. Body weights are expressed in grams (g), exercise time is expressed in minutes (min) and work is expressed in Joules (J). Data are presented as the mean \pm the standard error. **a:** $p < 0.05$ compared to wild type

Exercise Performance				
	Laforin+/+	Laforin-/-	Malin+/+	Malin-/-
n	16	20	8	10
Body Weight (g)	37.7 \pm 1.4	37.6 \pm 1.1	36.4 \pm 1.0	40.3 \pm 1.2 ^a
Exercise Time (min)	41.1 \pm 3.0	44.0 \pm 3.7	56.5 \pm 4.7	43.2 \pm 5.4

Table 5. Blood glucose pre- and post-Exercise

Blood glucose (BG) analysis of mice before and after exercise. After mice were exercised until exhaustion some were given an oral glucose gavage and blood glucose was monitored for 15-180 minutes post gavage (PG). Blood glucose is expressed as mg per deciliter and the data are presented as the mean \pm the standard error. **b**: $p < 0.05$ compared to the pre-exercise blood glucose levels **b***: $p < 0.001$ compared to the pre-exercise blood glucose levels. There was no significant difference between the knockout animals and their respective wild types

Exercise Blood Glucose								
Blood Glucose (mg/dl)	Laforin+/+		Laforin-/-		Malin+/+		Malin-/-	
	n	Average	n	Average	n	Average	n	Average
BG Pre-EX	16	134 \pm 5.0	20	133 \pm 2.4	8	140 \pm 7.5	10	144 \pm 5.5
BG Post EX	16	174 \pm 8.4 ^{b*}	20	164 \pm 8.5 ^{b*}	8	167 \pm 19.8	10	164 \pm 10.0
BG 15 min PG	8	248 \pm 20.6 ^{b*}	6	229 \pm 15.7 ^{b*}	3	176 \pm 25.3	4	153 \pm 26.2 ^{b*}
BG 30 min PG	8	207 \pm 11.3 ^{b*}	8	217 \pm 15.6 ^{b*}	3	197 \pm 17.3	4	249 \pm 21.5 ^{b*}
BG 60 min PG	8	209 \pm 18.2 ^{b*}	8	233 \pm 14.1 ^{b*}	3	217 \pm 9.3 ^b	4	226 \pm 14.8 ^{b*}
BG 180 min PG	8	158 \pm 14.8 ^{b*}	8	127 \pm 5.0 ^{b*}	3	136 \pm 23.3	4	113 \pm 9.7 ^b

4.2 Effect of Exercise on Enzyme Phosphorylation and Distribution

It is well established that adenosine monophosphate activated kinase (AMPK) is activated by phosphorylation at Thr172 after exercise (130,189,267-270) and therefore can serve as a molecular indicator of a normal muscle response to muscular activity. Previous reports on young, 3 month old, laforin-/- mice had shown that there were no defects in AMPK phosphorylation in

response to exercise (238). In the present study, we find similar results with older, 12 month old mice, namely no impairment of exercise-induced AMPK phosphorylation in either the laforin^{-/-} or malin^{-/-} mice as compared to wild type mice (Figure 31).

A number of reports describe the activation, via dephosphorylation, of glycogen synthase following exercise, (127,128,189,270) although the exact mechanisms are complex and not fully understood (57). Therefore, we analyzed glycogen synthase after exercise of the laforin and malin knockout mice (Figure 32). In the 12 month old laforin and malin knockout mice, there was a noticeable increase in glycogen synthase protein levels over wild type (Figure 32), consistent with previous results in the laforin^{-/-} mice (13). In response to exercise, the laforin^{-/-} mice had a blunted dephosphorylation of glycogen synthase and the malin^{-/-} mice had a complete inhibition of glycogen synthase dephosphorylation (Figure 32). Even though AMPK activation in the skeletal muscle of the knockout mice may indicate a normal response to exercise, the impaired activation of glycogen synthase could indicate defects more specific to glycogen metabolism.

The knockout animals have increased total glycogen synthase protein levels and the bulk of the protein is associated with the LSP fraction of the muscle extracts (Figure 33). The levels of glycogen synthase in the LSS were similar to that in the wild type animals (Figure 33, A, B, C and D). The wild type animals from the laforin background had a significant decrease in glycogen synthase phosphorylation in both the LSS and LSP fractions in response to exercise (Figure 33 A and E), while the wild types from the malin background only showed a significant decrease in glycogen synthase dephosphorylation in the LSS.

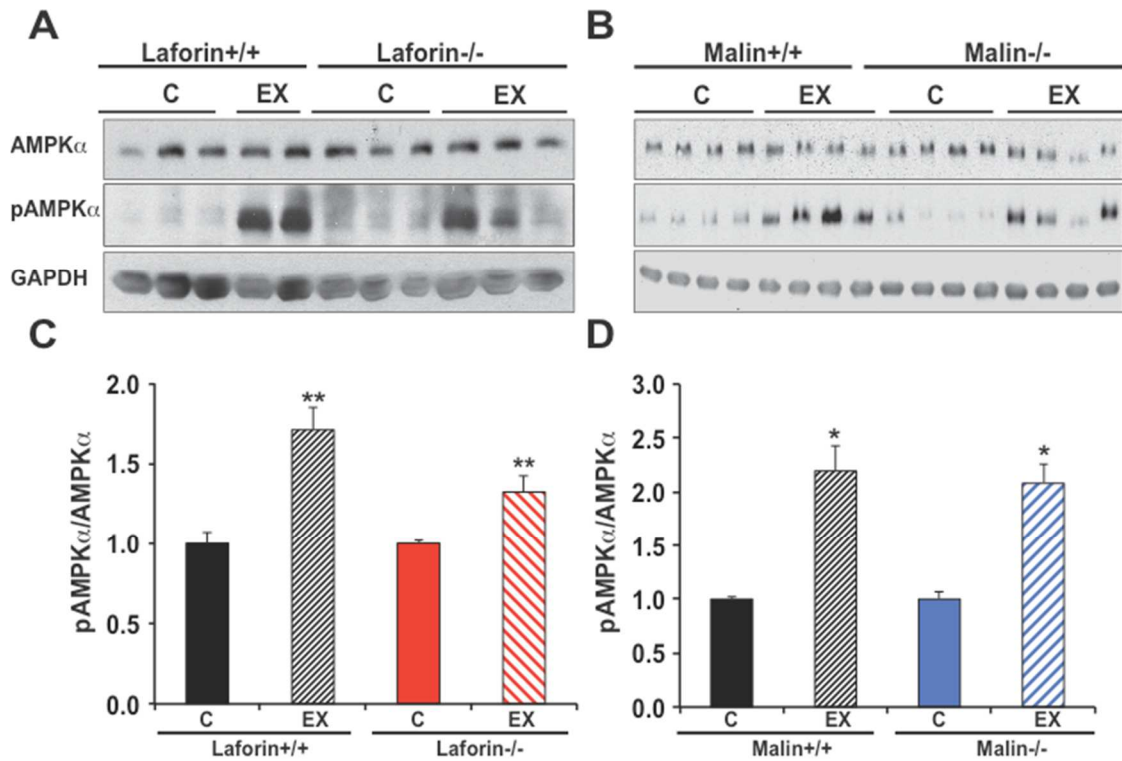


Figure 32. Effect of exercise on AMPK phosphorylation. Western analysis of AMPK and phosphorylation at Thr172 from skeletal muscle total extracts of 12 month old mice. **A.** Laforin+/+ and laforin-/- control (C) and post-exercise (EX) **B.** Malin+/+ and Malin-/- control (C) and post-exercise (EX) **C.** Quantitation of the ratio of P-AMPK over AMPK by densitometry of the control and exercise laforin+/+ and laforin-/- mice (n = 4-6). **D.** Quantitation of the ratio of P-AMPK over AMPK by densitometry of the control and exercise malin+/+ and malin-/- mice (n = 4).). Data are means +/- SEM, * indicates significance compared to the control with p < 0.05 and ** indicates p<0.01

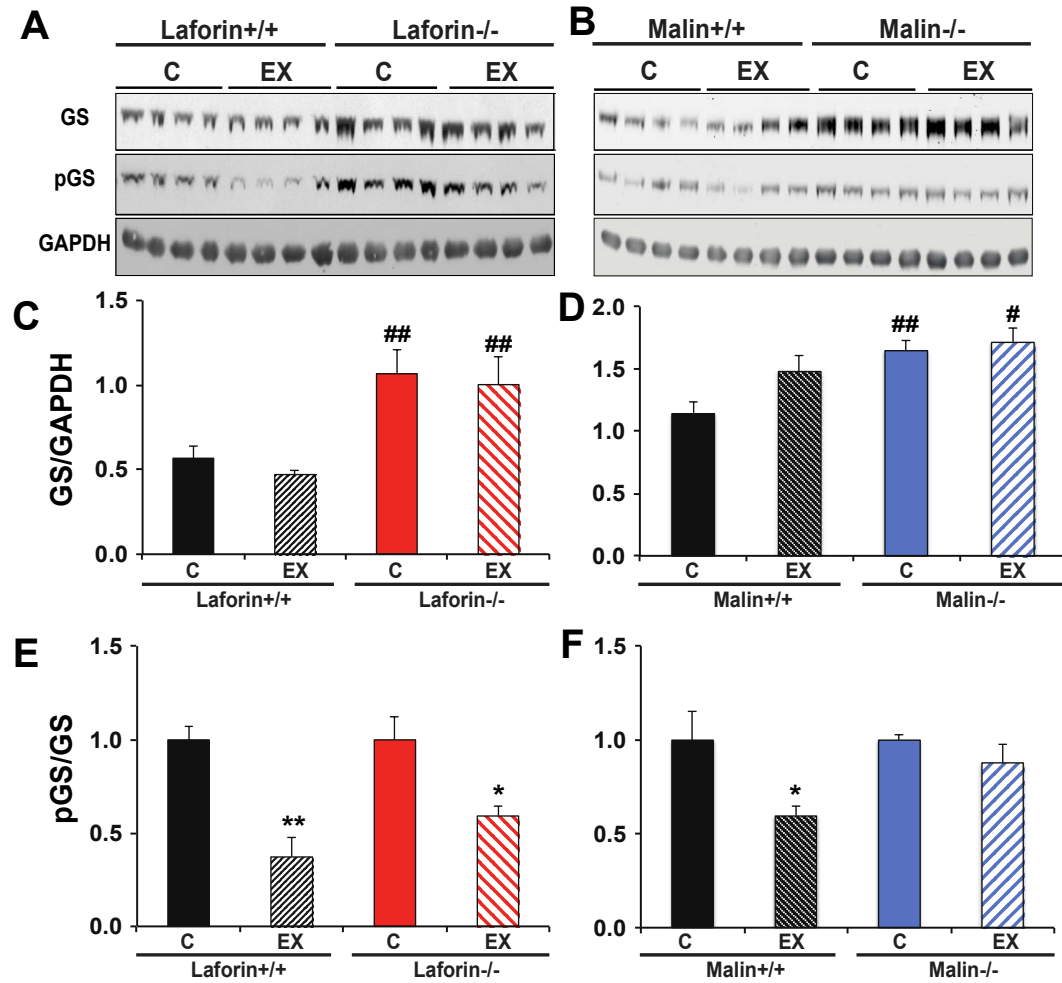


Figure 33. Effect of exercise on glycogen synthase and glycogen synthase phosphorylation Western analysis glycogen synthase protein and phosphorylation of total extracts of skeletal muscle from 12 month old laforin^{+/+}, laforin^{-/-}, malin^{+/+} and malin^{-/-} mice. **A.** Laforin^{+/+}, laforin^{-/-} control (C) and post-exercise (EX). **B.** Malin^{+/+} and Malin^{-/-} control (C) and post-exercise (EX). **C and D.** Quantitation of the ratio of GS over GAPDH by densitometry of the control and exercise **E and F.** Quantitation of the ratio of P-GS over GS by densitometry of the control and exercise (n = 4). Data are means +/- SEM, * indicates significance compared to the control and # indicates significance compared to wild type with p < 0.05 double symbols ** or ## indicate p < 0.01.

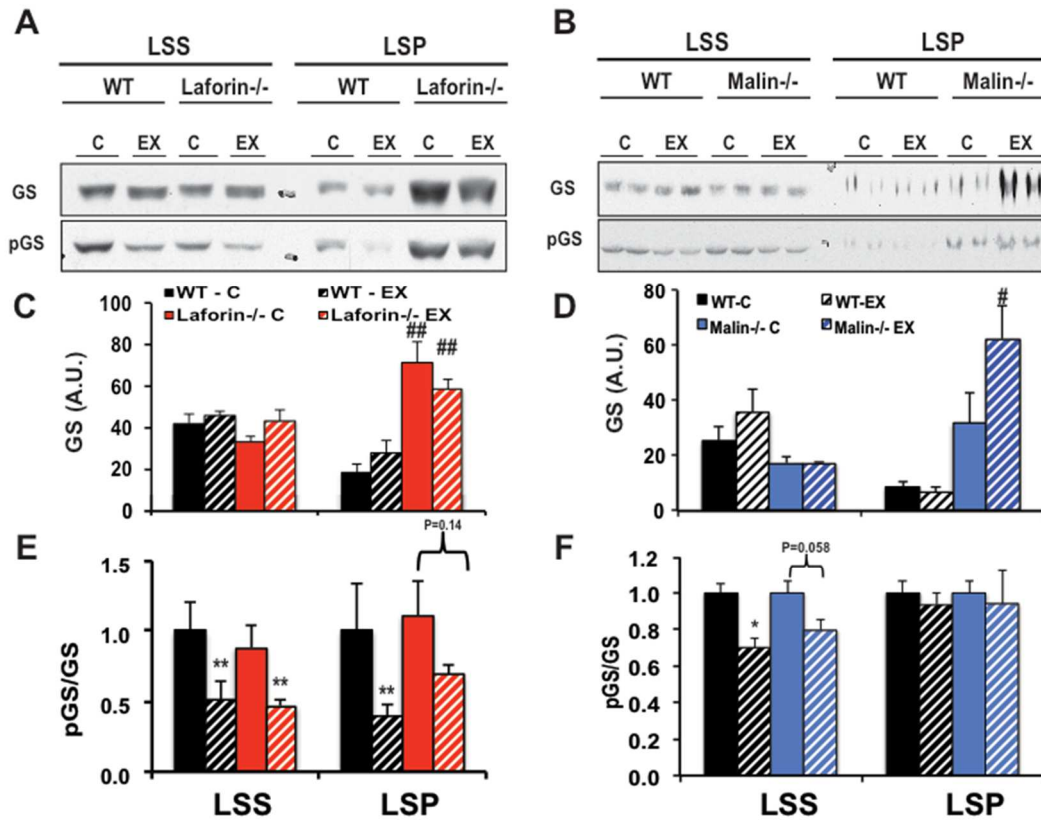


Figure 34. Effect of exercise on glycogen synthase and glycogen synthase phosphorylation in the LSS and LSP Western blot analysis of 12 month old laforin^{+/+} and laforin^{-/-} (**A**) and malin^{+/+} and malin^{-/-} (**B**) mice skeletal muscle LSS and LSP with antibodies against glycogen synthase (GS) and phospho-GS. **C and D.** Quantitation of GS in either the LSS or LSP of skeletal muscle extracts. **E and F.** Quantitation of the ratio of phospho-GS over GS densitometry of the control and exercise (n = 4). Data are means +/- SEM, * indicate significance compared to the control and # indicate significance compared to wild type with p < 0.05 double symbols ** or ## indicate p < 0.01.

The malin^{-/-} mice had a small, but not statistically significant, decrease in glycogen synthase phosphorylation in the LSS and no change in the LSP (Figure 34, B and F). The malin samples for the glycogen synthase and phosphorylated form of glycogen synthase, in the LSS and LSP, posed some technical challenges that may have contributed to the observed data, but from multiple attempts what is presented here is the best representation for such data. In both cases it would appear that glycogen synthase associated with the LSP, where the majority of glycogen synthase was found, the phosphorylation status of glycogen synthase does not appear to change in response to exercise, suggesting that it may not be subject to normal metabolism. After exercise, glycogen synthase associated with the LSP in the laforin^{-/-} mice trended towards a decrease in phosphorylation but was not statistically significant (Figure 34, A and E). Exercise-induced glycogen synthase dephosphorylation in the LSS fraction of the laforin^{-/-} mice suggest that solubility of glycogen and its associated proteins is required for normal metabolism

In the malin^{-/-} mice there was a basal increase in laforin protein levels (Figure 35) similar to previous reports for young animals (189). The bulk of the laforin protein tracks in the LSP of skeletal muscle extracts with depletion from the LSS (Figure 36) and is associated with the abnormal glycogen found in the LSP (Figure 39), similar to previous observations (189). Exercise did not affect the distribution of laforin in the malin^{-/-} mice (Figure 37). Since there was no observable decrease in glycogen phosphate content in the malin^{-/-} mice, even with exercise (Figure 40 and 42), it is likely that the majority of laforin in the malin^{-/-} mice is most likely sequestered in the insoluble fraction and not active, as previously proposed (189).

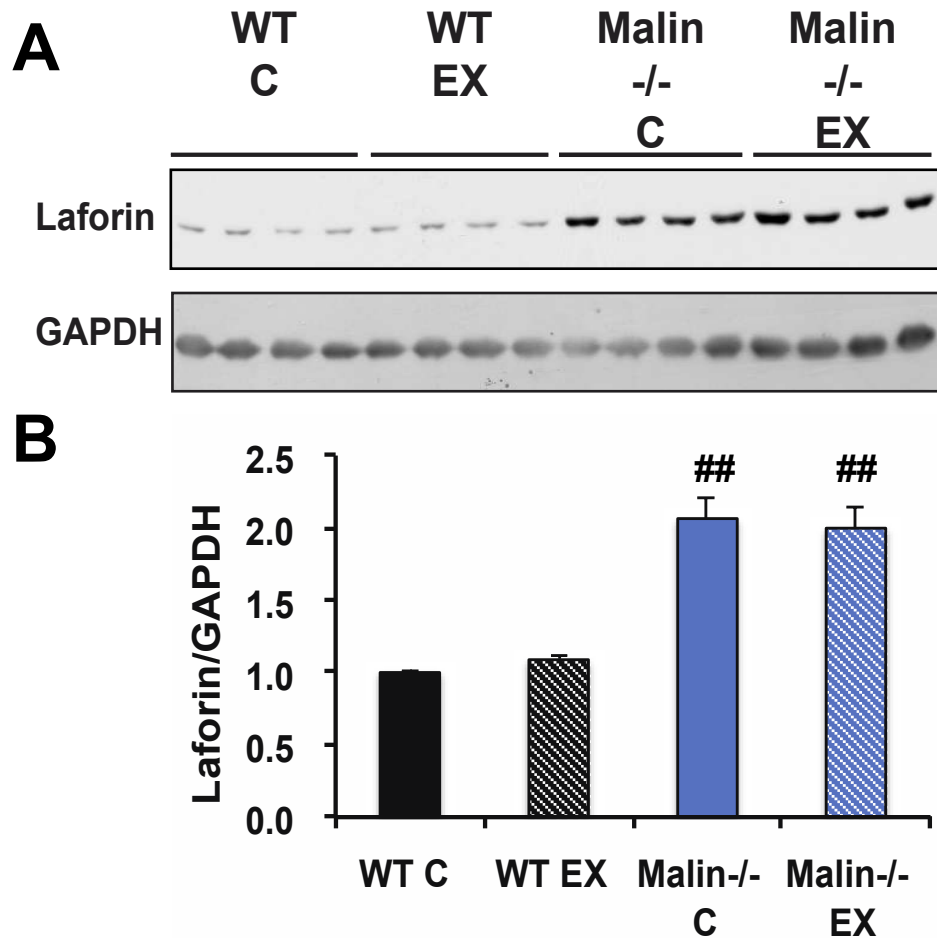


Figure 35. Laforin protein levels in the malin knockout mice. Western blot analysis of 12 month old malin^{+/+} and malin^{-/-} mice total skeletal muscle extracts analyzing laforin protein levels. **A.** Skeletal muscle extract western blots for antibodies against laforin and GAPDH. **B.** Quantitation of the ratio of laforin over GAPDH densitometry of the control and exercise (n = 4). Data are means \pm SEM, # indicate significance compared to wild type with $p < 0.05$ double symbols ** or ## indicate $p < 0.01$.

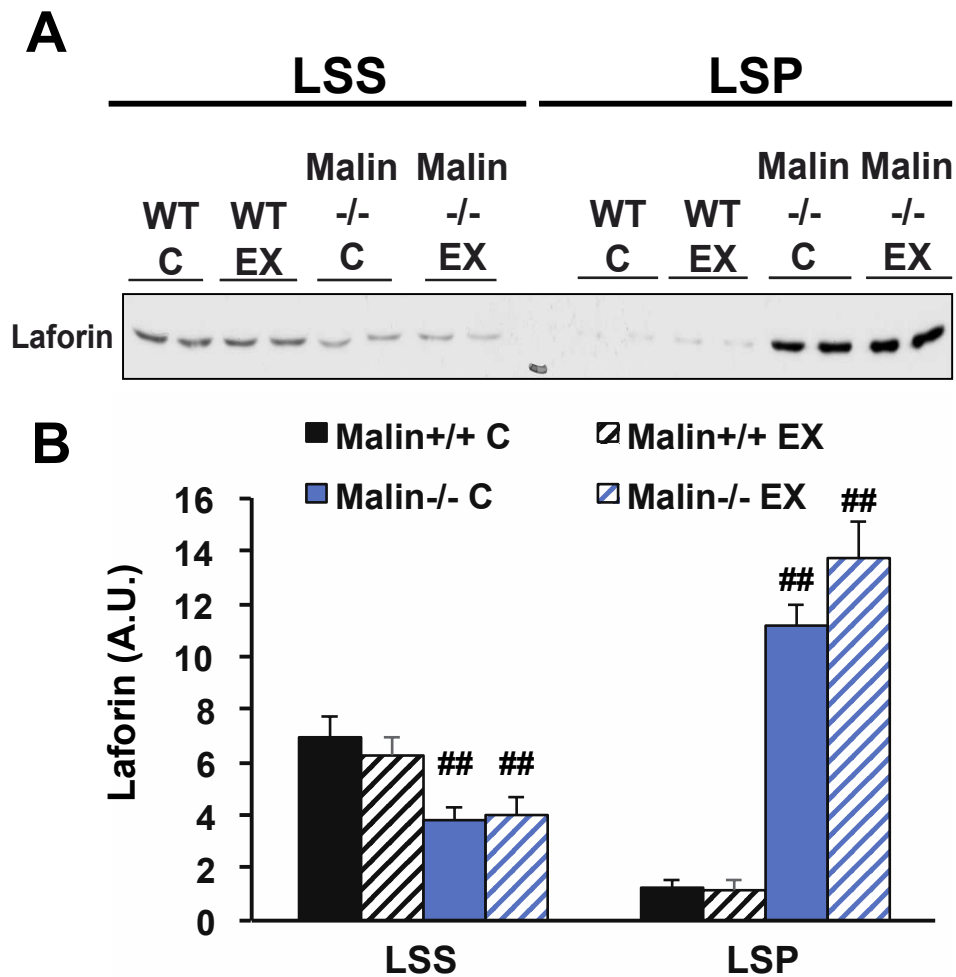


Figure 36. Laforin protein levels in the LSS and LS of malin knockout mice. Western blot analysis on 12 month old malin^{+/+} and malin^{-/-} mice skeletal muscle LSS and LSP. **A.** Skeletal muscle LSS and LSP western blots for antibodies against laforin. **B.** Quantitation of laforin in the LSS and LSP. Data are means \pm SEM, ## indicate significance compared to the wild type with $p < 0.01$.

4.3 Effect of Exercise on Glycogen and Glycogen Phosphate

Metabolism

During exhaustive exercise glycogen is utilized as a major source of energy in the skeletal muscle, while liver glycogen is broken down in order to maintain blood glucose levels (4). The laforin^{-/-} and the malin^{-/-} mice had an increase in total skeletal muscle glycogen content of 3 or 2.6-fold increase over wild type, respectively (Figure 38, A and B). Wild type animals consumed 75-80 % of their total muscle glycogen during the exercise protocol while the knockout animals had no statistically significant decrease in the levels of their skeletal muscle glycogen though there was a trend to be slightly lower than the non-exercised group (Figure 37, A). However, there is a relatively large error associated with the measurement of skeletal muscle glycogen in the laforin^{-/-} mice. The wild type mice consumed 15 μmol glucose/g tissue during exercise, a decrease that may be lost within the measurement errors of the much higher glycogen levels in the laforin^{-/-} mice. A similar argument can be made for the malin^{-/-} mice (Figure 37 B). Skeletal muscle glycogen levels were restored 3 hours post exercise but there was minimal or no supercompensation, unlike what was observed in younger mice (238).

The glycogen levels in the liver were decreased by exercise but there was no difference between the wild type and knockout animals (Figure 37, C and D). On the other hand, although the brain glycogen was higher in the knockout mice as previously reported (13,189,210) (Figure 37, E and F), no difference was observed between control and exercise animals. Consistent with no significant decrease of total glycogen we also did not observe a noticeable decrease in Lafora bodies in the skeletal muscle of laforin^{-/-} mice after exercise (Figure 38)

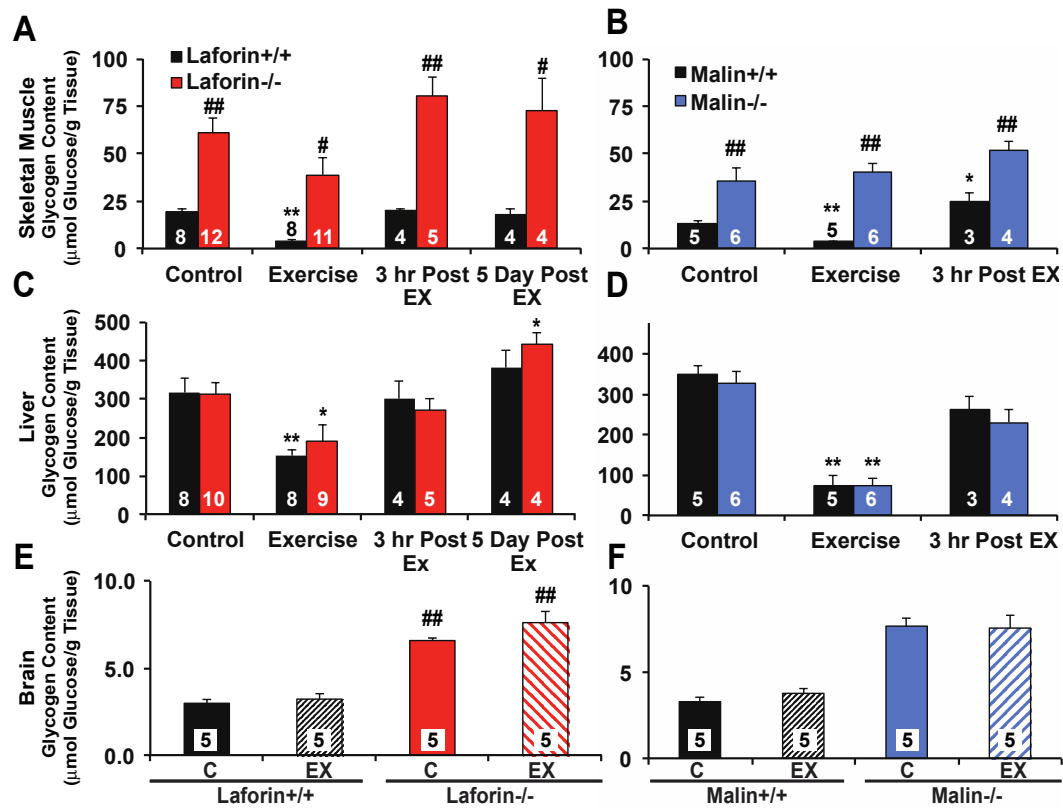


Figure 37. Effect of exercise on glycogen. Total glycogen content expressed as μmol of glucose/g tissue in the 12 month old male laforin^{-/-} (red bars), malin^{-/-} (blue bars) and in the corresponding wild type litter mate (black bars) mice. **A and B.** Total skeletal muscle glycogen in response to exercise and post exercise. **C and D.** Total liver glycogen in response to exercise and post exercise. **E and F.** Total brain glycogen in response to exercise. The number in the data bar indicates the number of mice for each group. Data are means +/- SEM, * indicate significance compared to the control and # indicate significance compared to wild type with p < 0.05 double symbols ** or ## indicate p < 0.01.

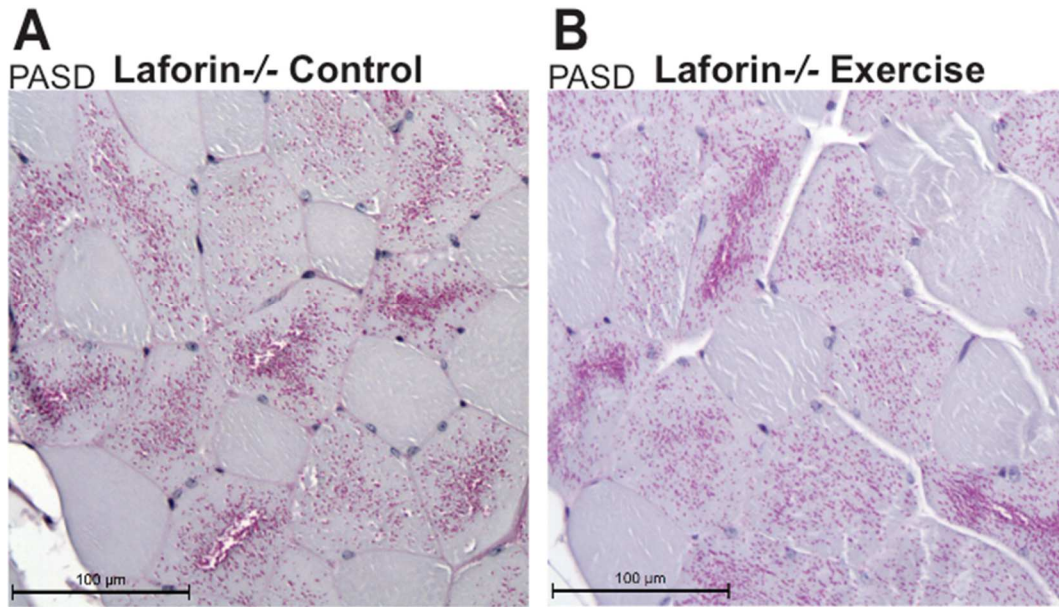


Figure 38. Lafora bodies and response to exercise. Sections quadriceps muscle from a control laforin^{-/-} mouse **A** and an exercise laforin^{-/-} **B** were stained with periodic acid/Schiff/diastase (PASD) to visualize Lafora bodies as α -amylase resistant polysaccharide, visualized as dark purple spots.

In response to exercise, the wild type animals utilized glycogen both from the LSS and LSP (Figure 39, A and B), suggesting that both pools of glycogen are metabolically active and likely explained by the fact that the LSP glycogen is normal glycogen that is trapped in the pellet during centrifugation. The LSS glycogen, from both knockout mouse lines, was clearly utilized during exercise. In both knockout mouse lines, the LSP glycogen is elevated and does not significantly decrease in response to exercise although a small amount of utilization would not have been detectable.

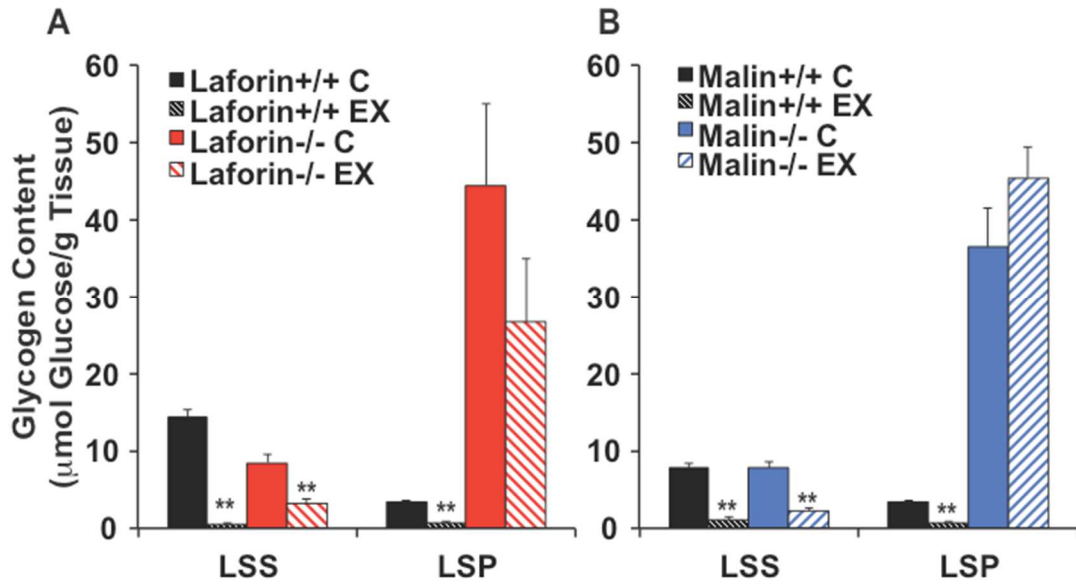


Figure 39. Skeletal muscle glycogen distribution in response to exercise. Total skeletal muscle extracts were subjected to low speed centrifugation to generate a low speed supernatant (LSS) and pellet (LSP). Glycogen content was measured and expressed as μmol of glucose/g tissue in the LSS and LSP for the (A) laforin $+/+$, laforin $-/-$ ($n = 4-8$), (B) Malin $+/+$ and malin $-/-$ ($n = 5-6$) for the control exercised mice. Data are means \pm SEM, * indicate significance compared to the control with $p < 0.05$ and ** indicating $p < 0.01$.

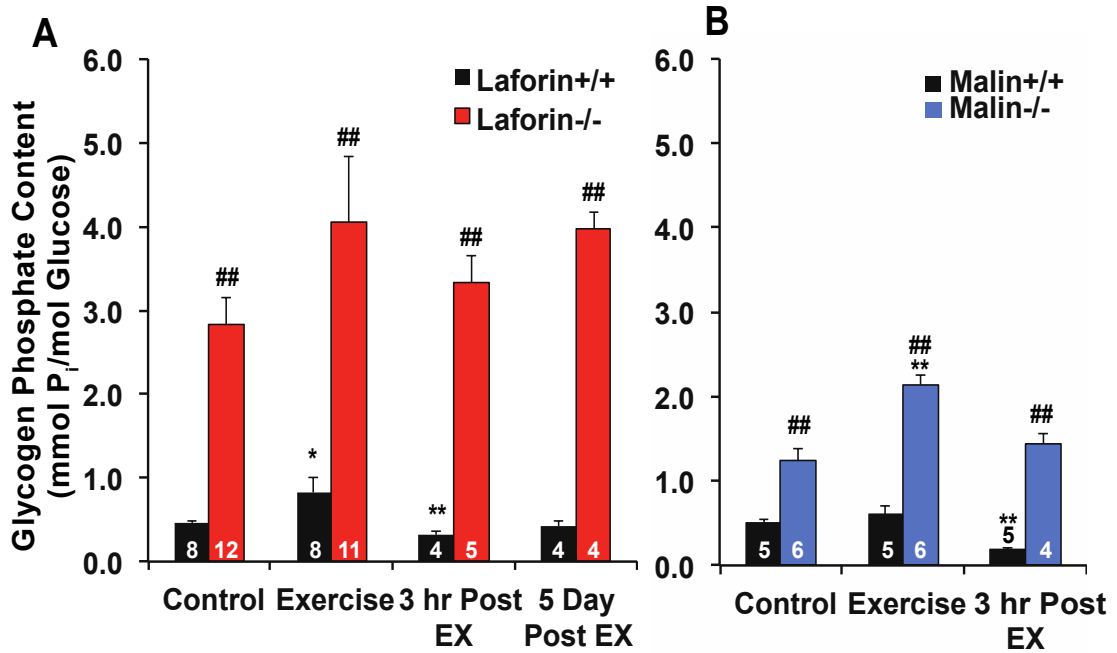


Figure 40. Glycogen phosphate levels in response to exercise. Glycogen phosphate (mmol of phosphate/mol glucose) in laforin^{-/-} (red bars) (A), malin^{-/-} (blue bars) (B) and corresponding wild type littermates (black bars). The number in the data bar indicates the number of mice for each group. Data are means +/- SEM, * indicate significance compared to the control and # indicate significance compared to wild type with p < 0.05 double symbols ** or ## indicate p < 0.01.

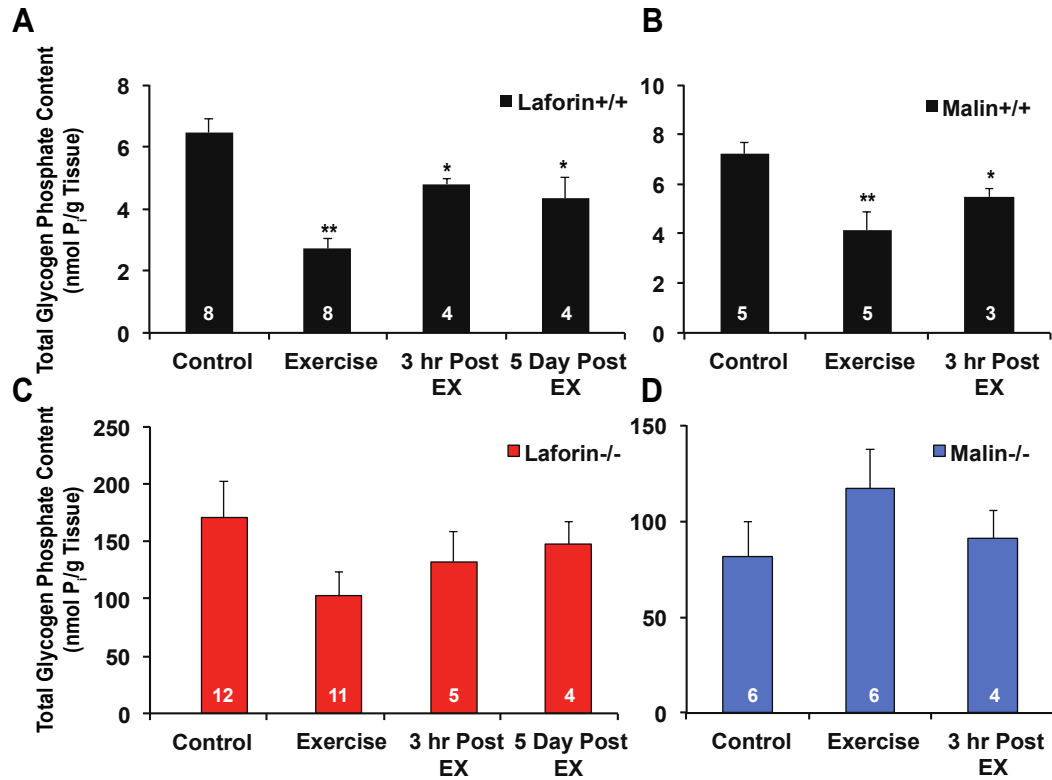


Figure 41. Total glycogen phosphate in response to exercise.

A, Total glycogen phosphate expressed as nmol phosphate/g tissue in laforin+/+ (**A**), malin+/+ (**B**), laforin-/- (**C**), and malin-/- (**D**) in response to exercise and post exercise. The number in the data bar indicates the number of mice for each group. Data are means +/- SEM, * indicate significance compared to the control with $p < 0.05$ and ** indicating $p < 0.01$.

Glycogen phosphorylation was also measured through the exercise protocol. In the old, 12 month old, wild type mice glycogen phosphate content, expressed as the molar ratio of phosphate to mole of glucose, tended to increase after exercise and then decreased 3 hours post-exercise following glucose gavage (Figure 40). Irimia et al. (238) observed similar results in 3 month old mice and interpreted the decrease in glycogen phosphorylation following exercise as due to resynthesis with little phosphate introduction by glycogen synthase. Thus, even though glycogen levels have been restored, the steady state phosphorylation state has not yet been re-established. Total glycogen

phosphate (nmol phosphate/g tissue) was reduced after exercise and restored over time (Figure 41).

As previously mentioned, glycogen can be fractionated by subjecting tissue extracts to low speed centrifugation to define a soluble fraction in the low speed supernatant (LSS) and an insoluble fraction in the low speed pellet (LSP). In wild type mice, the distribution of glycogen between the LSS and LSP is about 70% to 30%, respectively (Figure 42, D). This is in agreement with previous observations, and there was no change in the distribution of glycogen from wild type animals as they aged, at least up to 12 months of age (12). However, at 9-10 months of age the laforin^{-/-} and malin^{-/-} mice have a glycogen distribution that is different from wild type, with ~70% of the glycogen being present in the insoluble, LSP, fraction (Figure 39, D). Analysis of branching of glycogen from the LSS and LSP by HPAEC indicated that skeletal muscle glycogen from wild type was identically branched in both fractions, as indicated by the superimposable profiles (Figure 42, A). Interestingly, the branching profiles of the LSS glycogen from the laforin and malin knockout mice were also superimposable (Figure 42, B), indicating that the soluble glycogen in the knockout mice is normally branched. The HPAEC profiles for the laforin^{-/-} or malin^{-/-} of the LSP were strikingly different from the profile of the wild type animals (Figure 42, C). Both knockout LSP profiles have fewer short chain length branches and more long chains (DP 14 and above), suggesting that the glycogen in the LSP is less branched and the average chain length is increased, which contribute to its insolubility.

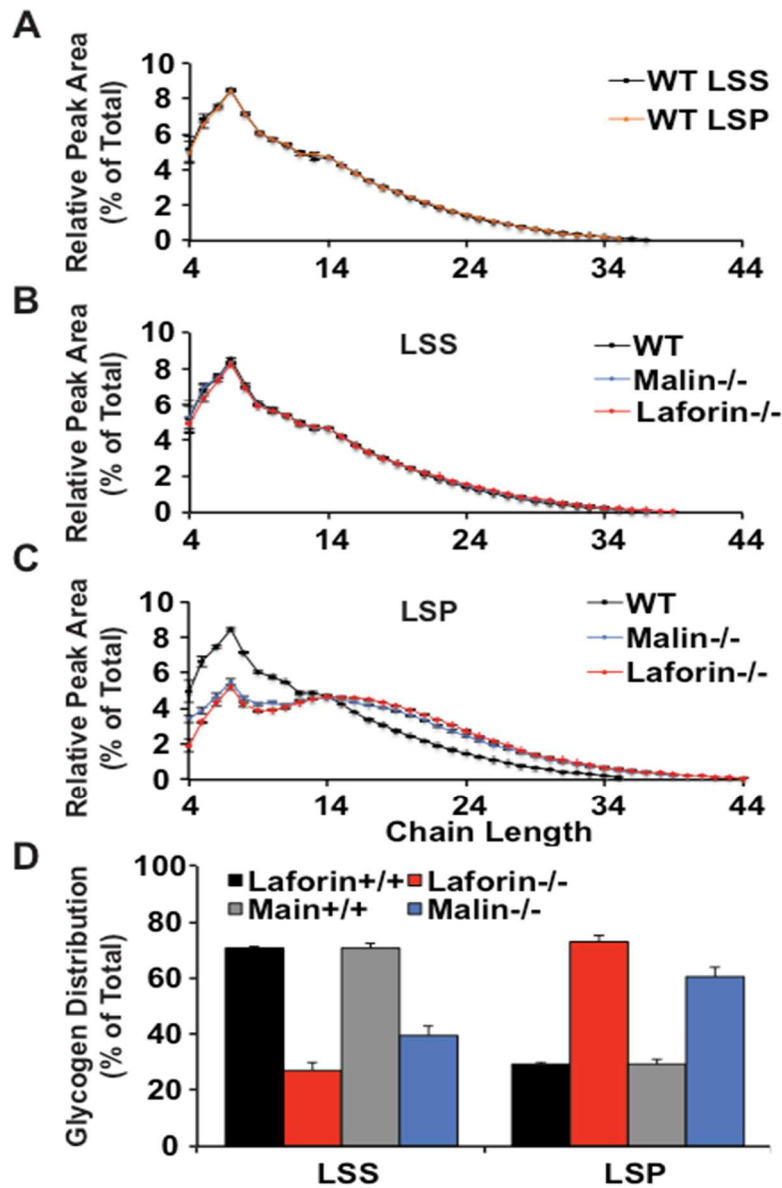


Figure 42. Skeletal muscle glycogen distribution and branching. High performance anionic exchange chromatography (HPAEC) analysis of the chain length distribution from glycogen purified from either the LSS or LSP fractions of skeletal muscle extracts and digested with isoamylase. **A**, chain length distribution of the LSS and LSP for the laforin^{+/+} and malin^{+/+}, indicated as WT with n = 6 for the LSS and n = 5 for the LSP. **B**, Is the chain length analysis for the LSS of the WT, malin^{-/-} (n = 3) and the laforin^{-/-} (n = 3). **C**, Represents the chain length analysis for the LSP of the WT, malin^{-/-} (n = 3) and the laforin^{-/-} (n = 3). **D**, Shows the percent of glycogen found in the LSS or LSP from the 10-11 month old mice used for the LSS/LSP branching analysis (n = 4-5). Data are means +/- SEM

DISCUSSION

1. Location of the Phosphate in Glycogen

We had previously reported that glycogen contained phosphate at the C2 and C3 locations (16). Nitschke *et al* (15) reported that C6 was the major site of phosphorylation in glycogen and that C6 phosphorylation would effectively block the action of the branching enzyme and result in the poorly branched glycogen found in Lafora disease. To address the discrepancy in the results we re-evaluated the location of glycogen phosphate by NMR analysis. One possibility for the difference in results between the two studies could be due to glycogen purification process. Therefore, we purified glycogen by two methods, one being a more gentle method and the other being a more harsh method, which involved hydrolyzing skeletal muscle in hot KOH. The rationale was to determine whether the purification process for glycogen affected the outcome and in particular whether harsh conditions promoted phosphate ester migration, a known phenomenon in sugar phosphates chemistry (229-231). Based on the NMR analyses, the glycogen preparation method did not seem to effect the distribution of phospho-monoesters found in the phospho-oligosacharides. Additionally, in this study, we observed phosphate monoester at the C2, C3 and C6 locations, which is in agreement with the study of Nitschke *et al*. (15).

In addition to the NMR analysis, a newly developed, highly sensitive assay that measures glucose-6-P in hydrolysates of glycogen was used to quantitate C6 phosphorylation. From our results, in glycogen isolated from skeletal muscle of either rabbit or mouse, the proportion of C6 phosphorylation was ~20% of the total arguing that C6 is not the dominant location of the phosphate. Furthermore, even when glycogen phosphorylation was significantly increased in the mouse models of Lafora disease, the proportion of C6 phosphate remained the same. We argue, therefore, that there are no grounds to propose that C6 phosphorylation is any more or less important to the altered glycogen structure associated with Lafora disease. A phospho-monoester at C6 of a glucose residue within glycogen would obviously block the formation of C1-C6 branchpoint.

However, considering the model for glycogen structure, described in the Introduction, where a full size glycogen molecule, consisting of ~55,000 glucose residues arranged in a series of tiers, there would be ~4,000 branch points and with C6 phosphate accounting for ~20% of the total phosphate found in glycogen, there would be 3 – 4 C6 phosphates per glycogen molecule and ~17 phosphates located at C2 and C3. Therefore, C6 phosphorylation could only block no more than 0.1% of the potential branch points, which makes it hard to imagine that C6 phosphorylation would be directly responsible for wide spread reduction of branching. Rather, we favor the idea that phosphate has a wider ranging effect on the overall structure of glycogen (12,214) by disrupting hydrogen bonding and interactions that are needed for glucose helix stabilization (202). The idea that phosphate interferes with glucose polymer helical structure has been described as part of the degradative process for amylopectin (17,233,235,236), where C3 phosphorylation induces helical strain and C6 phosphorylation can affect the packing of the helix (236). This may provide an explanation for the physical chemical properties of glycogen in Lafora disease but the exact mechanism by which elevated phosphorylation of glycogen is linked to the decreased branching of glycogen is unknown and remains an important unanswered question in the field.

2. Origin of the Phosphate in Glycogen.

The source of the phosphate in glycogen remains an active area of investigation. Lomako *et al* had proposed that an uncharacterized enzyme, distinct from glycogen synthase, was responsible for phosphate incorporation into glycogen (2). They suggested that the enzyme, a glucose-1-P-transferase, would form the proposed C1-C6 phosphodiester bond by transferring a glucose-1-P moiety, including the β -phosphate, from UDP-glucose (2). Tagliabracci *et al* (16) demonstrated such an activity in skeletal muscle extracts from wild type mice but not from mice lacking the muscle isoform of glycogen synthase, suggesting that glycogen synthase may be capable of incorporating phosphate into glycogen. Additionally, Tagliabracci *et al* (16) proposed a mechanism for

phosphate incorporation, where a glucose cyclic phosphate compound would be formed in the active site of glycogen synthase and result in the transfer of glucose-2 or glucose-3 phosphate into glycogen. The event was rare, occurring at a rate of one phosphate per 10,000 glucose residues incorporated into glycogen. As noted, Nitschke *et al* (15) suggested that the ^{32}P signal we had observed in glycogen was due to non-specific binding of the $[\beta^{32}\text{P}]\text{-UDP}$ that is produced during the normal glycogen synthase reaction. We performed many experiments to address this issue and we have provided evidence that glycogen synthase can incorporate phosphate into glycogen. However, this would only provide a possible mechanism for C2 and perhaps C3 phosphate incorporation by glycogen synthase via a cyclic phosphodiester intermediate. How phosphate is introduced at the C6 position remains unknown at this time and is incompatible with a cyclic phosphate mechanism. There are several possibilities (18). One, is that the phosphate can be introduced by an uncharacterized phosphotransferase enzyme, which would most likely use ATP or some other high-energy molecule as a phosphate donor. The second would be the existence of a mutase, which could transfer phosphate groups similar to the phosphoglucomutase reaction of intermediary metabolism. However, no evidence for either mechanism has appeared to date.

3. Glycogen Metabolism in Mouse Models of Lafora Disease

There is a correlation between glycogen accumulation, insolubility and phosphate levels in mouse models of Lafora disease (12,14,15,19). We therefore investigated the skeletal muscle branching, solubility and phosphate content of glycogen from the double knockout mice. As expected, the double knockout, PTG/*laforin*^{-/-} and the PTG/*malin*^{-/-}, mice had reduced or normalized skeletal muscle glycogen levels, similar to that of the PTG^{-/-} animals. The glycogen phosphate content of the PTG/*laforin*^{-/-} mice was still elevated and at the same level as the *laforin*^{-/-} mice, consistent with *laforin* acting as a glycogen phosphatase *in vivo*. Interestingly, even though the phosphate content, expressed as the molar ratio of phosphate to glucose, was not rescued by PTG

KO and remained the same as in the laforin^{-/-} mice, the branching of the glycogen from the PTG/laforin^{-/-} mice was rescued and became similar to that of the PTG^{-/-} mice. Additionally, knockout of PTG improved glycogen solubility in the laforin knockout mice, as a majority of the glycogen was found in the soluble LSS fraction in the double knockout mice. The distribution of glycogen between the LSS and LSP in the PTG/laforin KO mice was similar to that of the wild type or PTG^{-/-} mice. These data suggest that increased phosphate alone is not sufficient to impair glycogen solubility and result in formation of Lafora bodies. The branching of the double knockout skeletal muscle glycogen was similar to the PTG^{-/-} mice, which is also consistent with the solubility properties of the glycogen. Therefore we favor the idea that Lafora body formation is dependent on the accumulation of poorly branched and highly phosphorylated glycogen, which would aggregate and form Lafora bodies. However, increased glycogen branch length alone does not seem to result in Lafora body formation or Lafora disease. For instance, in Anderson disease, GSD IV, where there is impaired or loss of function of the branching enzyme (148), the result is poorly branched glycogen but patients do not develop Lafora disease, but rather have a different pathology. Tagliabracci *et al* (12) showed, by electron microscopy, that glycogen from laforin^{-/-} mice has a drastically different physical appearance, where wild type glycogen was visualized as rosette like structures whereas the laforin^{-/-} glycogen had a "globular" appearance, in some areas forming massive aggregates containing many glycogen molecules. After treating the glycogen with recombinant laforin, thus removing at least the superficial and accessible phosphate, the glycogen particles changed to resemble more, though not completely, the rosette-like appearance of the wild type glycogen. However, the removal of the phosphate, presumably, would not affect branch length and solubility. These results argue that the high glycogen phosphate content along with decreased branching both contribute to aggregation and the formation of Lafora bodies.

The PTG/malin^{-/-} mice gave similar results as the PTG/laforin^{-/-} mice, in that they had normalized glycogen levels, branching was similar to the PTG^{-/-}

mice and glycogen solubility was also normalized. However, there was one distinct difference between the PTG/laforin^{-/-} and the PTG/malin^{-/-} and that is the phosphate content of glycogen. The malin^{-/-} mice had elevated glycogen and glycogen phosphate in skeletal muscle but the phosphate content of the PTG/malin^{-/-} mice was normalized, similar to the levels of the wild type and PTG^{-/-} mice. Several reports have proposed that malin regulates laforin, either by regulating its protein levels or because it is needed for laforin activity (187,205,207,208). We have previously observed that the levels of laforin increase in the malin^{-/-} mice and that the majority of the laforin protein is sequestered with the abnormal glycogen in the LSP (189). In our current studies, the glycogen phosphate levels of the PTG/malin^{-/-} mice were normalized, arguing that laforin activity is not dependent on malin. Additionally, in the skeletal muscle of the PTG/malin^{-/-} mice, the levels of laforin protein were normalized and a majority of the laforin was associated with the soluble LSS fraction (data not shown, unpublished data), suggesting that laforin is not a malin substrate *in vivo*. This also supports our hypothesis that in the malin^{-/-} mice, and most likely in humans with malin mutations, that the increase in laforin is due to its association with the insoluble abnormal glycogen (189), which is likely metabolically inactive.

A number of studies have probed the role of laforin phosphatase activity in the development of Lafora bodies. In the first, Chan et al. (175) characterized mice over-expressing a human laforin C266S mutant, demonstrated the generation of Lafora bodies and concluded that the mutant allele acted as a dominant negative even though no neurological defects were noted. They also suggested that laforin preferentially bound to polyglucosan and that laforin's role in preventing Lafora body formation occurs after polyglucosan starts to form. Tiberia et al (271) observed the formation of diastase resistant material that stained positive with PAS, similar to Lafora bodies, when overexpressing either wild type or catalytically inactive laforin in cells in culture. However, they did not see Lafora body like aggregates in cells where laforin with a non-functional carbohydrate domain was overexpressed. Therefore, Tiberia et al concluded that

the physical binding of excess laforin contributed to the formation of Lafora bodies. Gayarre et al (272), however, reported that when a catalytically inactive C265S mutant of murine laforin, is expressed in laforin^{-/-} mice, the animals did not develop Lafora bodies or have any neurological abnormalities. Therefore, they concluded that the pathogenic process causing abnormal glycogen accumulation requires the interaction of laforin and malin to form a complex but not the phosphatase activity of laforin. They did not, however, measure glycogen phosphorylation. More recently, Nitschke et al (257) revisited this issue and reported results similar to those of Gayarre et al. (272). By crossing either the Gayarre et al. (272) mice or a previously generated mouse line (175) over-expressing the human laforin C266S catalytically inactive mutant with laforin^{-/-} mice, Lafora body formation was suppressed in the resulting double knockout animals. Additionally, analysis of glycogen from the transgenic mice showed that in the laforin^{-/-} background, when the catalytically inactive laforin is expressed, the phosphate content of the glycogen remained elevated but the branching of glycogen was rescued and is similar to the wild type controls. Interestingly, when the catalytically inactive laforin was expressed in the malin^{-/-} mice, Lafora body formation and glycogen branching was not restored to wild type levels. From this study, Nitschke et al (257) concluded that laforin's action to prevent Lafora body formation is mediated through malin and that laforin phosphatase activity is not needed to prevent Lafora body formation.

The studies described above yielded some complex, interesting and sometimes conflicting results. A priori, it is difficult to imagine that the evolved phosphatase activity of laforin, the only human protein with a phosphatase domain housed in the same polypeptide as a glycogen binding module, is dispensable and does not have any role in Lafora body formation or in Lafora disease. However, besides being a glycogen phosphatase, there may be other roles for laforin that are not yet understood. The first of these studies (175) suggested that expression of a catalytically inactive laforin acted as a dominant negative and Lafora body formation was observed in those mice. Gayarre et al (272) performed a similar experiment and took it a step further to express the

catalytically inactive laforin in mice lacking laforin, where they observed a rescuing effect and minimal to no Lafora body formation. The authors even monitored mice out to two years of age and still did not observe significant Lafora body formation. A rationalization of the Chan et al study (175) with the later ones is that there may have been some Lafora body formation but not close to the frequency observed in laforin^{-/-} mice. Nitschke et al (257) took the investigation a step further, in that they expressed the catalytically inactive laforin also in malin knockout mice, and observed a rescuing affect in the laforin knockout background but not in the malin knockout, which suggests that malin and laforin protein must both be present to prevent Lafora body formation. However, not addressed is whether expressing wild type laforin in the malin knockout mice would rescue the Lafora disease phenotype. In comparison to data presented in this thesis, mainly with the PTG/laforin^{-/-} and PTG/malin^{-/-} double knockout mice, we can also agree that glycogen phosphate does not seem to be the sole contributor to the insolubility of glycogen. However, our observation with the PTG/malin^{-/-} mice that Lafora body formation is rescued, glycogen phosphate content is normalized and branching is also normalized is in contrast to the results presented by Nitschke et al (257). Our data would suggest that laforin can act independently of malin and that the reduction of overall glycogen levels is key to preventing Lafora body formation. The same argument can be made for the laforin^{-/-}PTG^{-/-} mice since the decrease of glycogen levels was sufficient to prevent Lafora body formation. The relevance of reducing glycogen levels to prevent Lafora body formation is consistent with the data of Nitschke et al (257) who reported that over-expression of catalytically inactive laforin in laforin^{-/-} mice restored glycogen to wild type levels, although the mechanism is unknown. There is clearly much more to be learned about the mechanism of Lafora body formation, the relative significance of glycogen branching and phosphorylation, and the normal physiological roles of laforin and malin. However, even without a consensus on mechanism, reducing glycogen levels seems a key to preventing Lafora body formation

4. Glycogen Metabolism During Exercise in Mouse Models of Lafora Disease

In 9 – 12 month old laforin^{-/-} or malin^{-/-} mice there is a significant increase in glycogen, Lafora bodies are abundantly present and glycogen is hyper-phosphorylated (12,14,19). One goal of this work was to determine if the abnormal glycogen in the older laforin^{-/-} and malin^{-/-} mice could be metabolized during exhaustive exercise. We have shown that the soluble fraction of glycogen in both the laforin^{-/-} and malin^{-/-} mice is clearly utilized during exercise. The soluble fraction of glycogen from the laforin^{-/-} and malin^{-/-} mice accounts for only ~25% of the total skeletal muscle glycogen, making it difficult to measure any significant utilization of glycogen from the total glycogen pool. Additionally, there was no significant depletion of glycogen in the LSP of either the laforin^{-/-} or malin^{-/-} mice after exercise, suggesting that the insoluble and poorly branched glycogen found in the LSP is not subject to normal metabolism. Interestingly, in the laforin^{-/-} mice there was a clear difference in glycogen synthase phosphorylation state between the LSS and LSP in response to exercise. The glycogen synthase associated with the LSS was dephosphorylated in response to exercise in both the wild type and laforin^{-/-} mice, while the glycogen synthase in the LSP of the laforin^{-/-} mice did not respond to exercise, supporting the idea that enzymes associated with the abnormal glycogen are also not metabolically active. In the malin^{-/-} mice, there is an increase in laforin level associated with the LSP, presumably sequestered by the abnormal glycogen; given that there was no change in glycogen phosphate content after exercise, it is likely that a majority of laforin is inactive.

Besides knowing the location of the phospho-monoesters on carbon atoms of glucose residues, we also know that ~25% of the phosphate is located on the outer tiers of glycogen and that the majority is found in the inner tiers of the glycogen molecules (12). Studies of exercised 3-month-old mice have shown that as glycogen is utilized the glycogen phosphorylation (mmol phosphate/mol glucose) increases after exercise (238), which is consistent with the phosphate being more concentrated in the inner tiers of glycogen. In wild type animals, after

a bout of exercise followed by a period of rest, the phosphorylation of the exercised mice decreased, as the glycogen was being resynthesized and remodeled, suggesting that laforin was able to access and remove the exposed phosphate from glycogen. However, in 3-month-old mice lacking laforin, the phosphate levels remained high and the remodeling of glycogen was slower than in the wild type mice. Additionally, there was no noticeable loss of glycogen phosphate in response to exercise despite a significant loss of total skeletal muscle glycogen. These results were also consistent in older laforin^{-/-} and malin^{-/-} mice and suggest that the phosphate in glycogen could affect its degradation and inhibit its remodeling.

5. Overall Discussion

Loss of function mutations in either the *EPM2A* or *EPM2B* genes, which encode the laforin or malin proteins respectively, result in Lafora disease with similar clinical outcomes. Therefore, much of the focus of Lafora disease research has been to determine the function(s) of both laforin and malin so as to understand the mechanism underlying the disease and hence the design of potential therapy. At the present time, there is no cure available for Lafora disease and the only treatments are aimed at alleviating epileptic symptoms with antiepileptic drugs (273). A hallmark of Lafora disease is the accumulation of Lafora bodies in various tissues. There is now growing evidence that glycogen over-accumulation is a major factor in the formation of Lafora bodies, and therefore that Lafora disease is a type of glycogenosis (198,210-212,214). At the outset of this thesis research, the hypothesis had evolved, largely from work of our laboratory, that glycogen phosphorylation played a leading role in the generation of Lafora bodies and Lafora disease. Increased glycogen phosphorylation correlated with many of the properties of the polyglucosan in Lafora bodies, although the connection between phosphorylation and decreased glycogen branching was never understood. Work from this thesis, as well as from other laboratories, has now shown that matters are more complex since hyperphosphorylation of glycogen alone does not guarantee Lafora body

formation. The evidence strongly supports the idea that laforin can function as a glycogen phosphatase *in vivo* but the question now emerging is whether it has other roles relevant to glycogen metabolism and Lafora body formation. There is a disease causing mutation in laforin that disables the carbohydrate binding domain (174,239), while phosphatase activity is still present, which may suggest that binding of laforin to glycogen is necessary for preventing Lafora body formation. Glycogen from old laforin *-/-* mice aggregates and treatment with laforin makes the glycogen appear more rosette-like and more similar to wild type {Tagliabracci, 2008 #9}, which supports the idea that phosphate has a role in glycogen aggregation. However, this is an area that merits further exploration. The exact function of malin also remains largely undefined. Further work to understand the detailed mechanism for the formation of Lafora bodies and/or the development of Lafora disease is clearly necessary.

However, as shown by work in this thesis, reducing the accumulation of abnormal glycogen in Lafora mouse models does reduce or eliminate Lafora body formation leading to a good consensus within the Lafora research community that suppression of glycogen storage may be, at this time, one of the most promising therapeutic directions to follow. Several laboratories are following this lead, ours pursuing small molecules that can inhibit glycogen synthase or glycogen synthase dephosphorylation. Inhibiting glycogen synthesis in Lafora disease patients could minimally prevent further progression of the disease and in the best case scenario allow for the clearance of the abnormal glycogen that makes up Lafora bodies. In any event, this is a therapeutic approach that is worth pursuing.

References

1. Gambetti, P., Di Mauro, S., Hirt, L., and Blume, R. P. (1971) Myoclonic epilepsy with Lafora bodies: some ultrastructural, histochemical, and biochemical aspects. *Archives of neurology* **25**, 483-493
2. Lomako, J., Lomako, W. M., Whelan, W. J., and Marchase, R. B. (1993) Glycogen contains phosphodiester groups that can be introduced by UDPglucose: glycogen glucose 1-phosphotransferase. *FEBS letters* **329**, 263-267
3. Lomako, J., Lomako, W. M., Kirkman, B. R., and Whelan, W. J. (1994) The role of phosphate in muscle glycogen. *Biofactors* **4**, 167-171
4. Roach, P. J., Skurat, A. V., and Harris, R. A. (2010) Regulation of Glycogen Metabolism. in *Comprehensive Physiology*, John Wiley & Sons, Inc. pp
5. Gunja-Smith, Z., Marshall, J. J., Mercier, C., Smith, E. E., and Whelan, W. J. (1970) A revision of the Meyer-Bernfeld model of glycogen and amylopectin. *FEBS letters* **12**, 101-104
6. Melendez-Hevia, E., Waddell, T. G., and Shelton, E. D. (1993) Optimization of molecular design in the evolution of metabolism: the glycogen molecule. *Biochemical Journal* **295 (Pt 2)**, 477-483
7. Melendez, R., Melendez-Hevia, E., and Cascante, M. (1997) How did glycogen structure evolve to satisfy the requirement for rapid mobilization of glucose? A problem of physical constraints in structure building. *Journal of molecular evolution* **45**, 446-455
8. Goldsmith, E., Sprang, S., and Fletterick, R. (1982) Structure of maltoheptaose by difference Fourier methods and a model for glycogen. *Journal of molecular biology* **156**, 411-427
9. Shearer, J., and Graham, T. E. (2004) Novel aspects of skeletal muscle glycogen and its regulation during rest and exercise. *Exerc Sport Sci Rev* **32**, 120-126
10. Kirkman, B. R., and Whelan, W. J. (1986) Glucosamine is a normal component of liver glycogen. *FEBS letters* **194**, 6-11
11. Fontana, J. D. (1980) The presence of phosphate in glycogen. *FEBS letters* **109**, 85-92
12. Tagliabracci, V. S., Girard, J. M., Segvich, D., Meyer, C., Turnbull, J., Zhao, X., Minassian, B. A., Depaoli-Roach, A. A., and Roach, P. J. (2008) Abnormal metabolism of glycogen phosphate as a cause for Lafora disease. *J Biol Chem* **283**, 33816-33825
13. Tagliabracci, V. S., Turnbull, J., Wang, W., Girard, J. M., Zhao, X., Skurat, A. V., Delgado-Escueta, A. V., Minassian, B. A., Depaoli-Roach, A. A., and Roach, P. J. (2007) Laforin is a glycogen phosphatase, deficiency of which leads to elevated phosphorylation of glycogen in vivo. *Proc Natl Acad Sci U S A* **104**, 19262-19266
14. DePaoli-Roach, A. A., Contreras, C. J., Segvich, D. M., Heiss, C., Ishihara, M., Azadi, P., and Roach, P. J. (2015) Glycogen phosphomonoester

- distribution in mouse models of the progressive myoclonic epilepsy, lafora disease. *J Biol Chem* **290**, 841-850
15. Nitschke, F., Wang, P., Schmieder, P., Girard, J. M., Awrey, D. E., Wang, T., Israelian, J., Zhao, X., Turnbull, J., Heydenreich, M., Kleinpeter, E., Steup, M., and Minassian, B. A. (2013) Hyperphosphorylation of glucosyl C6 carbons and altered structure of glycogen in the neurodegenerative epilepsy Lafora disease. *Cell Metab* **17**, 756-767
 16. Tagliabracci, V. S., Heiss, C., Karthik, C., Contreras, C. J., Glushka, J., Ishihara, M., Azadi, P., Hurley, T. D., DePaoli-Roach, A. A., and Roach, P. J. (2011) Phosphate incorporation during glycogen synthesis and Lafora disease. *Cell Metab* **13**, 274-282
 17. Blennow, A., Nielsen, T. H., Baunsgaard, L., Mikkelsen, R., and Engelsen, S. B. (2002) Starch phosphorylation: a new front line in starch research. *Trends Plant Sci* **7**, 445-450
 18. Roach, P. J. (2015) Glycogen phosphorylation and Lafora disease. *Molecular aspects of medicine* **46**, 78-84
 19. Turnbull, J., Wang, P., Girard, J. M., Ruggieri, A., Wang, T. J., Draginov, A. G., Kameka, A. P., Pencea, N., Zhao, X., Ackerley, C. A., and Minassian, B. A. (2010) Glycogen hyperphosphorylation underlies lafora body formation. *Ann Neurol* **68**, 925-933
 20. Cavanagh, J. B. (1999) Corpora-amylacea and the family of polyglucosan diseases. *Brain Res Rev* **29**, 265-295
 21. Rosai, J., and Lascano, E. F. (1970) Basophilic (mucoïd) degeneration of myocardium: a disorder of glycogen metabolism. *Am J Pathol* **61**, 99-116
 22. Agius, L. (2008) Glucokinase and molecular aspects of liver glycogen metabolism. *Biochemical Journal* **414**, 1-18
 23. McGarry, J., Kuwajima, M., Newgard, C., Foster, D., and Katz, J. (1987) From dietary glucose to liver glycogen: the full circle round. *Annual review of nutrition* **7**, 51-73
 24. Thorens, B., and Mueckler, M. (2010) Glucose transporters in the 21st Century. *American Journal of Physiology-Endocrinology and Metabolism* **298**, E141-E145
 25. Kennedy, L. D., Kirkman, B. R., Lomako, J., Rodriguez, I. R., and Whelan, W. J. (1985) The biogenesis of rabbit-muscle glycogen. *Membranes and Muscle. IRL Press, Oxford*, 65-84
 26. KRISMAN, C. R., and BARENGO, R. (1975) A Precursor of Glycogen Biosynthesis: α -1, 4-Glucan-Protein. *European Journal of Biochemistry* **52**, 117-123
 27. PITCHER, J., SMYTHE, C., CAMPBELL, D. G., and COHEN, P. (1987) Identification of the 38 kDa subunit of rabbit skeletal muscle glycogen synthase as glycogenin. *European Journal of Biochemistry* **169**, 497-502
 28. Roach, P. J., Depaoli-Roach, A. A., Hurley, T. D., and Tagliabracci, V. S. (2012) Glycogen and its metabolism: some new developments and old themes. *The Biochemical journal* **441**, 763-787
 29. Hirschhorn, R., and Reuser, A. J. (2000) Glycogen Storage Disease Type II: Acid α -Glucosidase (Acid Maltase) Deficiency. in *he Metabolic and*

- Molecular Basis of Inherited Disease*. (Scriver, C. R., Beaudet, A. L., Sly, W. S., and Valle, D. eds.), McGraw-Hill, New York. pp 3389-3420
30. Cori, C. F. C. G. T. (1939) The activating effect of glycogen on the enzymatic synthesis of glycogen from glucose-1-phosphate. *J Biol Chem* **131**, 397-398
 31. Kennedy, L., Kirkman, B., Lomako, J., Rodriguez, I., and Whelan, W. (1985) The biogenesis of rabbit-muscle glycogen. *Membranes and muscle*, 65-84
 32. Butler, N. A., Lee, E. Y., and Whelan, W. J. (1977) A protein-bound glycogen component of rat liver. *Carbohydrate research* **55**, 73-82
 33. Alonso, M., Lomako, J., Lomako, W., and Whelan, W. (1995) A new look at the biogenesis of glycogen. *The FASEB journal* **9**, 1126-1137
 34. Gannon, M., and Nuttall, F. (1997) Effect of feeding, fasting, and diabetes on liver glycogen synthase activity, protein, and mRNA in rats. *Diabetologia* **40**, 758-763
 35. Henrissat, B., and Davies, G. (1997) Structural and sequence-based classification of glycoside hydrolases. *Current Opinion in Structural Biology* **7**, 637-644
 36. Campbell, J. A., Davies, G. J., Bulone, V., and Henrissat, B. (1997) A classification of nucleotide-diphospho-sugar glycosyltransferases based on amino acid sequence similarities. *Biochemical Journal* **326**, 929
 37. Mu, J., Skurat, A. V., and Roach, P. J. (1997) Glycogenin-2, a novel self-glucosylating protein involved in liver glycogen biosynthesis. *J Biol Chem* **272**, 27589-27597
 38. Zhai, L., Schroeder, J., Skurat, A. V., and Roach, P. J. (2001) Do Rodents Have a Gene Encoding Glycogenin α 2, the Liver Isoform of the Self α Glucosylating Initiator of Glycogen Synthesis? *IUBMB life* **51**, 87-91
 39. Moslemi, A. R., Lindberg, C., Nilsson, J., Tajsharghi, H., Andersson, B., and Oldfors, A. Glycogenin-1 deficiency and inactivated priming of glycogen synthesis. *N Engl J Med* **362**, 1203-1210
 40. Lomako, J., Mazuruk, K., Lomako, W. M., Alonso, M. D., Whelan, W. J., and Rodriguez, I. R. (1996) The human intron-containing gene for glycogenin maps to chromosome 3, band q24. *Genomics* **33**, 519-522
 41. Gibbons, B. J., Roach, P. J., and Hurley, T. D. (2002) Crystal structure of the autocatalytic initiator of glycogen biosynthesis, glycogenin. *Journal of molecular biology* **319**, 463-477
 42. Roach, P. J., and Skurat, A. V. (1997) Self-glucosylating initiator proteins and their role in glycogen biosynthesis. *Prog Nuc Acid Res Mol Biol* **57**, 289-316
 43. Lomako, J., Lomako, W. M., and Whelan, W. J. (2004) Glycogenin: the primer for mammalian and yeast glycogen synthesis. *Biochim Biophys Acta* **1673**, 45-55
 44. Smythe, C., and Cohen, P. (1991) The discovery of glycogenin and the priming mechanism for glycogen biogenesis. *European Journal Of Biochemistry*. **200**, 625-631

45. Cao, Y., Skurat, A., DePaoli-Roach, A., and Roach, P. (1993) Initiation of glycogen synthesis. Control of glycogenin by glycogen phosphorylase. *J Biol Chem* **268**, 21717-21721
46. Skurat, A. V., Cao, Y., and Roach, P. (1993) Glucose control of rabbit skeletal muscle glycogenin expressed in COS cells. *J Biol Chem* **268**, 14701-14707
47. Caudwell, F. B., and Cohen, P. (1980) Purification and subunit structure of glycogen-branching enzyme from rabbit skeletal muscle. *European Journal Of Biochemistry*. **109**, 391-394
48. Gibson, W. B., Illingsworth, B., and Brown, D. H. (1971) Studies of glycogen branching enzyme. Preparation and properties of -1,4-glucan- -1,4-glucan 6-glycosyltransferase and its action on the characteristic polysaccharide of the liver of children with Type IV glycogen storage disease. *Biochemistry* **10**, 4253-4262
49. Abad, M. C., Binderup, K., Rios-Steiner, J., Arni, R. K., Preiss, J., and Geiger, J. H. (2002) The X-ray crystallographic structure of Escherichia coli branching enzyme. *J Biol Chem* **277**, 42164-42170.
50. Pal, K., Kumar, S., Sharma, S., Garg, S. K., Alam, M. S., Xu, H. E., Agrawal, P., and Swaminathan, K. (2010) Crystal structure of full-length Mycobacterium tuberculosis H37Rv glycogen branching enzyme: insights of N-terminal beta-sandwich in substrate specificity and enzymatic activity. *J Biol Chem* **285**, 20897-20903
51. Friedman, D. L., and Lerner, J. (1963) Studies on Udp-g-Alpha-Glucan Transglucosylase. Iii. Interconversion of Two Forms of Muscle Udp-g-Alpha-Glucan Transglucosylase by a Phosphorylation-Dephosphorylation Reaction Sequence. *Biochemistry* **2**, 669-675
52. Roach, P. J., and Lerner, J. (1977) Covalent phosphorylation in the regulation of glycogen synthase activity. *Molecular and cellular biochemistry* **15**, 179-200
53. Bai, G., Zhang, Z., Werner, R., Nuttall, F., Tan, A., and Lee, E. (1990) The primary structure of rat liver glycogen synthase deduced by cDNA cloning. Absence of phosphorylation sites 1a and 1b. *J Biol Chem* **265**, 7843-7848
54. Nuttall, F. Q., Gannon, M. C., Bai, G., and Lee, E. Y. (1994) Primary structure of human liver glycogen synthase deduced by cDNA cloning. *Archives of biochemistry and biophysics* **311**, 443-449
55. Farkas, I., Hardy, T. A., Goebel, M. G., and Roach, P. J. (1991) Two glycogen synthase isoforms in Saccharomyces cerevisiae are coded by distinct genes that are differentially controlled. *J Biol Chem* **266**, 15602-15607
56. Zhang, W., Browner, M., Fletterick, R., DePaoli-Roach, A., and Roach, P. (1989) Primary structure of rabbit skeletal muscle glycogen synthase deduced from cDNA clones. *The FASEB journal* **3**, 2532-2536
57. Roach, P. J. (2002) Glycogen and its metabolism. *Current Molecular Medicine* **2**, 101-120
58. Hardy, T. A., and Roach, P. J. (1993) Control of yeast glycogen synthase-2 by COOH-terminal phosphorylation. *J Biol Chem* **268**, 23799-23805

59. Roach, P. J. (1990) Control of glycogen synthase by hierarchal protein phosphorylation. *FASEB journal : official publication of the Federation of American Societies for Experimental Biology* **4**, 2961-2968
60. Roach, P. J. (1991) Multisite and hierarchal protein phosphorylation. *J Biol Chem* **266**, 14139-14142
61. Picton, C., Woodgett, J., Hemmings, B., and Cohen, P. (1982) Multisite phosphorylation of glycogen synthase from rabbit skeletal muscle. Phosphorylation of site 5 by glycogen synthase kinase-5 (casein kinase-II) is a prerequisite for phosphorylation of sites 3 by glycogen synthase kinase-3. *FEBS letters* **150**, 191-196
62. DePaoli-Roach, A. A., Ahmad, Z., Camici, M., Lawrence, J. C., Jr., and Roach, P. J. (1983) Multiple phosphorylation of rabbit skeletal muscle glycogen synthase. Evidence for interactions among phosphorylation sites and the resolution of electrophoretically distinct forms of the subunit. *J Biol Chem* **258**, 10702-10709
63. Roach, P. J., DePaoli-Roach, A. A., and Lerner, J. (1978) Ca²⁺-stimulated phosphorylation of muscle glycogen synthase by phosphorylase b kinase. *J Cyclic Nucleotide Res* **4**, 245-257
64. Huang, T. S., and Krebs, E. G. (1977) Amino acid sequence of a phosphorylation site in skeletal muscle glycogen synthetase. *Biochem Biophys Res Commun* **75**, 643-650
65. Flotow, H., and Roach, P. J. (1989) Synergistic phosphorylation of rabbit muscle glycogen synthase by cyclic AMP-dependent protein kinase and casein kinase I. Implications for hormonal regulation of glycogen synthase. *J Biol Chem* **264**, 9126-9128
66. Flotow, H., Graves, P. R., Wang, A. Q., Fiol, C. J., Roeske, R. W., and Roach, P. J. (1990) Phosphate groups as substrate determinants for casein kinase I action. *J Biol Chem* **265**, 14264-14269
67. Fiol, C. J., Mahrenholz, A. M., Wang, Y., Roeske, R. W., and Roach, P. J. (1987) Formation of protein kinase recognition sites by covalent modification of the substrate. Molecular mechanism for the synergistic action of casein kinase II and glycogen synthase kinase 3. *J Biol Chem* **262**, 14042-14048
68. Carling, D., and Hardie, D. G. (1989) The substrate and sequence specificity of the AMP-activated protein kinase. Phosphorylation of glycogen synthase and phosphorylase kinase. *Biochim Biophys Acta* **1012**, 81-86
69. Wilson, W. A., Skurat, A. V., Probst, B., de Paoli-Roach, A., Roach, P. J., and Rutter, J. (2005) Control of mammalian glycogen synthase by PAS kinase. *Proc Natl Acad Sci U S A* **102**, 16596-16601
70. Skurat, A. V., and Dietrich, A. D. (2004) Phosphorylation of Ser640 in muscle glycogen synthase by DYRK family protein kinases. *J Biol Chem* **279**, 2490-2498
71. Kuma, Y., Campbell, D. G., and Cuenda, A. (2004) Identification of glycogen synthase as a new substrate for stress-activated protein kinase 2b/p38beta. *The Biochemical journal* **379**, 133-139

72. Skurat, A. V., Wang, Y., and Roach, P. J. (1994) Rabbit skeletal muscle glycogen synthase expressed in COS cells. Identification of regulatory phosphorylation sites. *J Biol Chem* **269**, 25534-25542
73. Skurat, A. V., and Roach, P. J. (1995) Phosphorylation of sites 3a and 3b (Ser640 and Ser644) in the control of rabbit muscle glycogen synthase. *J Biol Chem* **270**, 12491-12497
74. Rutter, J., Probst, B. L., and McKnight, S. L. (2002) Coordinate regulation of sugar flux and translation by PAS kinase. *Cell* **111**, 17-28
75. Bollen, M. (2001) Combinatorial control of protein phosphatase-1. *Trends in Biochemical Sciences* **26**, 426-431
76. Ceulemans, H., and Bollen, M. (2004) Functional diversity of protein phosphatase-1, a cellular economizer and reset button. *Physiol Rev* **84**, 1-39
77. Gasa, R., Jensen, P. B., Berman, H. K., Brady, M. J., DePaoli-Roach, A. A., and Newgard, C. B. (2000) Distinctive regulatory and metabolic properties of glycogen-targeting subunits of protein phosphatase-1 (PTG, GL, GM/RGI) expressed in hepatocytes. *J Biol Chem* **275**, 26396-26403
78. Tang, P. M., Bondor, J. A., Swiderek, K. M., and DePaoli-Roach, A. A. (1991) Molecular cloning and expression of the regulatory (RG1) subunit of the glycogen-associated protein phosphatase. *J Biol Chem* **266**, 15782-15789
79. DOHERTY, M. J., Cadefau, J., Stalmans, W., Bollen, M., and COHEN, P. T. (1998) Loss of the hepatic glycogen-binding subunit (GL) of protein phosphatase 1 underlies deficient glycogen synthesis in insulin-dependent diabetic rats and in adrenalectomized starved rats. *The Biochemical Journal* **333**, 253-257
80. Doherty, M. J., Moorhead, G., Morrice, N., Cohen, P., and Cohen, P. T. (1995) Amino acid sequence and expression of the hepatic glycogen-binding (G L-subunit of protein phosphatase-1. *FEBS letters* **375**, 294-298
81. Kelsall, I. R., Voss, M., Munro, S., Cuthbertson, D. J., and Cohen, P. T. (2011) R3F, a novel membrane-associated glycogen targeting subunit of protein phosphatase 1 regulates glycogen synthase in astrocytoma cells in response to glucose and extracellular signals. *Journal of Neurochemistry* **118**, 596-610
82. Baskaran, S., Roach, P. J., DePaoli-Roach, A. A., and Hurley, T. D. (2010) Structural basis for glucose-6-phosphate activation of glycogen synthase. *Proceedings of the National Academy of Sciences* **107**, 17563-17568
83. Zeqiraj, E., Tang, X., Hunter, R. W., García-Rocha, M., Judd, A., Deak, M., von Wilamowitz-Moellendorff, A., Kurinov, I., Guinovart, J. J., and Tyers, M. (2014) Structural basis for the recruitment of glycogen synthase by glycogenin. *Proceedings of the National Academy of Sciences* **111**, E2831-E2840
84. Mahalingan, K. K., Baskaran, S., Depaoli-Roach, A. A., Roach, P. J., and Hurley, T. D. (2016) Redox switch for the inhibited state of yeast glycogen synthase mimics regulation by phosphorylation. *Biochemistry*

85. Pederson, B. A., Csitkovits, A. G., Simon, R., Schroeder, J. M., Wang, W., Skurat, A. V., and Roach, P. J. (2003) Overexpression of glycogen synthase in mouse muscle results in less branched glycogen. *Biochem Biophys Res Commun* **305**, 826-830.
86. Cameron, J. M., Levandovskiy, V., MacKay, N., Utgikar, R., Ackerley, C., Chiasson, D., Halliday, W., Raiman, J., and Robinson, B. H. (2009) Identification of a novel mutation in GYS1 (muscle-specific glycogen synthase) resulting in sudden cardiac death, that is diagnosable from skin fibroblasts. *Molecular genetics and metabolism* **98**, 378-382
87. Kollberg, G., Tulinius, M., Gilljam, T., Östman-Smith, I., Forsander, G., Jotorp, P., Oldfors, A., and Holme, E. (2007) Cardiomyopathy and exercise intolerance in muscle glycogen storage disease 0. *New England Journal of Medicine* **357**, 1507-1514
88. Orho, M., Bosshard, N. U., Buist, N. R., Gitzelmann, R., Aynsley-Green, A., Blumel, P., Gannon, M. C., Nuttall, F. Q., and Groop, L. C. (1998) Mutations in the liver glycogen synthase gene in children with hypoglycemia due to glycogen storage disease type 0. *J Clin Invest* **102**, 507-515
89. McCue, M. E., Valberg, S. J., Miller, M. B., Wade, C., DiMauro, S., Akman, H. O., and Mickelson, J. R. (2008) Glycogen synthase (GYS1) mutation causes a novel skeletal muscle glycogenosis. *Genomics* **91**, 458-466
90. Irimia, J. M., Meyer, C. M., Peper, C. L., Zhai, L., Bock, C. B., Previs, S. F., McGuinness, O. P., DePaoli-Roach, A., and Roach, P. J. (2010) Impaired glucose tolerance and predisposition to the fasted state in liver glycogen synthase knock-out mice. *J Biol Chem* *iological Chemistry* **285**, 12851-12861
91. Hudson, J. W., Golding, G. B., and Crerar, M. M. (1993) Evolution of allosteric control in glycogen phosphorylase. *Journal of molecular biology* **234**, 700-721
92. Newgard, C. B., Hwang, P. K., and Fletterick, R. J. (1989) The Family of Glycogen Phosphorylases: Structure and Functio. *Critical Reviews in Biochemistry and Molecular Biology* **24**, 69-99
93. Newgard, C. B., Littman, D., van Genderen, C., Smith, M., and Fletterick, R. (1988) Human brain glycogen phosphorylase. Cloning, sequence analysis, chromosomal mapping, tissue expression, and comparison with the human liver and muscle isozymes. *J Biol Chem* **263**, 3850-3857
94. Titani, K., Koide, A., Ericsson, L. H., Kumar, S., Hermann, J., Wade, R. D., Walsh, K. A., Neurath, H., and Fischer, E. H. (1978) Sequence of the carboxyl-terminal 492 residues of rabbit muscle glycogen phosphorylase including the pyridoxal 5'-phosphate binding site. *Biochemistry* **17**, 5680-5695
95. Johnson, L. (1992) Glycogen phosphorylase: control by phosphorylation and allosteric effectors. *The FASEB journal* **6**, 2274-2282
96. Johnson, L., and Barford, D. (1990) Glycogen phosphorylase. The structural basis of the allosteric response and comparison with other allosteric proteins. *J Biol Chem* **265**, 2409-2412

97. Madsen, N. B. (1986) 9 Glycogen Phosphorylase. *The Enzymes* **17**, 365-394
98. Nakano, K., Hwang, P. K., and Fletterick, R. J. (1986) Complete cDNA sequence for rabbit muscle glycogen phosphorylase. *FEBS letters* **204**, 283-287
99. Fischer, E., Pocker, A., and Saari, J. (1970) The structure, function and control of glycogen phosphorylase. *Essays in biochemistry* **6**, 23-68
100. Fischer, E., and Heilmeyer, L. (1971) Jr. & RH Haschke: *Curr. Topics Cell. Reg* **4**, 211
101. Graves, D. J., and Wang, J. H. (1972) 15 α -Glucan Phosphorylases—Chemical and Physical Basis of Catalysis and Regulation. *The Enzymes* **7**, 435-482
102. Krebs, E. G., and Fischer, E. H. (1956) The phosphorylase b to a converting enzyme of rabbit skeletal muscle. *Biochimica et Biophysica Acta* **20**, 150-157
103. Kasvinsky, P. J., Fletterick, R. J., and Madsen, N. B. (1981) Regulation of the dephosphorylation of glycogen phosphorylase a and synthase b by glucose and caffeine in isolated hepatocytes. *Canadian journal of biochemistry* **59**, 387-395
104. Heilmeyer, L. M. (1991) Molecular basis of signal integration in phosphorylase kinase. *Biochimica et Biophysica Acta (BBA)-Molecular Cell Research* **1094**, 168-174
105. Meyer, W. L., Fischer, E. H., and Krebs, E. G. (1964) Activation of skeletal muscle phosphorylase b kinase by Ca²⁺. *Biochemistry* **3**, 1033-1039
106. Cohen, P. (1973) The role of phosphorylase kinase in the nervous and hormonal control of glycogenolysis in muscle. in *Biochemical Society symposium*
107. Sutherland, E. W., and Robison, G. A. (1969) The role of cyclic AMP in the control of carbohydrate metabolism. *Diabetes* **18**, 797-819
108. Gilboe, D. P., Larson, K. L., and Nuttall, F. Q. (1972) Radioactive method for the assay of glycogen phosphorylases. *Anal Biochem* **47**, 20-27
109. Stalmans, W., Bollen, M., and Mvumbi, L. (1987) Control of glycogen synthesis in health and disease. *Diabetes/Metabolism Research and Reviews* **3**, 127-161
110. White, M. F. (1998) The IRS-signalling system: a network of docking proteins that mediate insulin action. in *Insulin Action*, Springer. pp 3-11
111. Pessin, J. E., and Saltiel, A. R. (2000) Signaling pathways in insulin action: molecular targets of insulin resistance. *The Journal of clinical investigation* **106**, 165-169
112. Taniguchi, C. M., Emanuelli, B., and Kahn, C. R. (2006) Critical nodes in signalling pathways: insights into insulin action. *Nature reviews Molecular cell biology* **7**, 85-96
113. Dent, P., Lavoigne, A., Nakielny, S., Caudwell, F. B., Watt, P., and Cohen, P. (1990) The molecular mechanism by which insulin stimulates glycogen synthesis in mammalian skeletal muscle. *Nature* **348**, 302-308

114. Armstrong, C. G., Browne, G. J., Cohen, P., and Cohen, P. T. (1997) PPP1R6, a novel member of the family of glycogen-targetting subunits of protein phosphatase 1. *FEBS letters* **418**, 210-214
115. Suzuki, Y., Lanner, C., Kim, J. H., Vilardo, P. G., Zhang, H., Yang, J., Cooper, L. D., Steele, M., Kennedy, A., Bock, C. B., Scrimgeour, A., Lawrence, J. C., Jr., and DePaoli-Roach, A. A. (2001) Insulin control of glycogen metabolism in knockout mice lacking the muscle-specific protein phosphatase PP1G/RGL. *Molecular & Cellular Biology* **21**, 2683-2694
116. Printen, J. A., Brady, M. J., and Saltiel, A. R. (1997) PTG, a protein phosphatase 1-binding protein with a role in glycogen metabolism. *Science* **275**, 1475-1478
117. Brady, M. J., and Saltiel, A. R. (2001) The role of protein phosphatase-1 in insulin action. *Recent Progress in Hormone Research* **56**, 157-174
118. EMBI, N., PARKER, P. J., and COHEN, P. (1981) A Reinvestigation of the Phosphorylation of Rabbit Skeletal Muscle Glycogen Synthase by Cyclic AMP-Dependent Protein Kinase. *The FEBS Journal* **115**, 405-413
119. PARKER, P. J., EMBI, N., CAUDWELL, F. B., and COHEN, P. (1982) Glycogen synthase from rabbit skeletal muscle. *The FEBS Journal* **124**, 47-55
120. POULTER, L., ANG, S. G., GIBSON, B. W., WILLIAMS, D. H., HOLMES, C. F., CAUDWELL, F. B., PITCHER, J., and COHEN, P. (1988) Analysis of the in vivo phosphorylation state of rabbit skeletal muscle glycogen synthase by fast-atom bombardment mass spectrometry. *The FEBS Journal* **175**, 497-510
121. Sheorain, V. S., Khatra, B., and Soderling, T. (1982) Hormonal regulation of glycogen synthase phosphorylation in rabbit skeletal muscle. *J Biol Chem* **257**, 3462-3470
122. FOULKES, J. G., and COHEN, P. (1979) The hormonal control of glycogen metabolism. *European Journal of Biochemistry* **97**, 251-256
123. Alemany, S., and Cohen, P. (1986) Phosphorylase a is an allosteric inhibitor of the glycogen and microsomal forms of rat hepatic protein phosphatase-1. *FEBS letters* **198**, 194-202
124. Moorhead, G., MacKintosh, C., Morrice, N., and Cohen, P. (1995) Purification of the hepatic glycogen-associated form of protein phosphatase-1 by microcystin-Sepharose affinity chromatography. *FEBS letters* **362**, 101-105
125. Ørtenblad, N., Westerblad, H., and Nielsen, J. (2013) Muscle glycogen stores and fatigue. *The Journal of physiology* **591**, 4405-4413
126. Bergström, J., Hermansen, L., Hultman, E., and Saltin, B. (1967) Diet, muscle glycogen and physical performance. *Acta Physiologica Scandinavica* **71**, 140-150
127. Nielsen, J. N., and Richter, E. A. (2003) Regulation of glycogen synthase in skeletal muscle during exercise. *Acta Physiologica Scandinavica* **178**, 309-319

128. Nielsen, J. N., and Wojtaszewski, J. F. (2004) Regulation of glycogen synthase activity and phosphorylation by exercise. *Proceedings of the Nutrition Society* **63**, 233-237
129. Shulman, R., and Rothman, D. (2001) The “glycogen shunt” in exercising muscle: a role for glycogen in muscle energetics and fatigue. *Proceedings of the National Academy of Sciences* **98**, 457-461
130. Wojtaszewski, J. F., Higaki, Y., Hirshman, M. F., Michael, M. D., Dufresne, S. D., Kahn, C. R., and Goodyear, L. J. (1999) Exercise modulates postreceptor insulin signaling and glucose transport in muscle-specific insulin receptor knockout mice. *The Journal of clinical investigation* **104**, 1257-1264
131. McManus, E. J., Sakamoto, K., Armit, L. J., Ronaldson, L., Shpiro, N., Marquez, R., and Alessi, D. R. (2005) Role that phosphorylation of GSK3 plays in insulin and Wnt signalling defined by knockin analysis. *The EMBO journal* **24**, 1571-1583
132. Aschenbach, W. G., Suzuki, Y., Breeden, K., Prats, C., Hirshman, M. F., Dufresne, S. D., Sakamoto, K., Vilaro, P. G., Steele, M., Kim, J. H., Jing, S. L., Goodyear, L. J., and DePaoli-Roach, A. A. (2001) The muscle-specific protein phosphatase PP1G/R(GL)(G(M)) is essential for activation of glycogen synthase by exercise. *J Biol Chem* **276**, 39959-39967
133. Lai, Y.-C., Stuenkel, J. T., Kuo, C.-H., and Jensen, J. (2007) Glycogen content and contraction regulate glycogen synthase phosphorylation and affinity for UDP-glucose in rat skeletal muscles. *American Journal of Physiology-Endocrinology and Metabolism* **293**, E1622-E1629
134. Richter, E. A., and Ruderman, N. B. (2009) AMPK and the biochemistry of exercise: implications for human health and disease. *Biochemical Journal* **418**, 261-275
135. Hardie, D. G. (2007) AMP-activated/SNF1 protein kinases: conserved guardians of cellular energy. *Nature reviews Molecular cell biology* **8**, 774-785
136. McBride, A., and Hardie, D. G. (2009) AMP-activated protein kinase--a sensor of glycogen as well as AMP and ATP? *Acta Physiol (Oxf)* **196**, 99-113
137. McBride, A., Ghilagaber, S., Nikolaev, A., and Hardie, D. G. (2009) The glycogen-binding domain on the AMPK β subunit allows the kinase to act as a glycogen sensor. *Cell metabolism* **9**, 23-34
138. Milan, D., Jeon, J.-T., Looft, C., Amarger, V., Robic, A., Thelander, M., Rogel-Gaillard, C., Paul, S., Iannuccelli, N., and Rask, L. (2000) A mutation in PRKAG3 associated with excess glycogen content in pig skeletal muscle. *Science* **288**, 1248-1251
139. Arad, M., Seidman, C. E., and Seidman, J. G. (2007) AMP-activated protein kinase in the heart: role during health and disease. *Circ Res* **100**, 474-488
140. Pederson, B. A., Cope, C. R., Schroeder, J. M., Smith, M. W., Irimia, J. M., Thurberg, B. L., DePaoli-Roach, A. A., and Roach, P. J. (2005) Exercise capacity of mice genetically lacking muscle glycogen synthase: in mice,

- muscle glycogen is not essential for exercise. *J Biol Chem* **280**, 17260-17265
141. Koeberl, D. D., Kishnani, P. S., Bali, D., and Chen, Y. T. (2009) Emerging therapies for glycogen storage disease type I. *Trends in endocrinology and metabolism: TEM* **20**, 252-258
 142. Chou, J. Y., Matern, D., Mansfield, B. C., and Chen, Y. T. (2002) Type I glycogen storage diseases: disorders of the glucose-6-phosphatase complex. *Current molecular medicine* **2**, 121-143
 143. Koster, J. F., Busch, H. F., Slee, R. G., and Van Weerden, T. W. (1978) Glycogenosis type II: the infantile- and late-onset acid maltase deficiency observed in one family. *Clinica chimica acta; international journal of clinical chemistry* **87**, 451-453
 144. Raben, N., Plotz, P., and Byrne, B. J. (2002) Acid alpha-glucosidase deficiency (glycogenosis type II, Pompe disease). *Current molecular medicine* **2**, 145-166
 145. Raben, N., Danon, M., Lu, N., Lee, E., Shliselfeld, L., Skurat, A. V., Roach, P. J., Lawrence, J. C., Jr., Musumeci, O., Shanske, S., DiMauro, S., and Plotz, P. (2001) Surprises of genetic engineering: a possible model of polyglucosan body disease. *Neurology* **56**, 1739-1745
 146. Douillard-Guilloux, G., Raben, N., Takikita, S., Ferry, A., Vignaud, A., Guillet-Deniau, I., Favier, M., Thurberg, B. L., Roach, P. J., and Caillaud, C. (2009) Restoration of muscle functionality by genetic suppression of glycogen synthesis in a murine model of Pompe disease. *Human molecular genetics*, ddp535
 147. Shen, J. J., and Chen, Y. T. (2002) Molecular characterization of glycogen storage disease type III. *Current molecular medicine* **2**, 167-175
 148. Wolfsdorf, J. I., and Weinstein, D. A. (2003) Glycogen storage diseases. *Reviews in endocrine & metabolic disorders* **4**, 95-102
 149. Raju, G. P., Li, H. C., Bali, D. S., Chen, Y. T., Urion, D. K., Lidov, H. G., and Kang, P. B. (2008) A case of congenital glycogen storage disease type IV with a novel GBE1 mutation. *Journal of child neurology* **23**, 349-352
 150. Burrow, T. A., Hopkin, R. J., Bove, K. E., Miles, L., Wong, B. L., Choudhary, A., Bali, D., Li, S. C., and Chen, Y. T. (2006) Non-lethal congenital hypotonia due to glycogen storage disease type IV. *American journal of medical genetics. Part A* **140**, 878-882
 151. Mommaerts, W. F., Illingworth, B., Pearson, C. M., Guillory, R. J., and Seraydarian, K. (1959) A functional disorder of muscle associated with the absence of phosphorylase. *Proc Natl Acad Sci U S A* **45**, 791-797
 152. Schmid, R., and Mahler, R. (1959) Chronic progressive myopathy with myoglobinuria: demonstration of a glycogenolytic defect in the muscle. *J Clin Invest* **38**, 2044-2058
 153. Chen, Y., and Burchell, A. (2001) The metabolic and molecular bases of inherited disease. *McGraw-Hill, New York*, 1521-1553

154. DiMauro, S., Andreu, A., Bruno, C., and Hadjigeorgiou, G. (2002) Myophosphorylase Deficiency (Glycogenosis Type V McArdle Disease). *Current molecular medicine* **2**, 189-196
155. Ozen, H. (2007) Glycogen storage diseases: new perspectives. *World journal of gastroenterology* **13**, 2541
156. Nakajima, H., Raben, N., Hamaguchi, T., and Yamasaki, T. (2002) Phosphofructokinase deficiency; past, present and future. *Current Molecular Medicine*. **2**, 197-212
157. Delgado-Escueta, A. V. (2007) Advances in lafora progressive myoclonus epilepsy. *Current neurology and neuroscience reports* **7**, 428-433
158. Chan, E. M., Omer, S., Ahmed, M., Bridges, L. R., Bennett, C., Scherer, S. W., and Minassian, B. A. (2004) Progressive myoclonus epilepsy with polyglucosans (Lafora disease): evidence for a third locus. *Neurology* **63**, 565-567
159. Lafora, G. R., and Glueck, B. (1911) Beitrag zur Histopathologie der myoklonischen Epilepsie. *Zeitschrift für die gesamte Neurologie und Psychiatrie* **6**, 1-14
160. DiMauro, S., and Lamperti, C. (2001) Muscle glycogenoses. *Muscle & nerve* **24**, 984-999
161. Carpenter, S., and Karpati, G. (1981) Ultrastructural findings in Lafora disease. *Annals of neurology* **10**, 63-64
162. Nishimura, R., Ishak, K., Reddick, R., Porter, R., James, S., and Barranger, J. (1980) Lafora disease: diagnosis by liver biopsy. *Annals of neurology* **8**, 409-415
163. Berkovic, S. F., Andermann, F., Carpenter, S., and Wolfe, L. S. (1986) Progressive myoclonus epilepsies: specific causes and diagnosis. *N Engl J Med* **315**, 296-305
164. Harriman, D. G., Millar, J. H., and Stevenson, A. C. (1955) Progressive familial myoclonic epilepsy in three families: its clinical features and pathological basis. *Brain* **78**, 325-349
165. Minassian, B. A., Andrade, D. M., Ianzano, L., Young, E. J., Chan, E., Ackerley, C. A., and Scherer, S. W. (2001) Laforin is a cell membrane and endoplasmic reticulum-associated protein tyrosine phosphatase. *Annals of neurology* **49**, 271-275
166. Minassian, B. A. (2001) Lafora's disease: towards a clinical, pathologic, and molecular synthesis. *Pediatric neurology* **25**, 21-29
167. Yokoi, S., Austin, J., Witmer, F., and Sakai, M. (1968) Studies in myoclonus epilepsy (Lafora body form). I. Isolation and preliminary characterization of Lafora bodies in two cases. *Archives of neurology* **19**, 15-33
168. Singh, S., and Ganesh, S. (2009) Lafora progressive myoclonus epilepsy: a meta-analysis of reported mutations in the first decade following the discovery of the EPM2A and NHLRC1 genes. *Hum Mutat* **30**, 715-723
169. Minassian, B. A., Lee, J. R., Herbrick, J. A., Huizenga, J., Soder, S., Mungall, A. J., Dunham, I., Gardner, R., Fong, C. Y., Carpenter, S., Jardim, L., Satishchandra, P., Andermann, E., Snead, O. C., 3rd, Lopes-Cendes,

- I., Tsui, L. C., Delgado-Escueta, A. V., Rouleau, G. A., and Scherer, S. W. (1998) Mutations in a gene encoding a novel protein tyrosine phosphatase cause progressive myoclonus epilepsy. *Nature Genetics* **20**, 171-174
170. Gentry, M. S., Downen, R. H., 3rd, Worby, C. A., Mattoo, S., Ecker, J. R., and Dixon, J. E. (2007) The phosphatase laforin crosses evolutionary boundaries and links carbohydrate metabolism to neuronal disease. *J Cell Biol* **178**, 477-488
171. Gentry, M. S., and Pace, R. M. (2009) Conservation of the glucan phosphatase laforin is linked to rates of molecular evolution and the glucan metabolism of the organism. *BMC evolutionary biology* **9**, 138
172. Ganesh, S., Amano, K., Delgado-Escueta, A. V., and Yamakawa, K. (1999) Isolation and characterization of mouse homologue for the human epilepsy gene, EPM2A. *Biochem Biophys Res Commun* **257**, 24-28
173. Ganesh, S., Agarwala, K. L., Amano, K., Suzuki, T., Delgado-Escueta, A. V., and Yamakawa, K. (2001) Regional and developmental expression of Epm2a gene and its evolutionary conservation. *Biochem Biophys Res Commun* **283**, 1046-1053
174. Wang, J., Stuckey, J. A., Wishart, M. J., and Dixon, J. E. (2002) A unique carbohydrate binding domain targets the lafora disease phosphatase to glycogen. *J Biol Chem.* **277**, 2377-2380
175. Chan, E. M., Ackerley, C. A., Lohi, H., Ianzano, L., Cortez, M. A., Shannon, P., Scherer, S. W., and Minassian, B. A. (2004) Laforin preferentially binds the neurotoxic starch-like polyglucosans, which form in its absence in progressive myoclonus epilepsy. *Human molecular genetics* **13**, 1117-1129
176. Wang, H., Wang, L., Erdjument-Bromage, H., Vidal, M., Tempst, P., Jones, R. S., and Zhang, Y. (2004) Role of histone H2A ubiquitination in Polycomb silencing. *Nature* **431**, 873-878
177. Minassian, B. A., Ianzano, L., Meloche, M., Andermann, E., Rouleau, G. A., Delgado-Escueta, A. V., and Scherer, S. W. (2000) Mutation spectrum and predicted function of laforin in Lafora's progressive myoclonus epilepsy. *Neurology* **55**, 341-346.
178. Wang, W., and Roach, P. J. (2004) Glycogen and related polysaccharides inhibit the laforin dual-specificity protein phosphatase. *Biochem Biophys Res Commun* **325**, 726-730
179. Wang, W., Parker, G. E., Skurat, A. V., Raben, N., DePaoli-Roach, A. A., and Roach, P. J. (2006) Relationship between glycogen accumulation and the laforin dual specificity phosphatase. *Biochem Biophys Res Commun* **350**, 588-592
180. Chen, Y.-T., and Burchell, A. (1995) Glycogen storage diseases. in *The Metabolic and Molecular Bases of Inherited Disease* (Scriver, C. R., Beaudet, A. L., Sly, W. S., and Valle, D. eds.), 7 th Ed., McGraw-Hill, New York. pp 935-965
181. Moses, S. W., and Parvari, R. (2002) The variable presentations of glycogen storage disease type IV: a review of clinical, enzymatic and molecular studies. *Current molecular medicine* **2**, 177-188

182. Puri, R., Suzuki, T., Yamakawa, K., and Ganesh, S. (2009) Hyperphosphorylation and aggregation of Tau in laforin-deficient mice, an animal model for Lafora disease. *J Biol Chem* **284**, 22657-22663
183. Solaz-Fuster, M. C., Gimeno-Alcaniz, J. V., Ros, S., Fernandez-Sanchez, M. E., Garcia-Fojeda, B., Criado Garcia, O., Vilchez, D., Dominguez, J., Garcia-Rocha, M., Sanchez-Piris, M., Aguado, C., Knecht, E., Serratosa, J., Guinovart, J. J., Sanz, P., and Rodriguez de Cordoba, S. (2008) Regulation of glycogen synthesis by the laforin-malin complex is modulated by the AMP-activated protein kinase pathway. *Human molecular genetics* **17**, 667-678
184. Worby, C. A., Gentry, M. S., and Dixon, J. E. (2006) Laforin: A dual specificity phosphatase that dephosphorylates complex carbohydrates. *J Biol Chem* **281**, 30412-30418
185. Fernandez-Sanchez, M. E., Criado-Garcia, O., Heath, K. E., Garcia-Fojeda, B., Medrano-Fernandez, I., Gomez-Garre, P., Sanz, P., Serratosa, J. M., and Rodriguez de Cordoba, S. (2003) Laforin, the dual-phosphatase responsible for Lafora disease, interacts with R5 (PTG), a regulatory subunit of protein phosphatase-1 that enhances glycogen accumulation. *Human molecular genetics* **12**, 3161-3171
186. Lohi, H., Ianzano, L., Zhao, X. C., Chan, E. M., Turnbull, J., Scherer, S. W., Ackerley, C. A., and Minassian, B. A. (2005) Novel glycogen synthase kinase 3 and ubiquitination pathways in progressive myoclonus epilepsy. *Human molecular genetics* **14**, 2727-2736
187. Gentry, M. S., Worby, C. A., and Dixon, J. E. (2005) Insights into Lafora disease: malin is an E3 ubiquitin ligase that ubiquitinates and promotes the degradation of laforin. *Proc Natl Acad Sci U S A* **102**, 8501-8506
188. Wang, Y., Liu, Y., Wu, C., Zhang, H., Zheng, X., Zheng, Z., Geiger, T. L., Nuovo, G. J., and Zheng, P. (2006) Epm2a suppresses tumor growth in an immunocompromised host by inhibiting Wnt signaling. *Cancer Cell* **10**, 179-190
189. DePaoli-Roach, A. A., Tagliabracci, V. S., Segvich, D. M., Meyer, C. M., Irimia, J. M., and Roach, P. J. (2010) Genetic depletion of the malin E3 ubiquitin ligase in mice leads to lafora bodies and the accumulation of insoluble laforin. *J Biol Chem* **285**, 25372-25381
190. Wang, W., Lohi, H., Skurat, A. V., DePaoli-Roach, A. A., Minassian, B. A., and Roach, P. J. (2007) Glycogen metabolism in tissues from a mouse model of Lafora disease. *Arch Biochem Biophys* **457**, 264-269
191. Komatsu, M., Waguri, S., Chiba, T., Murata, S., Iwata, J., Tanida, I., Ueno, T., Koike, M., Uchiyama, Y., Kominami, E., and Tanaka, K. (2006) Loss of autophagy in the central nervous system causes neurodegeneration in mice. *Nature* **441**, 880-884
192. Rubinsztein, D. C. (2006) The roles of intracellular protein-degradation pathways in neurodegeneration. *Nature* **443**, 780-786
193. Williams, A., Jahreiss, L., Sarkar, S., Saiki, S., Menzies, F. M., Ravikumar, B., and Rubinsztein, D. C. (2006) Aggregate-prone proteins are cleared

- from the cytosol by autophagy: therapeutic implications. *Current topics in developmental biology* **76**, 89-101
194. Inoki, K., and Guan, K.-L. (2009) Tuberous sclerosis complex, implication from a rare genetic disease to common cancer treatment. *Human molecular genetics* **18**, R94-R100
 195. Kim, W., Bennett, E. J., Huttlin, E. L., Guo, A., Li, J., Possemato, A., Sowa, M. E., Rad, R., Rush, J., Comb, M. J., Harper, J. W., and Gygi, S. P. (2011) Systematic and quantitative assessment of the ubiquitin-modified proteome. *Mol Cell* **44**, 325-340
 196. Kim, J., and Guan, K.-L. (2011) Amino acid signaling in TOR activation. *Annual review of biochemistry* **80**, 1001-1032
 197. Jain, N., Rai, A., Mishra, R., and Ganesh, S. (2017) Loss of malin, but not laforin, results in compromised autophagic flux and proteasomal dysfunction in cells exposed to heat shock. *Cell Stress and Chaperones* **22**, 307-315
 198. Duran, J., Gruart, A., Garcia-Rocha, M., Delgado-Garcia, J. M., and Guinovart, J. J. (2014) Glycogen accumulation underlies neurodegeneration and autophagy impairment in Lafora disease. *Human molecular genetics*
 199. Niittyta, T., Comparot-Moss, S., Lue, W. L., Messerli, G., Trevisan, M., Seymour, M. D., Gatehouse, J. A., Villadsen, D., Smith, S. M., Chen, J., Zeeman, S. C., and Smith, A. M. (2006) Similar protein phosphatases control starch metabolism in plants and glycogen metabolism in mammals. *J Biol Chem* **281**, 11815-11818
 200. Kotting, O., Santelia, D., Edner, C., Eicke, S., Marthaler, T., Gentry, M. S., Comparot-Moss, S., Chen, J., Smith, A. M., Steup, M., Ritte, G., and Zeeman, S. C. (2009) STARCH-EXCESS4 is a laforin-like Phosphoglucan phosphatase required for starch degradation in *Arabidopsis thaliana*. *The Plant cell* **21**, 334-346
 201. Raththagala, M., Brewer, M. K., Parker, M. W., Sherwood, A. R., Wong, B. K., Hsu, S., Bridges, T. M., Paasch, B. C., Hellman, L. M., and Husodo, S. (2015) Structural mechanism of laforin function in glycogen dephosphorylation and lafora disease. *Molecular cell* **57**, 261-272
 202. Gessler, K., Uson, I., Takaha, T., Krauss, N., Smith, S. M., Okada, S., Sheldrick, G. M., and Saenger, W. (1999) V-Amylose at atomic resolution: X-ray structure of a cycloamylose with 26 glucose residues (cyclomaltohexaicosaoase). *Proc Natl Acad Sci U S A* **96**, 4246-4251
 203. Chan, E. M., Bulman, D. E., Paterson, A. D., Turnbull, J., Andermann, E., Andermann, F., Rouleau, G. A., Delgado-Escueta, A. V., Scherer, S. W., and Minassian, B. A. (2003) Genetic mapping of a new Lafora progressive myoclonus epilepsy locus (EPM2B) on 6p22. *Journal of medical genetics* **40**, 671-675
 204. Freemont, P. S. (2000) RING for destruction? *Current biology : CB* **10**, R84-87

205. Cheng, A., Zhang, M., Gentry, M. S., Worby, C. A., Dixon, J. E., and Saltiel, A. R. (2007) A role for AGL ubiquitination in the glycogen storage disorders of Lafora and Cori's disease. *Genes Dev* **21**, 2399-2409
206. Moreno, D., Towler, M. C., Hardie, D. G., Knecht, E., and Sanz, P. (2010) The laforin-malin complex, involved in Lafora disease, promotes the incorporation of K63-linked ubiquitin chains into AMP-activated protein kinase beta subunits. *Mol Biol Cell* **21**, 2578-2588
207. Vilchez, D., Ros, S., Cifuentes, D., Pujadas, L., Valles, J., Garcia-Fojeda, B., Criado-Garcia, O., Fernandez-Sanchez, E., Medrano-Fernandez, I., Dominguez, J., Garcia-Rocha, M., Soriano, E., Rodriguez de Cordoba, S., and Guinovart, J. J. (2007) Mechanism suppressing glycogen synthesis in neurons and its demise in progressive myoclonus epilepsy. *Nat Neurosci* **10**, 1407-1413
208. Worby, C. A., Gentry, M. S., and Dixon, J. E. (2008) Malin decreases glycogen accumulation by promoting the degradation of protein targeting to glycogen (PTG). *J Biol Chem* **283**, 4069-4076
209. Ganesh, S., Puri, R., Singh, S., Mittal, S., and Dubey, D. (2006) Recent advances in the molecular basis of Lafora's progressive myoclonus epilepsy. *J Hum Genet* **51**, 1-8
210. Turnbull, J., Epp, J. R., Goldsmith, D., Zhao, X., Pencea, N., Wang, P., Frankland, P. W., Ackerley, C. A., and Minassian, B. A. (2014) PTG depletion rescues malin-deficient Lafora disease in mouse. *Ann Neurol*
211. Turnbull, J., DePaoli-Roach, A. A., Zhao, X., Cortez, M. A., Pencea, N., Tiberia, E., Piliguian, M., Roach, P. J., Wang, P., Ackerley, C. A., and Minassian, B. A. (2011) PTG depletion removes Lafora bodies and rescues the fatal epilepsy of Lafora disease. *PLoS Genet* **7**, e1002037
212. Pederson, B. A., Turnbull, J., Epp, J. R., Weaver, S. A., Zhao, X., Pencea, N., Roach, P. J., Frankland, P., Ackerley, C. A., and Minassian, B. A. (2013) Inhibiting glycogen synthesis prevents lafora disease in a mouse model. *Ann Neurol*
213. Duran, J., Tevy, M. F., Garcia-Rocha, M., Calbo, J., Milan, M., and Guinovart, J. J. (2012) Deleterious effects of neuronal accumulation of glycogen in flies and mice. *EMBO Mol Med* **4**, 719-729
214. Roach, P. J., and DePaoli-Roach, A. A. (2013) Glycogen Metabolism and Lafora Disease. in *Protein Tyrosine Phosphatase Control of Metabolism* (Bence, K. K. ed.), Springer New York, New York, NY. pp 239-262
215. Hizukuri, S., Tabata, S., Kagoshima, and Nikuni, Z. (1970) Studies on Starch Phosphate Part 1. Estimation of glucose-6-phosphate residues in starch and the presence of other bound phosphate(s). *Starch - Stärke* **22**, 338-343
216. Mordoh, J., Krisman, C. R., and Leloir, L. F. (1966) Further studies on high molecular weight liver glycogen. *Arch Biochem Biophys* **113**, 265-272
217. Northcote, D. H. (1954) Electrophoresis of some neutral polysaccharides. *The Biochemical journal* **58**, 353-358
218. Wanson, J. C., and Drochmans, P. (1968) Rabbit skeletal muscle glycogen. A morphological and biochemical study of glycogen beta-

- particles isolated by the precipitation-centrifugation method. *J Cell Biol* **38**, 130-150
219. Contreras, C. J., Segvich, D. M., Mahalingan, K., Chikwana, V. M., Kirley, T. L., Hurley, T. D., DePaoli-Roach, A. A., and Roach, P. J. (2016) Incorporation of phosphate into glycogen by glycogen synthase. *Arch Biochem Biophys* **597**, 21-29
220. Ritte, G., Lloyd, J. R., Eckermann, N., Rottmann, A., Kossmann, J., and Steup, M. (2002) The starch-related R1 protein is an alpha -glucan, water dikinase. *Proc Natl Acad Sci U S A* **99**, 7166-7171
221. Mikkelsen, R., Baunsgaard, L., and Blennow, A. (2004) Functional characterization of alpha-glucan,water dikinase, the starch phosphorylating enzyme. *The Biochemical journal* **377**, 525-532
222. Kotting, O., Pusch, K., Tiessen, A., Geigenberger, P., Steup, M., and Ritte, G. (2005) Identification of a novel enzyme required for starch metabolism in Arabidopsis leaves. The phosphoglucan, water dikinase. *Plant Physiol* **137**, 242-252
223. Baunsgaard, L., Lutken, H., Mikkelsen, R., Glaring, M. A., Pham, T. T., and Blennow, A. (2005) A novel isoform of glucan, water dikinase phosphorylates pre-phosphorylated alpha-glucans and is involved in starch degradation in Arabidopsis. *Plant J* **41**, 595-605
224. DePaoli-Roach, A. A., Vilaro, P. G., Kim, J.-H., Mavila, N., Vemuri, B., and Roach, P. J. (2003) Determination of mammalian glycogen synthase phosphatase activity. *Methods in enzymology* **366**, 17-34
225. Khanna, M., Imasaki, T., Chikwana, V. M., Perez-Miller, S., Hunter, G. O., Mosley, A., Takagi, Y., and Hurley, T. D. (2013) Expression and purification of functional human glycogen synthase-1 (hGYS1) in insect cells. *Protein expression and purification* **90**, 78-83
226. Paladini, A. C., and Leloir, L. F. (1952) Studies on uridine-diphosphate-glucose. *The Biochemical journal* **51**, 426-430
227. Zmudzka, B., Szer, W., and Shugar, D. (1962) Preparation and chemical and enzymic properties of phosphate esters of 1-(beta-D-glucopyranosyl)uracil and -thymine. *Acta Biochim Pol* **9**, 321-341
228. Chikwana, V. M., Khanna, M., Baskaran, S., Tagliabracci, V. S., Contreras, C. J., DePaoli-Roach, A., Roach, P. J., and Hurley, T. D. (2013) Structural basis for 2'-phosphate incorporation into glycogen by glycogen synthase. *Proc Natl Acad Sci U S A* **110**, 20976-20981
229. MacDonald, D. L. (1972) Phosphates and other inorganic esters. *The Carbohydrates* **E2**, 253-278
230. Patel, M. K., and Davis, B. G. (2013) Control of Phosphoryl Migratory Transesterifications Allows Regioselective Access to Sugar Phosphates. *Organic Letters* **15**, 346-349
231. Teranishi, K., and Ueno, F. (2003) Mechanism of 2-O→3-O silyl migration in cyclomaltohexaose (α-cyclodextrin). *Tetrahedron Letters* **44**, 4843-4848
232. Collins, G. H., Cowden, R. R., and Nevis, A. H. (1968) Myoclonus epilepsy with Lafora bodies. An ultrastructural and cytochemical study. *Arch Pathol* **86**, 239-254

233. Fettke, J., Hejazi, M., Smirnova, J., Hochel, E., Stage, M., and Steup, M. (2009) Eukaryotic starch degradation: integration of plastidial and cytosolic pathways. *J Exp Bot* **60**, 2907-2922
234. Stitt, M., and Zeeman, S. C. (2012) Starch turnover: pathways, regulation and role in growth. *Curr Opin Plant Biol* **15**, 282-292
235. Zeeman, S. C., Kossmann, J., and Smith, A. M. (2010) Starch: its metabolism, evolution, and biotechnological modification in plants. *Annu Rev Plant Biol* **61**, 209-234
236. Blennow, A., and Engelsens, S. B. (2010) Helix-breaking news: fighting crystalline starch energy deposits in the cell. *Trends Plant Sci* **15**, 236-240
237. Pérez, S., and Bertoft, E. (2010) The molecular structures of starch components and their contribution to the architecture of starch granules: A comprehensive review. *Starch - Stärke* **62**, 389-420
238. Irimia, J. M., Tagliabracci, V. S., Meyer, C. M., Segvich, D. M., DePaoli-Roach, A. A., and Roach, P. J. (2015) Muscle glycogen remodeling and glycogen phosphate metabolism following exhaustive exercise of wild type and laforin knockout mice. *J Biol Chem* **290**, 22686-22698
239. Ganesh, S., Delgado-Escueta, A. V., Suzuki, T., Francheschetti, S., Riggio, C., Avanzini, G., Rabinowicz, A., Bohlega, S., Bailey, J., Alonso, M. E., Rasmussen, A., Thomson, A. E., Ochoa, A., Prado, A. J., Medina, M. T., and Yamakawa, K. (2002) Genotype-phenotype correlations for EPM2A mutations in Lafora's progressive myoclonus epilepsy: exon 1 mutations associate with an early-onset cognitive deficit subphenotype. *Human molecular genetics* **11**, 1263-1271
240. DePaoli-Roach, A. A., Segvich, D. M., Meyer, C. M., Rahimi, Y., Worby, C. A., Gentry, M. S., and Roach, P. J. (2012) Laforin and malin knockout mice have normal glucose disposal and insulin sensitivity. *Human molecular genetics* **21**, 1604-1610
241. Zhai, L., Choi, C. S., Irimia-Dominguez, J., McGuire, A. C., Kim, S., Bock, C. B., Roach, P. J., Shulman, G. I., and DePaoli-Roach, A. A. (2007) Enhanced insulin sensitivity and energy expenditure in PPP1R3C (PTG) deleted mice. *Diabetes* **56 Supplement 1**, A62
242. Bergmeyer, H. U. (1974) *Methods of Enzymatic Analysis*, 2nd English ed., Academic Press, New York
243. Hess, H. H., and Derr, J. E. (1975) Assay of inorganic and organic phosphorus in the 0.1-5 nanomole range. *Anal Biochem* **63**, 607-613
244. Zhu, A., Romero, R., and Petty, H. R. (2009) An enzymatic fluorimetric assay for glucose-6-phosphate: application in an in vitro Warburg-like effect. *Analytical biochemistry* **388**, 97-101
245. Bradford, M. M. (1976) A rapid and sensitive method for the quantitation of microgram quantities of protein utilizing the principle of protein-dye binding. *Anal Biochem* **72**, 248-254
246. Heyen, C. A., Tagliabracci, V. S., Zhai, L., and Roach, P. J. (2009) Characterization of mouse UDP-glucose pyrophosphatase, a Nudix hydrolase encoded by the Nudt14 gene. *Biochemical and biophysical research communications* **390**, 1414-1418

247. Lamerz, A.-C., Haselhorst, T., Bergfeld, A. K., von Itzstein, M., and Gerardy-Schahn, R. (2006) Molecular cloning of the *Leishmania major* UDP-glucose pyrophosphorylase, functional characterization, and ligand binding analyses using NMR spectroscopy. *J Biol Chem* **281**, 16314-16322
248. Murphy, D. M., Ivanenkov, V. V., and Kirley, T. L. (2003) Bacterial expression and characterization of a novel, soluble, calcium-binding, and calcium-activated human nucleotidase. *Biochemistry* **42**, 2412-2421
249. Smith, T. M., Hicks-Berger, C. A., Kim, S., and Kirley, T. L. (2002) Cloning, expression, and characterization of a soluble calcium-activated nucleotidase, a human enzyme belonging to a new family of extracellular nucleotidases. *Archives of biochemistry and biophysics* **406**, 105-115
250. Wishart, D. S., Bigam, C. G., Yao, J., Abildgaard, F., Dyson, H. J., Oldfield, E., Markley, J. L., and Sykes, B. D. (1995) ¹H, ¹³C and ¹⁵N chemical shift referencing in biomolecular NMR. *J Biomol NMR* **6**, 135-140
251. Hawker, J., Ozbun, J., Ozaki, H., Greenberg, E., and Preiss, J. (1974) Interaction of spinach leaf adenosine diphosphate glucose α -1, 4-glucan α -4-glucosyl transferase and α -1, 4-glucan, α -1, 4-glucan-6-glycosyl transferase in synthesis of branched α -glucan. *Archives of Biochemistry and Biophysics* **160**, 530-551
252. Devillers, C. H., Piper, M. E., Ballicora, M. A., and Preiss, J. (2003) Characterization of the branching patterns of glycogen branching enzyme truncated on the N-terminus. *Arch Biochem Biophys* **418**, 34-38
253. Waffenschmidt, S., and Jaenicke, L. (1987) Assay of reducing sugars in the nanomole range with 2, 2'-bicinchoninate. *Analytical biochemistry* **165**, 337-340
254. Zmudzka, B. S., D. (1964) Preparation and chemical and enzymic properties of cyclic phosphates of D-glucopyranose and synthesis of derivatives of N-(D-glucopyranosyl) pyridine. *Acta Biochimica Polonica* **11**, 509-525
255. De Clercq, E., Zmudzka, B., and Shugar, D. (1972) Antiviral activity of polynucleotides: role of the 2'-hydroxyl and a pyrimidine 5-methyl. *FEBS letters* **24**, 137-140
256. Piras, R. (1963) Synthesis of Some Aldose 2-Phosphates. *Arch Biochem Biophys* **103**, 291-292
257. Nitschke, F., Sullivan, M. A., Wang, P., Zhao, X., Chown, E. E., Perri, A. M., Israelian, L., Juana-López, L., Bovolenta, P., and de Córdoba, S. R. (2017) Abnormal glycogen chain length pattern, not hyperphosphorylation, is critical in Lafora disease. *EMBO Molecular Medicine*, e201707608
258. Andrade, D. M., Turnbull, J., and Minassian, B. A. (2007) Lafora disease, seizures and sugars. *Acta Myol* **26**, 83-86
259. Gentry, M. S., Dixon, J. E., and Worby, C. A. (2009) Lafora disease: insights into neurodegeneration from plant metabolism. *Trends Biochem Sci* **34**, 628-639

260. Ritte, G., Heydenreich, M., Mahlow, S., Haebel, S., Kotting, O., and Steup, M. (2006) Phosphorylation of C6- and C3-positions of glucosyl residues in starch is catalysed by distinct dikinases. *FEBS letters* **580**, 4872-4876
261. Lomako, J., Lomako, W. M., Whelan, W. J., and Marchase, R. B. (1993) Glycogen contains phosphodiester groups that can be introduced by UDPglucose: glycogen glucose 1-phosphotransferase. *FEBS letters* **329**, 263-267
262. Koro, L. A., and Marchase, R. B. (1982) A UDP-glucose: glycoprotein glucose-1-phosphotransferase in embryonic chicken neural retina. *Cell* **31**, 739-748
263. Criado, O., Aguado, C., Gayarre, J., Duran-Trio, L., Garcia-Cabrero, A. M., Vernia, S., San Millan, B., Heredia, M., Roma-Mateo, C., Mouron, S., Juana-Lopez, L., Dominguez, M., Navarro, C., Serratos, J. M., Sanchez, M., Sanz, P., Bovolenta, P., Knecht, E., and Rodriguez de Cordoba, S. (2012) Lafora bodies and neurological defects in malin-deficient mice correlate with impaired autophagy. *Human molecular genetics* **21**, 1521-1533
264. Ganesh, S., Delgado-Escueta, A. V., Sakamoto, T., Avila, M. R., Machado-Salas, J., Hoshii, Y., Akagi, T., Gomi, H., Suzuki, T., Amano, K., Agarwala, K. L., Hasegawa, Y., Bai, D. S., Ishihara, T., Hashikawa, T., Itohara, S., Cornford, E. M., Niki, H., and Yamakawa, K. (2002) Targeted disruption of the Epm2a gene causes formation of Lafora inclusion bodies, neurodegeneration, ataxia, myoclonus epilepsy and impaired behavioral response in mice. *Human Molecular Genetics*. **11**, 1251-1262
265. Garcia-Cabrero, A. M., Marinas, A., Guerrero, R., de Cordoba, S. R., Serratos, J. M., and Sanchez, M. P. (2012) Laforin and malin deletions in mice produce similar neurologic impairments. *J Neuropathol Exp Neurol* **71**, 413-421
266. Valles-Ortega, J., Duran, J., Garcia-Rocha, M., Bosch, C., Saez, I., Pujadas, L., Serafin, A., Canas, X., Soriano, E., Delgado-Garcia, J. M., Gruart, A., and Guinovart, J. J. (2011) Neurodegeneration and functional impairments associated with glycogen synthase accumulation in a mouse model of Lafora disease. *EMBO Mol Med* **3**, 667-681
267. Jorgensen, S. B., and Rose, A. J. (2008) How is AMPK activity regulated in skeletal muscles during exercise? *Frontiers in bioscience: a journal and virtual library* **13**, 5589-5604
268. Egan, B., and Zierath, J. R. (2013) Exercise metabolism and the molecular regulation of skeletal muscle adaptation. *Cell metabolism* **17**, 162-184
269. Winder, W., and Hardie, D. (1996) Inactivation of acetyl-CoA carboxylase and activation of AMP-activated protein kinase in muscle during exercise. *American Journal of Physiology-Endocrinology And Metabolism* **270**, E299-E304
270. Aschenbach, W. G., Suzuki, Y., Breeden, K., Prats, C., Hirshman, M. F., Dufresne, S. D., Sakamoto, K., Vilardo, P. G., Steele, M., and Kim, J.-H. (2001) The muscle-specific protein phosphatase PP1G/RGL (GM) is

- essential for activation of glycogen synthase by exercise. *J Biol Chem* **276**, 39959-39967
271. Tiberia, E., Turnbull, J., Wang, T., Ruggieri, A., Zhao, X. C., Pencea, N., Israelian, J., Wang, Y., Ackerley, C. A., Wang, P., Liu, Y., and Minassian, B. A. (2012) Increased laforin and laforin binding to glycogen underlie Lafora body formation in malin-deficient Lafora disease. *J Biol Chem* **287**, 25650-25659
272. Gayarre, J., Duran-Trío, L., Criado Garcia, O., Aguado, C., Juana-López, L., Crespo, I., Knecht, E., Bovolenta, P., and Rodríguez de Córdoba, S. (2014) The phosphatase activity of laforin is dispensable to rescue *Epm2a*^{-/-} mice from Lafora disease. *Brain* **137**, 806-818
273. Striano, P., Zara, F., Turnbull, J., Girard, J.-M., Ackerley, C. A., Cervasio, M., De Rosa, G., Del Basso-De Caro, M. L., Striano, S., and Minassian, B. A. (2008) Typical progression of myoclonic epilepsy of the Lafora type: a case report. *Nature Reviews. Neurology* **4**, 106

CURRICULUM VITAE

Christopher J. Contreras

Education

Indiana University, Indianapolis, IN

PhD in Biochemistry & Molecular Biology

Minor in Diabetes and Obesity Research

PhD Mentor: Dr. Peter J. Roach

Dissertation title: **Abnormal Glycogen Metabolism in Lafora Disease**

August 2009 – January 2018

University of New Mexico, Albuquerque, NM

Bachelor of Arts and Science in Biochemistry and Molecular Biology

Graduated: May 2008

Research and Work Experience

Graduate Research

Indiana University School of Medicine

Indianapolis, IN

August 2009 – January 2018

PhD Mentor: Dr. Peter J. Roach

PhD Candidate

Main Projects

1. Designed and performed exercise experiments to investigate glycogen metabolism in mouse models of Lafora disease
2. Investigate how phosphate is incorporated into glycogen and how phosphate can affect physical, morphological and structural changes within glycogen.

Techniques

Conducting mouse exercise experiments

Glycogen purification from mouse and rabbit tissues

Measuring trace amounts of phosphate in glycogen and amylopectin

Synthesize radiolabeled substrates for glycogen synthase

Analyzing carbohydrates using high performance anionic

chromatography (Dionex ICS 3000)

Immunoblotting

Teaching and working with rotating graduate students

Research Technician III

University of New Mexico School of Medicine

Albuquerque, NM

Summer 2008 – Summer 2009

Principal Investigator: Dr. Angela Wandinger-Ness

Main Responsibilities

1. Designing and creating expression vectors for Rab-7 and a potential effector protein (VPS39)

2. Develop and test flow cytometry based enzymatic assays for Rab-7 GTPase activity
3. Maintain common supplies and solution stocks used in the lab

Techniques

Immunoblotting
Expression vector cloning
Transfection, transduction and maintaining mammalian cell cultures
FACS scan flow cytometry
Immunofluorescent microscopy
Training and teaching new students

Undergraduate Research

University of New Mexico –Initiative for Maximizing Student Development (IMSD)
Albuquerque, NM

August 2006 – May 2000

Undergraduate mentor: Dr. Scott Ness

Undergraduate Researcher

Main Projects

1. Investigating the role of the 3' UTR in post-transcriptional regulation of the oncogene *c-myb*.
2. Developing methods to knock down endogenous levels of c-Myb using siRNAs.

Techniques

Immunoblotting
RT-PCR
Expression vector cloning
Transfection, transduction and maintaining mammalian cell cultures
FACS scan flow cytometry
Training and teaching new students

Food and Drug Administration (FDA) Internship: Hispanic Association of Colleges & Universities (HACU)

Food and Drug Administration: Center for Drug Evaluation and Research (CDER)

Rockville, MD

June 2004-August 2004

Main Project:

1. Comparison of bone mineral density in normal and osteoporotic patients that were taking Fosamax and present findings to FDA-CDER personal.

Awards

- 2015 Indiana University Center for Diabetes and Metabolic Diseases Symposium Graduate Student Research Poster Award
- 2010 - 2013 NIH T32 Diabetes Training Grant (T32-DK064466)

- 2013 Society for Advancement of Chicanos and Native Americans in Science (SACNAS) National Conference Graduate Student Presentation Award in Biochemistry
- 2006 - 2008 UNM Initiative for Maximizing Student Development (IMSD) undergraduate research program
- 2007 SACNAS National Conference Travel Award
- 2005 & 2006 NIH Sponsored Summer Research Internship Program (Grant number: 5T35HL076595)
- 2004 Summer internship at Food & Drug Administration (FDA) as part of the Hispanic Association of Colleges & Universities (HACU) program

Meetings & Presentations

- 2016 June, Lafora Disease Workshop: UCSD
- 2015 Indiana University Center for Diabetes and Metabolic Diseases Symposium Graduate Student Research Poster
- Impaired Glycogen Metabolism in Mouse Models of Lafora Disease
- 2014 November, Indiana University Center for Diabetes Research (CDR) oral presentation
- Impaired Glycogen Metabolism in Mouse Models of Lafora Disease
- 2013 SACNAS National Conference graduate student oral presentation
- Impaired Metabolism of the Abnormal Glycogen in Laforin Knockout Mice
- 2007 SACNAS National Conference undergraduate research poster presentation

Publications

Christopher J. Contreras, Dyann M. Segvich, Anna A. DePaoli-Roach and Peter J. Roach (2017) Abnormal Glycogen Metabolism During Exercise in Mouse Models of Lafora Disease. (In Preparation)

Christopher J. Contreras, Dyann M. Segvich, Krishna Mahalingan, Vimbai M. Chikwana, Terry L. Kirley, Thomas D. Hurley, Anna A. DePaoli-Roach and Peter J. Roach (2016) Incorporation of phosphate into glycogen by glycogen synthase. *Archives of Biochemistry and Biophysics* **597**, 21-19

Anna A. DePaoli-Roach^{*}, **Christopher J. Contreras**^{*}, Dyann M. Segvich, Christian Heiss, Mayumi Ishihara, Parastoo Azadi and Peter J. Roach (2014) Glycogen Phosphomonoester Distribution in Mouse Models of the Progressive Myoclonic Epilepsy, Lafora Disease. *The J Biol Chem* **290**(2): 841-850

Chikwana, V. M., Khanna, M., Baskaran, S., Tagliabracci, V. S., **Contreras, C. J.**, DePaoli-Roach, A., Roach, P. J., and Hurley, T. D. (2013) Structural basis for 2'-phosphate incorporation into glycogen by glycogen synthase. *Proceedings of the National Academy of Sciences of the United States of America* **110**, 20976-20981

Baskaran, S., Chikwana, V. M., **Contreras, C. J.**, Davis, K. D., Wilson, W. A., DePaoli-Roach, A. A., Roach, P. J., and Hurley, T. D. (2011) Multiple glycogen-binding sites in eukaryotic glycogen synthase are required for high catalytic efficiency toward glycogen. *The J Biol Chem* **286**, 33999-34006

Tagliabracci, V. S., Heiss, C., Karthik, C., **Contreras, C. J.**, Glushka, J., Ishihara, M., Azadi, P., Hurley, T. D., DePaoli-Roach, A. A., and Roach, P. J. (2011) Phosphate incorporation during glycogen synthesis and Lafora disease. *Cell Metab* **13**, 274-282

*** Co-First Author**

Service

- 2014 October-February 2015, Student representative on search committee for the new Program and Evaluation Director for Indiana University School of Medicine Office of Diversity Affairs
- 2014 July - July 2017, SACNAS-IUPUI chapter member.

Other

- Analyzing and quantifying carbohydrate profiles from yeast fermentations for Xylogenics